NEURAL MECHANISMS OF HIPPOCAMPAL PLACE CELL SEQUENCES

by
Ting Feng

A dissertation submitted to Johns Hopkins University in conformity with the requirements for the degree of Doctor of Philosophy

Baltimore, Maryland

December, 2015

Abstract

The hippocampus is important for learning and memory. Specifically, a type of pyramidal neuron in the rodent hippocampus, namely the "place cell", encodes the current location of the animal in space. Sequential activations of hippocampal place cells occurs when the animal is under active exploration (theta sequence), and during the animal's quiet immobility or sleep (hippocampal replay). These hippocampal place cell sequences have been proposed as fundamental neural substrates of learning and memory, because they carry precise temporal coordination between individual neurons. However, the mechanisms contributing to their development with experience have not been well understood. To address this gap in knowledge, we applied high-density electrophysiological recording techniques to simultaneously monitor the activities of hundreds of hippocampal place cells, and compared neuronal activities before and after, or between early and late experiences, while the animal explored a novel environment. I found that both theta sequences and hippocampal replay emerged immediately after the first experience, and were absent prior to that. In contrast, the activities of individual place cells advanced to earlier phases of hippocampal theta rhythm (the phenomenon of "phase precession") independently with experience, and only became synchronized and formed temporally coordinated sequential activities after the first running experience. Further, the hippocampal replays, once developed, were continuously modulated by individual experiences, where the propagation speed of their represented spatial trajectories slowed down with learning. Examination of hippocampal replays in a fine temporal scale revealed that their spatial representations were discretized in alternating stages of static representation and rapid movement, and phase-locked to the slow-gamma rhythm. The change of the propagation speed of replay was reflected by an increased number of discrete alternating stages in the represented trajectory,

accompanied by an increase in duration of the static representations, and a decrease of the duration of the rapid movements. In conclusion, hippocampal place cell sequences undergo rapid plasticity with experience, which involves synchronization between individual neurons, and a dynamic change in the content of spatial information represented by the place cell sequences.

Thesis Committee

David J. Foster, Ph.D. (Advisor, Reader)

Marshall G. Hussain Shuler, Ph.D. (Second reader)

James J. Knierim, Ph.D.

Kechen Zhang, Ph.D.

Preface and Acknowledgements

First I would like to thank you for your interest in reading my dissertation. This dissertation contains five years of my work as a PhD student, where I investigated the cognitive function of learning and memory in the brain area of hippocampus by studying a particular type of neuron – "hippocampal place cell", and by examining the relationship of spike timing between different neurons via high density in-vivo electrophysiology techniques in behaving rodents. I included three of my projects in separate chapters, the contents of which come from two published papers (chapter 3 – Journal of Neuroscience 2015, chapter 4 – Nature Neuroscience 2015; see Curriculum Vitae) and a manuscript in preparation (chapter 5).

Words cannot express my gratitude for those who helped me along my way to complete the PhD degree. I would like to first thank my thesis advisor, Dr. David Foster, who introduced me to the world of place cells and directed me step by step to exciting discoveries. I would like to thank all my thesis committee members, Dr. James Knierim, Dr. Marshall Shuler and Dr. Kechen Zhang, who gave valuable suggestions to my research and ensured that I was in good standing with my progress every year. I would like to thank all my lab mates for their tremendous support, especially Dr. Delia Silva, who collaborated with me on the Nature Neuroscience publication. I would also like to thank accompanies of my friends in the Neuroscience department and the Johns Hopkins Chinese community through my six years in Baltimore. Finally, I would not succeed without my beloved family: special regards here to my parents Mr. Chaozhang Feng, Ms. Dexiu Zeng and my husband Dr. Gerald Sun.

Table of Contents

List of Figure

Chapter 1 — Background

1.1 Learning, memory and synaptic plasticity

Learning and memory are essential cognitive functions in humans. Throughout daily life, we rapidly learn new information and skills, and store acquired knowledge in the form of memories that can be retrieved in the future. Learning is the process of how new information is acquired, and memory is the expression of what you have learned. Although learning is the prerequisite to forming memory, learning and memory are interdependent processes, as memory helps generalization and learning of new information.

Depending on the type of information that acquired and stored, memory can be classified into two categories: declarative memory and non-declarative memory (Graf and Schacter, 1985; Tulving, 1992). The former is memory of explicit information that can be verbally described (Ullman, 2004), for example semantic memory stores facts and terms, and episodic memory stores personal experiences of past events (Tulving, 2002b). The latter is implicit memorized information that cannot be verbally recalled, such as procedural memory, which enables us to carry on daily tasks (mostly motor tasks) that may not require consciousness. Because different types of memory require different processes to learn and involve different areas of the brain (Squire, 1992b; Squire and Zola, 1996; Squire, 2004), this dissertation focuses on one type of memory: declarative

memory - the “conscious” category of memory. More specifically, I am asking how the brain encodes and consolidates episodic memories of spatial information.

The neurology substrate of learning and memory lies in individual neurons in the brain, particularly the molecular and structural change within and between individual neurons (Thompson, 1986). Individual neurons communicate with each other via their synapses, and are able to constantly modify their synaptic connections in response to changes of their activities, an ability named synaptic plasticity (Bear and Malenka, 1994). During learning, the numbers and/or strengths of different synaptic connections undergo long-term changes, such as long-term potentiation/depression (LTP/LTD), to enhance memory formation and storage (Abbott and Nelson, 2000). The synaptic plasticity changes between individual neurons follow the Hebb’s rule – “Cells that fire together, wire together” (Shatz, 1992), where repeated and persistent stimulations from a presynaptic neuron result in an increase of synaptic strength between presynaptic and postsynaptic neurons (Hebb et al., 1994). The spike timing between presynaptic and postsynaptic neurons are critical for the plasticity change, as the synaptic connection will only strengthen if the presynaptic neuron fires immediately ahead of the postsynaptic neuron, a plasticity rule named “spike-timing-dependent plasticity (STDP)” (Levy and Steward, 1983; Bi and Poo, 1998a).

Synaptic plasticity is currently one of the most featured research topics in Neuroscience, and is studied through a large range of technologies including, but not limited to, genetic modifications, electrophysiology recordings, imaging studies and behavior assays. The scale of synaptic plasticity research ranges from the molecular level

where neurotransmitters and receptors are examined (Gaiarsa et al., 2002), to cognitive level where the performances of learned tasks or perceptions are evaluated (Hubel et al., 1977). In this dissertation, we simultaneously monitor plasticity changes of activities of hundreds of neurons from high-density electrophysiology recordings in behaving animals, to probe the neuronal substrate of learning and memory.

1.2 The function and anatomy of hippocampus

The importance of the hippocampus in encoding and consolidation episodic memories has been widely recognized after a surgical treatment for epilepsy in the late 1950s resulted in patients' loss of ability to form new memories. The most well-known patient among them was H.M. (Corkin, 2013), who underwent a bilateral temporal lobectomy that removed most of his hippocampal formation and adjacent brain structures. Even though H.M.'s epilepsy symptoms lessened as a result of the surgery, he was unable to form any memory of events that he experienced post-surgery for the rest of his life. Interestingly, the loss of his ability to form memories was only restricted to episodic and semantic memories; his ability to hold working memory and form procedural memory seems intact. For example, H.M. can successfully carry on conversations with people, and learn new motor skills, despite not remembering he had learned them. The unique case of H.M. has inspired many influential studies, and provides direct evidence for the differentiation of declarative and procedural memories, as well as the important functional role of the hippocampus in episodic memory.

The importance of hippocampus in learning and memory has also been suggested in animal lesion studies. For example, rats with hippocampal lesion cannot effectively learn the location of a hidden platform to escape in a water maze (Morris et al., 1982). This impairment of behavior is restricted to hippocampal lesions, as animals with lesions in other cortical areas performed as well as intact animals. Furthermore, the hippocampal lesion group can successfully escape in the water maze, if the task is not memory-dependent, such as finding the platform above the water via visual guidance. Studies using pharmacological approaches, such as disabling the hippocampus with muscimol, and lesion studies on other animal models all support the important role of the hippocampus in learning and memory (Squire, 1992a; Holt and Maren, 1999; Corcoran et al., 2005).

Anatomically, the hippocampus is one of the brain areas at the top of the information process pyramid, as it receives highly processed, multimodal sensory information from many cortical areas (Andersen et al., 2006). External stimuli, such as light, sound, smell, and pressure, are first processed by primary sensory areas, and then integrated by secondary or higher sensory areas before relayed to the hippocampus. The hippocampus is also anatomically connected to areas of the brain that underlie other high-level cognitive functions. For example the hippocampus has connections with the amygdala, which is an important area of the brain for processing emotion (Pitkanen et al., 2000), thus both of these areas have been extensively studied in fear conditioning tasks (Selden et al., 1991; Phillips and Ledoux, 1992; Kim et al., 1993). The hippocampus is also connected with the prefrontal cortex that governs decision making processes (Ferino

et al., 1987; Jay et al., 1989). The interconnections between the hippocampus and the ventral tegmental area, which is involved in reward and drug addiction, dictate these two brain areas as common candidates in reinforcement learning experiments (Lisman and Grace, 2005; Luo et al., 2011).

Within the hippocampus, several dense layers of neurons, with abundant directional projections, form an intricate circuit (Andersen et al., 2006). The core tri-synaptic circuit can be described as follows: (i) the input structure of hippocampus, the entorhinal cortex, projects to the dentate and the CA3 cell layers via the perforant pathway, and projects to the CA1 cell layer directly via temporoammonic pathway; (ii) the granule cells in the dentate project to the pyramidal cells in the CA3 layer via mossy fibers; (iii) the densely interconnected CA3 pyramidal cells relay information to the CA1 pyramidal cells via fibers named schaffer collaterals; (iv) the CA1 then projects to the subiculum, which is the output structure of the hippocampus; (v) the subiculum then projects back to entorhinal cortex, to complete the loop, and projects to other brain areas. This intricate distributed neuronal network suits the hippocampus's ability to compute and integrate information, thus it is a significant feature when examining hippocampal functions. The current dissertation only examined neuronal activities from the CA1 pyramidal cells. However, the hippocampal circuit infers that my findings may also be applied to CA3 pyramidal cells; this is discussed in length in subsequent chapters.

The densely packed, but distinctly segregated, cell layers in the hippocampal circuit make the hippocampus an idea candidate for examining synaptic plasticity, such as long-term potentiation/depression (LTP/LTD) in slice physiology. Numerous studies

and fruitful discoveries have emerged in this field. At the molecular level, the synaptic changes in the hippocampus depend on a particular glutamate receptor, the NMDA receptor, which allows calcium influx upon synchronized presynaptic activation and postsynaptic depolarization. Blocking the NMDA receptor prevents the occurrence of LTP, thus impairing encoding and consolidation of memory (Nakazawa et al., 2004). In this dissertation, I did not include the studies manipulating the activity of NMDA receptor. However, a discussion regarding how my findings may rely on the NMDA receptor is included in the final chapter.

In this section I have discussed the importance of the hippocampus in learning and memory, described the anatomy and neural circuits both within and outside of hippocampus, as well as the molecular substrates of learning and memory in hippocampus. In the following section, I focus on a specific type of neuron, the hippocampal place cell, which is of particular interest for my research.

1.3 Hippocampal place cells

The discovery of "place cells" leads to the award of the 2014 Nobel Prize in Physiology or Medicine to John O'Keefe. The pyramidal cells in the CA1 and CA3 cell layers of the hippocampus in rodents are neurons that encode specific locations in space, hence the name "place cell". These cells were first discovered in 1971 (O'Keefe and Dostrovs.J, 1971), where O'Keefe and his colleague recorded activities of single hippocampal neurons in freely foraging rats. He found that an individual hippocampal pyramidal cell tended to fire when the animal entered a specific location, and was largely

inactive when the animal was at other places. This cell responded to location, as it robustly became active every time the animal traversed the region of the environment that was preferred by the cell (the preferred area is named “place field”), regardless of the directions the animal came from (O'Keefe, 1976, 1979; Best et al., 2001; Moser et al., 2008). The spatial selectivity of the hippocampal pyramidal cells has been observed in many kinds of environment: restricted (single or multiple arm tracks), 2-D (open field), and 3-D (cuboid-shaped room where bats are flying; Ulanovsky and Moss, 2007; Yartsev and Ulanovsky, 2013). Different pyramidal cells have different spatial preference in the same environment, and they also change their spatial selectivity between different environments (a phenomenon named “place cell remapping”; Muller and Kubie, 1987; Fyhn et al., 2007; Colgin et al., 2008).

The discovery of place cells led the influential theory of “cognitive map” (O'Keefe and Nadel, 1978a), where each individual place cell uniquely code a specific location in space, thus a detailed map can be formed from the spatial information carried by all of the place cells. This map itself is a structured organization of memory stored within the hippocampus. A unique feature of this theory is that different maps can be stored in the same ensemble of neurons as a result of place cell remapping between different environments. During spatial exploration, animals constantly use these stored information to navigate through space, and make real-time decisions of their foraging path.

How does a place cell develop its place field? As mentioned in the previous section on the hippocampal anatomy, the input to the hippocampal CA1 and CA3 place

cells comes from the entorhinal cortex. The neurons in entorhinal cortex also exhibit spatial selectivity but interestingly they fire in a hexagonal grid pattern, hence their name of "grid cells" (Hafting et al., 2005). Grid cells have evenly spaced place fields covering the entire environment, and the grid spacing and orientation between different grid cells are different. It is suggested that, because a place cell receives multiple inputs from different grid cells, the overlapping of its upstream grid cells' receptive fields produced the tightly defined place fields of the place cell. Theta rhythm oscillations produced by medial septum has been suggested to be important in grid cell formation (Burgess et al., 2007; Giocomo et al., 2007; Jeewajee et al., 2008a; Brandon et al., 2011).

Once place cells form their place fields, which usually happens immediately when the animal encounters a new environment, the spatial selectivity of place cells may still undergo plasticity changes. Firstly, the "ensemble code" – the spatial information carried by groups of place cells - was initially less stable in a novel environment and takes minutes to stabilize (Wilson and McNaughton, 1993). Secondly, new place cells can emerge after several repeated experiences or even after several days of exploring the same environment (Frank et al., 2004; Monaco et al., 2014). Thirdly, the locations and or shapes of the place fields also express progressive changes during early experience (Mehta et al., 2000). Lastly, this dissertation is going to report and discuss new findings of plasticity induced changes of spiking orders between individual hippocampal place cells.

Hippocampal place cells exhibit different activities at different brain states. In the first brain state, while the animal is actively exploring the environment, the local field

potential (LFP) in the hippocampus undergoes a characteristic theta oscillation with a frequency range of 4-12 Hz (Buzsaki, 2002). Accompanied by the theta rhythm, the activities of hippocampal place cells fluctuate, with peak firing close to the trough of theta oscillation. The second brain state is when the animal is immobile and quiet awake, or during slow-wave sleep. In this brain state, the hippocampal LFP exhibits large irregular activity pattern, and is intermingled with high frequency ripples (100-400 Hz) carried by large slow-wave deflection, namely sharp-wave ripples (SWRs) (Buzsaki et al., 1983; Buzsaki et al., 1992; Ylinen et al., 1995). During SWRs, the hippocampal place cells exhibit bursting activities, whereas outside SWRs, the place cells are much less active.

The apparent dissociation of two brain states, accompanied by different neuronal activities, promotes a two-stage model of memory trace formation: (i) during the exploratory (theta wave) state, the neocortical information is encoded as transient heterosynaptic potentiation in a subgroup of CA3 pyramidal cells, and (ii) upon the termination of exploratory activity (sharp wave brain state), these weakly potentiated CA3 neurons will then initiate population bursts (Buzsaki, 1989). Both stages are equally important for memory formations.

In this section I presented hippocampal place cells, their unique spatial selectivity features, their plasticity changes induced by experience, and how their activity patterns match with different brain waves. I will now discuss the sequential firing activities of groups of hippocampal place cells, because ensemble activity is a unique feature of hippocampal neurobiology.

1.4 Hippocampal place cell sequences

The engram in the brain has been long sought for centuries. The discovery of place cell is exciting, yet it only reveals a tip of the iceberg of the complex neurobiology of memory.

While an animal is actively exploring an environment or performing a spatial task, an active place cell only tells the animal its current location, but does not indicate additional information about where the animal should go. However, at any given moment, the animal needs to constantly remind itself where it has just come from and the particular path it just took, and combine this information with its previous knowledge of the spatial structure of the environment, to decide its next movement path. All of these cognitive processes require stored spatial information provided from more than just one neuron, presumably from a large group of place cells. Further, the nature of episodic memory dictates that the information being encoded and retrieved is all sequential information of experiences and, or, events. For example, when thinking about what I ate for breakfast this morning, egg and toast are not the only things I remember, rather I think of the sequential events that happened around the same time, for example I washed my hands before I went to the dining table, and I added salt and pepper to the egg, and then started eating. Again, the complete memory trace of "what I ate for breakfast" lies beyond the neuron that encodes/stores the subject of "egg and toast"; rather, it relies on a group of neurons that code sequential information.

All the above reasons lead us to examine hippocampal place cell sequences in the current dissertation, with the idea that the precisely controlled temporal order of place cell activities is a plausible engram of episodic memory. Hippocampal place cell sequences exhibit different activities under the two different brain states mentioned in the previous section. During the theta wave brain state, place cell sequences occur when the animal is actively exploring the environment, and several place cells with overlapping place fields fire in a sequence within a theta cycle, which is named "theta sequence" (Dragoi and Buzsaki, 2006; Foster and Wilson, 2007). The second place cell sequence occurs when the animal is immobile and quietly awake, or during sleep, accompanied by SWRs events. The place cells are firing in a compressed temporal order corresponding to previously experienced behavior sequences during SWRs events, hence these place cell sequences are called "hippocampal replays" (Skaggs and McNaughton, 1996; Lee and Wilson, 2002; Foster and Wilson, 2006).

In the following two sections, 1.4.1 and 1.4.2, I will describe hippocampal theta sequences and hippocampal replay in detail. Contrasting with previous studies, we used a high-density electrophysiology recording technique, and examined the precise temporal relationship of spike timing not just from pairs of neurons, but from hundreds of neurons simultaneously, to truly uncovered the sequential form. Our advanced technique revealed new features of hippocampal place cell sequences that would not have been revealed using traditional techniques.

1.4.1 Hippocampal theta sequences

Hippocampal theta sequences were not directly reported until technologies allowed simultaneous recording of large population of place cells (Dragoi and Buzsaki, 2006; Foster and Wilson, 2007). However, the hippocampal theta sequences had long been predicted. After O'Keefe discovered the place cell, he examined the relationship between the activities of place cells and theta rhythm in the hippocampus. He found that when the animal traversed a place cell's place field, the place cell emitted consecutive spikes that occurred earlier and earlier in phase in reference to the concurring theta oscillations, and the precession of phase in a single traverse is always restricted within 360 degree (Okeefe and Recce, 1993). This spike timing and theta phase relationship in individual place cells is named "phase precession", and is one of the first temporal coding properties that was discovered in place cell. Specifically, each location within the place field is uniquely encoded by a particular theta phase, thus even though the firing rate of the place cell may be indistinguishable between the animals' entry and exit point of the place field, the spatial location is not ambiguous encoded given the phase information. O'Keefe examined the phase precession of many place cells, and reported that they all share similar phase advancement properties, for example the theta phases of spikes emitted at animals' entry point of place fields are near the trough of the theta oscillation. From these observations he concluded that place cells with overlapping place fields will fire in a precise temporal order during each theta cycle (theta sequence). This is because the place cell of whose place field the animal is at the exit point, will fire at an early theta phase, and the place cell at which place field the animal just entered, will fire at a late theta phase, according to their spike phase advancement properties.

Following these early discoveries, the theta sequence has long been considered an experiment analogy of individual neuronal phase precession. As investigations progressed, several reports pointed out that the relationship between theta sequences and phase precession were not trivial (Dragoi and Buzsaki, 2006; Foster and Wilson, 2007). Several factors including the variability between individual place cells and phase precession properties complicate the relationship. In chapter 3 in this dissertation, I will present the first direct experimental evidence to dissociate theta sequences and phase precession during learning, and explain the reason behind their divergence.

Previous researches tended to infer the properties of theta sequences from examining the phase advancements of individual neurons, possibly because they were unaware of the dissociation between theta sequences and phase precession. Despite incomplete information, many aspects of the properties of theta sequences inferred from phase precession are consistent, and generally acknowledged by recent studies. A widely recognized function of the theta sequence (and phase precession) is its role in encoding of episodic memory (Okeefe and Recce, 1993; Skaggs et al., 1996; Tsodyks et al., 1996; Dragoi and Buzsaki, 2006; Foster and Wilson, 2007). Because place cells fire within tenth of milliseconds of each other during each theta sequence, and fire in the spatial order of their place fields, the synaptic connections between place cells that have overlapping place fields will strengthen in the direction that the animal is running, according to the spike-timing-dependent plasticity (STDP) rule. Because the sequential firing order occurs repeatedly for several theta cycles, groups of place cells form strong asymmetric network connections that are suitable for generating sequence. This

asymmetric synaptic connection is a result of experience, and can be considered as a neural form of episodic memory.

Other functional roles of theta sequences have been suggested with the recent development of multi-unit recording techniques, which enabled researchers to directly examine the sequential structures of theta sequences. Johnson and Redish (2007) reported that ensemble activities during theta oscillations represented spatial sequences that swept to candidate future trajectories through a choice point, indicating theta sequence may predict animals' future behavior (Johnson and Redish, 2007). This report is also consistent with theoretical predictions of theta sequences, that each theta sequence is composed of expressions of both past and future spatial locations, and the brain should be able to extract this information in real time to constantly recall the past and predict the future. Subsequently other investigations from the same laboratory reinforced this theory, where they examined structural details of the spatial representations of individual theta sequences, and reported that the lengths of the "recall" and "prediction" segments vary between different theta sequences (Gupta et al., 2012). In particular, the length of the "prediction" segment varied on a moment-by-moment basis, depending on the animal's goals (Wikenheiser and Redish, 2015).

Currently, there is still debate over the development of theta sequences with experience, perhaps due to both technical and historical reasons. Firstly, there is a lack of direct experimental evidence, due to either the limitation of techniques or lack of awareness of the importance of directly examining sequence given the prior knowledge of phase precession. Secondly, theta sequences are ensemble activities among individual

neurons, so it is difficult to dissociate the plasticity induced changes of individual neurons from the changes of sequential structures. Thirdly, as mentioned before, theta sequence plays a role in encoding experience into episodic memory; if experience in turn is required to form theta sequences, caution must be exercised in distinguishing a positive feedback loop between theta sequence and experience, from a seemly "chicken or egg" causality dilemma. In chapter 3 and 6 of this dissertation, all these problems are addressed with detailed discussions.

In summary, in this section I introduced the theta sequence and its relationship with phase precession, discussed its functional role in learning and memory, as well as the challenges researchers face when examining its experience-dependent properties.

1.4.2 Hippocampal replay

Hippocampal replays are "offline" reactivations of place cells outside their place fields during SWRs events. The first experimental evidence of such place cell reactivation was reported by Wilson and McNaughton (1994), who observed that pairs of hippocampal place cells that were co-activated when the animal was exploring a new environment, increased firing correlations during the sleep after the exploration, compared with the sleep prior to experience. Subsequently, Lee and Wilson (2002) recorded more place cells simultaneously, and analyzed the temporal firing order among them during SWRs events. They reported that those place cells fire in the same order as when the animal was running in the previous environment, but in a compressed temporal scale, as if place cell ensembles are "replaying" the previous experience. In other words,

the replayed sequence of a linear track contains information representing the spatial trajectory along the track.

These replayed sequences not only occur during sleep, they also occur during SWRs events when the animal is awake and immobile (Foster and Wilson, 2006; Diba and Buzsaki, 2007b), such as when the animal stops at the end of a linear track after running from the other end. Because place cells may fire at different locations along the linear track, when the animal is running in different directions (Muller et al., 1994), the awake replays can be divided into two categories, based on the relationship between the temporal spiking order of place cells in hippocampal replay and the order of their place fields in different running directions.

The first category of awake replays, "reverse replay", refers to the replays that are reactivations of recent episodes of spatial experience in a temporally reversed order (Foster and Wilson, 2006). On a linear track, the first place cell that is reactivated during a reverse replay is the most recently activated place cell during the run, the one that has place field closest to the animal's current location, and the last place cell in the reverse replay sequence is the most remotely activated place cell, the one that has place field near the other end of the track, thus the spatial representation of a reverse replay is as if the animal is running backwards in a faster speed. The second category of awake replays is "forward replay", which is when the reactivation of spatial experience is in the exact temporal order of the previous experience. Reverse and forward replays do not have to be mutually exclusive, as shown in a study of animals running on an extended, approximately 10 m long, linear track, in which there were mixed forward and reverse

replays within the same sequence (Davidson et al., 2009). Thus the recruitment of place cells for different replays is a dynamic process.

There are several other characteristic dynamic properties of replays. Firstly, the represented trajectory can traverse an extended distance that covers the entire experimental environment, such as 10 m long track used by Davidson et al., and 1.8 m tracks used in the research that is the focus of this dissertation. Secondly, the spatial trajectory of replay can start at any location in the experimental environment, even though the start location has a bias at the animal's current location. Thirdly, reports of awake remote replay (Karlsson and Frank, 2009b), which is reactivation of place cell sequences of a previously experienced environment that is different from the current running environment suggests that replays also recruit place cells other than the ones that are currently active. It is worth noting that all these initial observations were reported from experiments on linear tracks. Replays have also recently been studied in open field environment (Pfeiffer and Foster, 2013), where both their cell recruitment and spatial representation are much more dynamic as a result of increased dimensions.

The discovery of hippocampal replay has elicited many exciting studies about its functional role in learning and memory. As discussed previously in the two-stage model of episodic memory, the SWRs associated brain stage is important for memory consolidation. This has been confirmed by animal studies showing impaired performance in spatial memory task upon electrical perturbation of SWRs events both during sleep and when the animal is awake (Girardeau et al., 2009b; Ego-Stengel and Wilson, 2010; Jadhav et al., 2012b).

However, SWRs/replay's role is not just memory consolidation, especially since awake replay has been reported. During awake replay, the place cells are firing in a similar temporally compressed manner as in theta sequences (Davidson et al., 2009), thus the spike timing differences between neighboring place cells that are active in the sequence, also fit the STDP rule for enhancing synaptic connections. Awake replay occurs really fast in a novel environment, for example after only one or two running laps on a novel linear track (Foster and Wilson, 2006; Wu and Foster, 2014). All these evidence point to the potential role of replay in encoding of episodic memory.

The functional role of replay goes beyond encoding and consolidation of episodic memory. Gupta et al. (2010) reported that replay is not a simple function of experience, because it can represent novel combinations of learned trajectories. A study from our laboratory by Pfeiffer and Foster (2013), that examined replays in an open field environment when the animal alternated between a goal-directed foraging task and a random foraging task, suggested that replay may be a process of retrieving learned information to predict/guide future behavior. More generally, the encoding and consolidation of place-cell sequences may critically support the well-established hippocampal roles in navigation (Olton and Samuelson, 1976b; O'Keefe and Nadel, 1978b), and episodic memory (Scoville and Milner, 1957b; Gaffan, 1994a; Steele and Morris, 1999; Wood et al., 1999).

The mechanism underlying replay generation is still under investigation. One classic view is that neuronal networks firstly undergo plasticity changes during learning, to form asymmetric connections. This asymmetric network, when triggered properly,

either due to a release from inhibition (Foster and Wilson, 2006), or due to strong local activation, will have a chain reaction, hence reactivated as previously learned sequences. However, a recent study by Dragoi and Tonegawa (2011) challenged the idea that hippocampal replay is itself a learned sequence. This study proposed that asymmetric connections can exist prior to any experience, and replay is merely a reflected sequence that mapped from the pre-established neuronal network structure (Dragoi and Tonegawa, 2014). These report greatly challenged the traditional view of the experience-dependence of hippocampal replay, which will be addressed in chapter 4 of this dissertation.

Once replay is generated and established, will it continue to be modulated by experience? What are the other plasticity changes in the neuronal network? Addressing these questions are among the major focuses of the current dissertation. Similar to the development of theta sequences, the development of replay has not been directly addressed due to the limitation of technologies. Previous studies have attempted to examine the plasticity change of place cell reactivations (Csicsvari et al., 2007; Cheng and Frank, 2008), but they either did not directly address sequence, for example only used pair-wise correlation, or they were looking at an extended time period between days of exploration of an environment (Cheng and Frank, 2008).

In chapter 5 of this dissertation, I will present results examining replays between individual experiences, for example between consecutive running laps of animals on a linear track, hence effectively examining the plasticity changes of replay on a minute to minute basis. The chapter will also include discussion about the computational models of replay generation and development with experience.

In summary, in this section I have introduced hippocampal replay, discussed its characteristic properties and potential functional roles, and briefly introduced the questions that will be addressed in my dissertation.

Chapter 2 — General Methodology

The major technology this dissertation used is in vivo electrophysiological recording, specifically, single-unit recording of extracellular potential of individual neurons in behaving animals. Neurons are basic functional units in the brain, thus the ability to accurately measure their individual responses to external stimuli is essential for understanding the brain and cognition. Fine-tipped, high-impedance microelectrodes implanted in the brain can provide recoding of electrical potential at single-neuron resolution and are widely used by Neuroscientists. The recording techniques from our lab have the following advantages: firstly, we build a high-density array of microelectrode that allows simultaneous recordings of hundreds of neurons; secondly, microelectrodes in the array are independently adjustable as bundles of four (tetrode) to ensure maximum recording accuracy; thirdly, the electric signal from the same neuron can be picked up by four different channels on the same tetrode, which allows accurate segregation of multiple simultaneously activated neurons; finally, we carry out the recordings on fully functional animals without anesthesia, in order to probe the neuronal mechanism underlying behavior and cognition. In this chapter, I will go through the general methodology and basic experimental protocol utilizing these techniques. However, because this dissertation includes three separate projects, I will leave detailed methodology of each project to their own respective chapters.

2.1 Experiment protocol and subjects

All procedures were approved by the Johns Hopkins University Animal Care and Use Committee and followed US National Institutes of Health animal use guidelines. Adult male Long-Evans rats (4-6 months old, 450–550 g) were housed on a standard, non-inverted, 12 h light cycle. Rats were habituated to daily handling and food-restricted to 85–90% of their free-feeding weight, and subsequently trained to traverse a 1.8-m linear track to receive a liquid chocolate-flavored reward (200 ml, Carnation Breakfast Essentials) through a tubing system at either end after a complete traversal of the track. The tubing system allowed each well at the end of the track to be independently and soundlessly filled by the experimenter via a hand-held syringe. All rats were trained on a separate linear track designated for training and in a room visually distinct from the recording room. Each training session lasted 30-45 min or when rats completed 20-30 laps. After training, rats were surgically implanted with a microdrive array (see next Section) and were allow recovery with free-feeding. Following recovery from surgery, animals were food-deprived again and retrained on the training linear track with recording cables attached for approximately two days before recording sessions began. All data were collected either when rats running back and forth on novel linear tracks where each lap was composed of two traverses along the track in opposite directions, or in a separate "sleep box" before or after a novel running experience. Each track was 1.8 m long (including two ends), 6 cm wide, and 4 cm in height of the walls, with two 15 cm long and 13 cm wide ends where the reward delivery wells were located. Different tracks were placed in different locations in the recording room. All tracks were equally novel at

the time of recording, and rats did not experience the same track twice. The distal cues in the recording room were also rearranged between different recording days.

2.2 Surgery and data acquisition

A microdrive array (25-30 g) containing 40 independently adjustable, gold-plated tetrodes aimed at area CA1 of dorsal hippocampus (20 tetrodes per hemisphere; 4.00 mm posterior and 2.85 mm lateral to bregma) was implanted in animals after training. Following surgical implantation, tetrodes were slowly lowered into the CA1 pyramidal layer over the course of 7-10 days. Final tetrode placement, unit recording and local field potential (LFP) recording were as previously described (Foster and Wilson, 2006; Pfeiffer and Foster, 2013). Each tetrode consisted of a twisted bundle of four 17.8 μm 90% platinum/10% iridium wires (Neuralynx), and each wire was electroplated with gold to an impedance of <150 KOhms prior to surgery. A bone screw firmly attached to the skull served as ground. All data were collected using a Digital Lynx data acquisition system (Neuralynx, Boseman, MT). The animal's position was tracked via independently colored LEDs mounted on the microdrive array, and recorded continuously at 60 Hz via an overhead video system. Analog neural signals were digitized at 32,556 Hz. Spike threshold crossings (50 μV) were recorded at 32,556 Hz. Continuous local field potential (LFP) data were digitally filtered between 0.1 and 500 Hz and recorded at 3,255.6 Hz. Individual units were identified by manual clustering based on spike waveform peak amplitudes using custom software (xclust2, Matt A. Wilson). Only well-isolated units were included in the analysis. Clustered units identified as putative inhibitory neurons on

the basis of spike width were excluded from further analysis. Well isolated clusters were confirmed with $L_{ratio} < 0.05$, with values calculated using the peak amplitude of each waveform as the feature set (Schmitzer-Torbert and Redish, 2004; Pfeiffer and Foster, 2013). Briefly, the L_{ratio} value of cluster C is

$$L_{ratio} = \left(\sum_{i \neq C} \left(1 - CDF_{\chi^2_{df}(D^2_{i,c})} \right) \right) / n_s$$

where n_s is the total number of spikes recorded on the tetrode throughout the recording epoch, $i \notin C$ is the set of spikes which are not members of cluster C, and $CDF_{\chi^2_{df}}$ is the cumulative distribution function of the χ^2 distribution with $df = 4$.

2.3 Position reconstruction from activity of hippocampal place cells

Position reconstruction from neural activity is an important method used throughout the dissertation. Because the neuron of interest in this dissertation codes for information of the space in the environment, accurate and effective extraction of spatial information carried by various patterns of neuronal activities under different conditions and behavior paradigms is essential. Here I applied a memoryless decoding algorithm based on Bayesian probabilities (Zhang et al., 1998a; Davidson et al., 2009) to uncover the spatial representation of hippocampal place cell activities. This decoding algorithm is especially robust to noise, and suitable to assess ensemble activity patterns across a large population of neurons. In this chapter, I will describe the basic mathematics behind this powerful method. In chapter 3, I will introduce a useful modification to this algorithm.

And in chapter 4, I will touch upon some caveats and cautions that are required when using this technique.

Position was linearized and binned into 2.5 cm bins. Directional place fields were calculated as the smoothed histogram of firing activity normalized by the time spent per bin. Place cells with peak firing rates less than 1 Hz along the track were excluded. A memoryless probability-based decoding algorithm was used to estimate the animal's position based on the directional place fields and the spike trains (Davidson et al., 2009; Pfeiffer and Foster, 2013). Briefly, the posterior probability of the animal's position (pos) across M total position bins given a time window (τ) containing neural spiking ($spikes$) is

$$Pr(pos|spikes) = \cup \Big/ \sum_{j=1}^{M} \cup$$

where

$$\cup = \sum_{k=1}^{2} \left(\prod_{i=1}^{N} f_i(pos, dir_k)^{n_i} \right) e^{-\tau \sum_{i=1}^{N} f_i(pos, dir_k)}$$

and $f_i(pos, dir_k)$ is the place field of one running direction of the i-th unit, assuming independent rates and Poisson firing statistics for all N units and a uniform prior over position. Decoded errors were calculated as the differences between the animal's current running position and the peak decoded position in each time window. A time window of 20 ms, moving with 5 ms steps, was used to examine theta sequence structure (chapter 3)

and hippocampal replay (chapter 5) in a fine timescale. The detection of trajectory events was based on non-overlapping decoding window of 20 ms (chapter 4, 5).

2.4 Analysis of place cell sequences

The analysis of place cell sequences focuses on examining the temporal relationship of spike timings between different neurons. More specifically, I am asking how coordinated the place cells are when firing in the same order as during behavior sequences. This can be done by measuring the correlations between the time of emitted spike and the order of the cells, as has been used in multiple occasions in this dissertation. However, because the previously mentioned decoding algorithm provides a more robust method to evaluate the spatial representation carried by these place cell sequences, I can also measure the weighted correlation on these reconstructed trajectories. The mathematic basics are as follows:

Decoded probabilities ($prob$) were assigned as weights of position estimates to calculate the correlation coefficient between time (T) and decoded position (P):

$$corr(T, P; prob) = \frac{cov(T, P; prob)}{\sqrt{cov(T, T; prob)cov(P, P; prob)}}$$

where weighted covariance between time and decoded position is

$$cov(T, P; prob) = \frac{\sum_i prob_i \big(T_i - m(T; prob)\big)\big(P_i - m(P; prob)\big)}{\sum_i prob_i}$$

and weighted means of time and decoded position are

$$m(T; prob) = \frac{\sum_i prob_i T_i}{\sum_i prob_i} \ \ and \ \ m(P; prob) = \frac{\sum_i prob_i P_i}{\sum_i prob_i}$$

Weighted correlation of each reconstructed theta sequence was calculated from the decoded probabilities of positions 50 cm behind and ahead of the animal's current location, in a time window of ¼ theta cycle before and after the mid-time point of each theta sequence. Weighted correlation of each candidate event was calculated from the decoded probabilities within the time window of candidate events.

Further, as frequently emphasized in this dissertation, because the decoding algorithm yields more distinct trajectories than that from raw spikes, and contains rich probability information at every location and at every time point; a lot of information can be extracted from the decoded trajectories of these sequences. I will leave the detailed descriptions of different quantifications in their own chapters because they are all critical for the related discoveries. Briefly, I can measure the slope, the duration and the sharpness of the represented trajectories, as well as the standard metrics of individual neuron activity during these place cell sequences, for example firing rates, phase of emitted spike in reference to a particular brain wave.

2.5 Analysis of Local Field Potentials

Local field potentials (LFPs) reflect ensemble activity from both excitatory and inhibitory neurons in the vicinity of the recording tetrode and are composed of different characteristic oscillatory rhythms corresponding to different brain stages. Examining the temporal relationship between individual place cells and characteristic brain waves from

LFP helps to understand how individual neurons are modulated by population activity. Here I extracted LFP from the electrode with the highest theta signal-to-noise ratio during animals' running (chapter 5) for each tetrode. When LFP from only one tetrode was needed for the data analysis, I choose the LFP from the tetrode with either highest theta signal-to-noise ratio or largest number of simultaneously recorded pyramidal cells (chapter 3). Raw LFP signal was then filtered through a 4-12 Hz band-pass filter to extract theta rhythms (chapter 3) or through a 25-50 Hz band-pass filter to extract slow gamma rhythms (chapter 5). The theta/gamma phase of an emitted spike ($\emptyset$) at time t was determined by linear interpolation of spike timing between the preceding reference phase zero at time t_0 and the following reference phase zero at time t_1 as the following:

$$\emptyset = mod(\frac{t - t_0}{t_1 - t_0} + 360)$$

where mod denotes the remainder when divided by 360 because the phase is always a number between 0 and 359. When calculating the slow-gamma phase of an emitted spike in chapter 5, reference phase zero was the peak of slow-gamma oscillation from the LFP of the tetrode where the spike was recorded. When calculating the theta phase of an emitted spike in chapter 3, the reference phase zero was the global phase zeros where maximal pyramidal cell activities occurred. The instantaneous theta/gamma frequency was determined as the reciprocal of duration of each theta/gamma cycle. When quantifying the amplitude or power of theta/gamma rhythm, z-scored value was calculated for each individual recording session when pooling data together to normalize across tetrodes with different impedances.

Chapter 3 — Dissociation between the experience-dependent development of hippocampal theta sequences and single-trail phase precession

3.1 Introduction

The hippocampus is important for navigational learning (O'Keefe and Nadel, 1978a; Morris et al., 1982) and episodic memory (Scoville and Milner, 1957a; Olton and Samuelson, 1976a; Gaffan, 1994b; Steele and Morris, 1999), both of which require temporal encoding of relationships between events and/or locations. Temporal coordination between hippocampal neurons during theta oscillations, namely theta sequences (Skaggs et al., 1996; Dragoi and Buzsaki, 2006; Foster and Wilson, 2007; Gupta et al., 2012) is thought to underlie this function via spike timing-dependent plasticity (Hebb et al., 1994; Jensen and Lisman, 1996; Skaggs et al., 1996). The "sweeping forward" structure of theta sequences also enables the retrieval of information about locations immediately ahead of the animal, which can be useful in guiding future behavior (Johnson and Redish, 2007; Gupta et al., 2012). However, little is known regarding the mechanisms underlying the development of hippocampal theta sequences with individual experiences, likely due to technical difficulties associated with simultaneously recording large cell ensembles. Because theta sequences generally recruit place cells only when the animal occupies their place fields, they are shorter and harder to detect than, for example, offline replay sequences that recruit cells with fields dispersed

widely throughout the environment (Lee and Wilson, 2002; Pfeiffer and Foster, 2013). Here we address this technical difficulty by implanting micro-drives containing 40 adjustable tetrodes targeted to the hippocampus, yielding up to hundreds of simultaneously recorded place cells.

Theta sequences were originally predicted as a consequence of phase precession (Okeefe and Recce, 1993; Skaggs et al., 1996), in which spikes fired by an individual place cell occur at progressively earlier theta phases during place field traversal. However, variability in place field sizes, instantaneous firing rates, phase precession offsets, phase precession slopes, and other properties between different cells complicate the relationship between phase precession and theta sequences (Dragoi and Buzsaki, 2006; Foster and Wilson, 2007; Schmidt et al., 2009). Theoretical models and experimental results also differ in how they view the dependence of phase precession and/or theta sequences on experience, with some regarding phase precession as intrinsic to individual place cells and independent of experience (Okeefe and Recce, 1993; Rosenzweig et al., 2000; Harvey et al., 2009), whereas others regard phase precession as merely an experimental corollary of theta sequences, which may themselves exist before experience (Itskov et al., 2011) or result from it (Samsonovich and McNaughton, 1997; Tsodyks, 1999; Mehta et al., 2002). Nevertheless, despite different accounts, the common assumption in most previous work is that ensemble-level theta sequences and single neuronal phase precession are manifestations of the same underlying phenomenon.

In this study, we recorded up to hundreds of hippocampal place cells simultaneously in freely behaving rats, to examine directly theta sequence structure and

single-trial phase precession during successive traversals along a novel track. I observed that theta sequence structure was absent on the first experience of a novel environment but emerged immediately thereafter, whereas the phase precession of individual hippocampal place cells was present from the first traversal and appeared to be an experience-independent phenomenon.

3.2 Methods

3.2.1 Subjects and experiment overview

Please refer to "Experiment protocol and subjects" in chapter 2 for general information. In this study, four adult male Long-Evans rats (4-6 months old) were food deprived and pre-trained to repeatedly traverse a linear track to obtain liquid reward at both ends in a room different from the recording room before implantation. Seven recording sessions of animals running on novel linear tracks that have never been experienced before were included in this study (track length, 165 cm not including the two ends; minimum of 14 laps per session). Of the seven recording sessions, two animals contributed more than one session by being introduced to other physically distinct novel linear tracks on different recording days. We also rearrange the distal cues in the recording room between different recording days. "Surgery and data acquisition" is as described in chapter 2.

3.2.2 Quantification methods for theta sequences

"Analysis of hippocampal theta rhythm" is as described in chapter 2. Theta sequences were quantified only when the animal was in the middle of the track (one-sixth to five-sixths of the track length), running faster than 10 cm/s, and when the durations of the corresponding theta cycles ranged from 100 to 200 ms. Four different quantification methods, either based on spikes, or based on reconstructed positions from the decoding algorithm (refer to "Position reconstruction from activity of hippocampal place cells" section in chapter 2; decoded window of 20 ms, moving every 5 ms) were used in this study. To construct the averaged theta sequence on each lap (Figure 2a, 3c, Figure 5a,c, Figure 7a), decoded probabilities over position during each theta cycle were aligned to the animal's current running position and direction before averaging. The mid-time point of theta sequences was defined as the theta phase where the center of the averaged theta sequence lies. To construct single-lap decoded theta sequence, single-lap directional place fields were calculated using spikes only from the current lap and the current running direction (each lap is composed of two traverses along the track in opposite directions) and then applied to the decoding algorithm that is described in chapter 2. The four quantification methods for theta sequences are as follows:

Method I: probability differences. Decoded probabilities ±50 cm around the animal's location, and ±¼ theta cycle around the mid-time point of the theta sequence, were divided equally into four quadrants. The region both physically and temporally behind the animal is represented as Quadrant II, while Quadrant IV represents the region physically and temporally ahead of the animal (Figure 2a, 3c, 5a,c, and Figure 7a, inset of

the subplot for lap 14). The summed decoded probabilities opposite with the animal's current running direction (Quadrants I and III) were subtracted from the summed decoded probabilities along the animal's current running direction (Quadrants II and IV), and then normalized by the summed decoded probabilities in all four quadrants. Positive differences would imply theta sequences sweeping in the running direction of the animal, whereas differences close to zero would indicate a lack of sequential structure in the decoded probabilities.

Method II: weighted correlation is as described in chapter 2. A distinct sequential structure sweeping along the animal's running direction would yield a large positive correlation, whereas a lack of sequential structure would produce a correlation close to zero.

Method III: theta sequence slope. The slope of each theta sequence was determined by the slope of a fitted line that yielded the maximum decoded probability in a 20 cm vicinity and within half a theta cycle centered by the mid-time point. To fit a line that best describes the series of position estimates during each theta cycle, I used a method similar to line finding in a 2-dimensional image, using a modified discrete approximation to the Radon transform (Toft, 1996; Davidson et al., 2009). The likelihood (R) that the decoded theta sequence (duration of n time bins) is along the fitted line with slope (V) and starting location (ρ) was calculated as the averaged decoded probability in a 20 cm vicinity along the fitted line as follows:

$$R(V,\rho) = \frac{1}{n}\sum_{k=0}^{n-1} P_r(|pos - (\rho + V \cdot k \cdot \Delta t)| \leq d)$$

Where Δt is the moving step of the decoding time window (5 ms), and the value of d was empirically set to 10 cm to fit theta sequences with small local variations in slope (for those time bins k when the fitted line would specify a location beyond the end of the track, the median probability of all possible locations is taken as the likelihood). To determine the most likely slope for each decoded theta sequence, I densely sampled the parameter space of V and ρ to find the values that maximize R. A larger slope would indicate a faster propagation speed of the sequence across participating neurons.

Method IV: spike train correlation. For each theta sequence, Pearson's linear correlation coefficient between spike timing and place cell peak firing positions was calculated for spikes emitted during 45-315 degree of individual theta cycle (referenced to global phase zero) and for cells whose peak firing positions were within 50 cm behind or in front of the animal's current position.

In order to produce error bars in Figure 4b, theta sequences on each lap were divided into five groups by the corresponding z-scored theta peak amplitudes, instantaneous theta frequencies, overall firing rate, or the animal's running speeds. Analysis controlling overall firing rate on each lap was conducted by randomly sampling spikes from each lap (Figure 3b, Figure 5a,b, Figure 6b,c, and Figure 7c). Analysis controlling the animal's running speed on each lap was conducted by matching theta sequences with the same animal's running speed in between laps (see Figure 5c,d).

3.2.3 Quantifications of individual neuronal phase precessions

Single-lap/trial phase precessions were examined in place fields that possessed peak firing rates no less than 5 Hz, peak firing positions in the middle of the track (one-fifth to four-fifths of the track length), field size (defined by 1 Hz firing rate boundary) more than two position bins and not including the end of the track. The definitions of center of mass, skewness and FRAI (see Figure 6d) were as previously described (Mehta et al., 2000). For group analysis, only stable place fields from cells emitting at least three spikes at no less than two different location bins on each lap were included. The phase-position correlation of spikes emitted by a place cell during a single traverse of its place field by the animal was determined by finding the optimal phase shift (P, referred as phase offset) that minimizes the negative Pearson's linear correlation ($corr$) between the animal's positions (pos) and shifted spike phases ($\emptyset + P$) as follows:

$$corr(\emptyset + P, pos) = \frac{cov(\emptyset + P, pos)}{\sigma_{\emptyset+P}\sigma_{pos}}$$

where $\emptyset$ is the original spike phase, cov is the covariance and σ is the standard deviation. Phase precession slope was calculated by least-square fit of spike locations of the animal and shifted spike phases. Phase range was defined as the phase difference between the spike with the highest shifted phase and the spike with the lowest shifted phase, rather than as the multiplication of phase precession slope and the size of the single-lap place field as previously has been defined (Schmidt et al., 2009). The latter method relies on the goodness of fit of the linear regression and, thus, can be imprecise or underestimate the real phase range when the spike phase and location are weakly or nonlinearly

correlated (e.g., bimodality of phase precession, Figure 6a, Cell 55 in Session 7) (Yamaguchi et al., 2002). The phase range of single-lap phase precession calculated through the latter method was indeed smaller (185 ± 1.64 degree, mean ± SEM) than through my method (see Results), and was close to half a theta cycle as Schmidt et al. (2009) previously reported. However, my phase range calculation is independent of the strength of phase precession thus was used throughout the study; although the method in Schmidt et al. (2009) did not change my main results. Polar plots of phase offset distributions were generated with $\pi/6$ bin size. The shuffled data were produced by independently replacing the phase of each emitted spike by a random phase for 5000 times (Figure 6b, top). The resultant vector length in Figure 7c was calculated as the magnitude of the resultant vector of single-lap phase offsets from all the stable place fields that included in the group analysis. I also quantified the resultant vector length of phase offset of all the pairs of place fields that were recorded on the same recording tetrode, or between different tetrodes (Figure 7d, left). Theta phase deviation was defined as the phase difference between global phase zero and the trough of theta oscillation of individual LFP. The calculation of spike modulation depth was as previously described (Carr et al., 2012). Circular statistics were performed using CircStat MATLAB Toolbox (Berens, 2009).

3.3 Results

In all of the seven recording sessions, we simultaneously recorded large numbers of hippocampal place cells that were active when animals ran laps on novel linear tracks

(78 ± 6.5 active place cells per session; mean ± SEM). Both recorded LFP and neuronal spiking activities demonstrated strong theta modulation during exploration (Figure 1a, b). Individual place cells emitted spikes in advancing theta phases as the animal ran across their place fields (single-lap phase precession: Figure 1a, magenta and green). Ordering place cells by their peak firing positions along the track revealed repetitive sequential spiking activities across the population of neurons that were phase-locked to each theta cycle (theta sequences: Figure 1a, middle). Decoded probabilities of the animal's position estimated from pyramidal cell activities (Davidson et al., 2009) revealed more distinct sequential structures of theta sequences (Figure 1a, bottom) which start and end on the descending phase of theta-modulated spike density oscillation (on average 80 degrees in reference to spike density peak; Figure 1b). Decoded errors were also modulated by theta oscillations, with minimum error near the center of theta sequences (Figure 1b, middle).

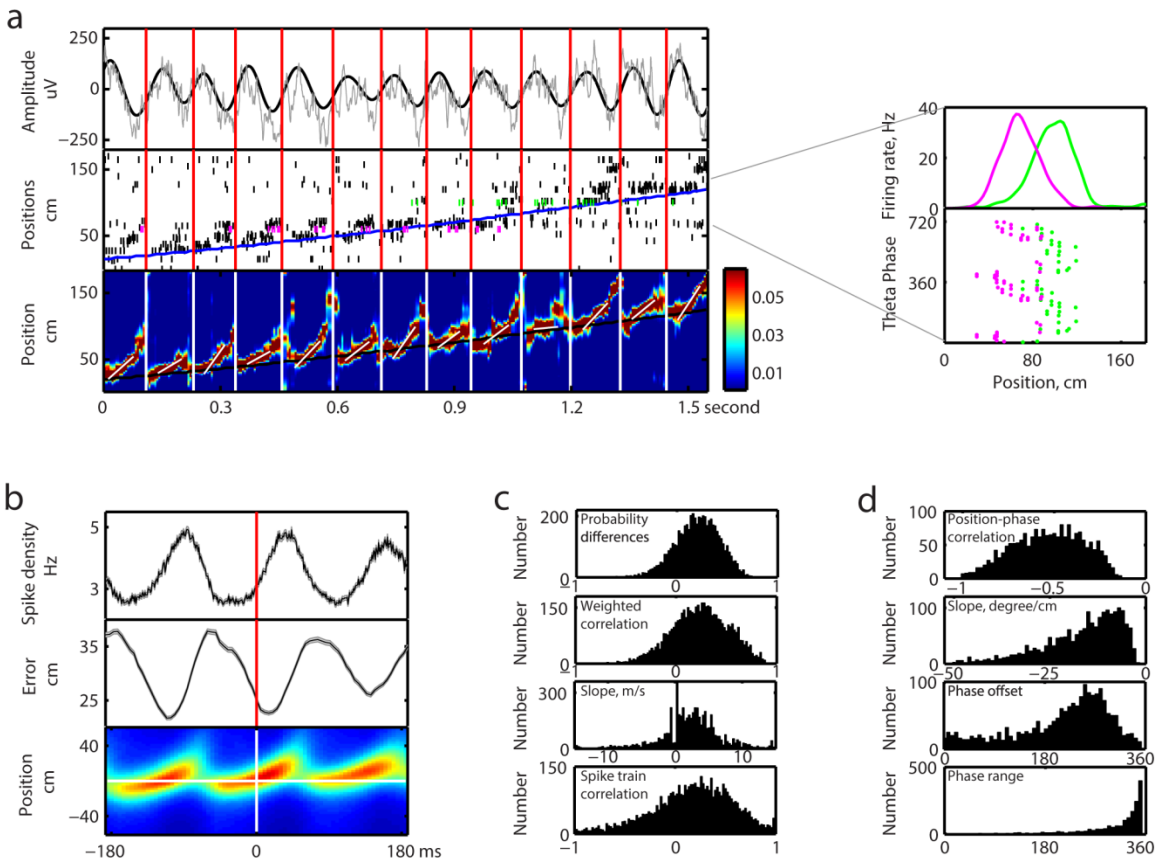

Figure 1. Individual theta sequences and single-lap phase precession.

a) Left, Concurrent LFP (top panel, raw LFP in gray, 4-12 Hz band-pass filtered theta rhythm in black), spikes from 107 CA1 pyramidal cells ordered by place cells' peak firing positions along the track (middle, black bars; magenta and green represent the spikes from the cells in right panel), and theta sequences constructed from raw spikes (bottom, probability estimates were color scaled) during 1.55 s of the animal's running. Overlay white line indicates the speed of each theta sequence. The running trajectory of the animal was indicated as overlay blue (middle) or black line (bottom). The beginning and end of theta sequences were indicated as white (bottom) or red bars (other panels). Right, Examples of single-lap phase precession. Top, two overlapping place fields.

Bottom, phase-position relationship of emitted spikes during the running lap shown in the left panel. **b)** Spike density of neuronal population (top), decoded errors (middle), and theta sequences (bottom) were theta modulated. **c)** Histogram of theta sequence strength measured by probability differences (first panel), weighted correlation (second panel), slope (third panel), and spike train correlation (fourth panel). **d)** Histogram of phase-position correlation (first panel), slope (second panel), phase offset (third panel), and phase range (fourth panel) of single-lap phase precession.

3.3.1 Individual theta sequences and single-lap phase precession

In order to compare theta sequence strength on each lap accurately, I used four distinct methods, based on decoded probabilities or spike trains to quantify individual theta sequences during 5513 theta cycles. Consistent with previous reports (Dragoi and Buzsaki, 2006; Foster and Wilson, 2007; Davidson et al., 2009), the majority of theta sequences demonstrated stronger decoded probabilities along the animal's current running direction than the opposite direction (normalized probability differences: 0.22 ± 0.00, median ± SEM; Figure 1c, first panel), positive weighted correlations between decoded position and time (0.26 ± 0.00; median ± SEM; Figure 1c, second panel), positive slopes (2.50 ± 0.06, median ± SEM; Figure 1c, third panel), and positive correlations between spike timing and place cell peak firing positions (0.21 ± 0.01; median ± SEM; Figure 1c, fourth panel), all with $p < 10^{-10}$ from Wilcoxon signed rank test .

I also quantified single-lap phase precessions in place cells that had stable place fields throughout the recording session. Consistent with previous reports (Schmidt et al., 2009), the majority of 1946 single-lap phase precessions demonstrated negative correlations between spike location and spike phase (-0.52 ± 0.00; mean ± SEM Figure 1d, first panel), negative slopes (-19.22 ± 0.67; mean ± SEM; Figure 1d, second panel), phase offsets around 259 degrees (mean; 1.44, SEM; Figure 1d, third panel), and phase ranges around 330 degrees (median; 0.99, SEM; Figure 1d, fourth panel; see Methods). Given our ability to measure both theta sequences and theta phase precession, I next

asked whether either or both varied as a function of experience on a lap-by-lap basis after exposure to a novel environment.

3.3.2 Theta sequence structure emerged rapidly after experience on a novel track

To examine the development of theta sequences, I centered the decoded position estimates by the animal's current running location and the mid-time point of theta sequence at each theta cycle and averaged the resulting sequences. I observed no clear sequential structure when the animal was running on the first lap across the novel track (Figure 2a, first subplot, average of decoding during 440 theta cycles). However, by the second lap on the track, distinct theta sequences emerged in the decoded positions. These sequences swept forward along the animal's running direction and persisted across subsequent laps once established (Figure 2a, second to 14th subplot).

All four quantification methods for theta sequences demonstrated significant positive correlations between theta sequence strength and the number of running experiences (Figure 2b; Pearson's linear correlation coefficient $r=0.13$, $p<10^{-10}$, probability differences, first panel; $r=0.11$, $p<10^{-10}$, weighted correlation, second panel; $r=0.07$, $p=2.02*10^{-7}$, slope, third panel; $r=0.06$, $p=3.83*10^{-5}$, spike train correlation, fourth panel). Theta sequence strength increased dramatically between the first lap and following laps, resembling a negative acceleration curve. There was a significant difference in theta sequence strength between running laps (Figure 2b; Kruskal-Wallis test: $H_{(13)}=236.08$, $p<10^{-10}$, probability differences, first panel; $H_{(13)}=215.77$, $p<10^{-10}$, weighted correlation, second panel; $H_{(13)}=52.61$, $p=1.06*10^{-6}$, slope, third panel;

$H_{(13)}$=54.4, p=5.16*10^{-7}, spike train correlation, fourth panel), and the significance of the effect was mainly due to a near-zero theta sequence strength on the first lap indicated by *post hoc* multiple comparison with Scheffé correction (the first lap was included in all pairs of laps that were significantly different under all four quantification methods, with a single exception of probability difference between lap 2 and lap 8). I further verified the absence of clear sequential structure on the first lap in individual recording sessions, and the rapid development of theta sequences was universal across all the animals and recording sessions (Kruskal-Wallis test of probability differences measurement: p=1.62*10^{-8}, session 1; p=2.59*10^{-7}, session 2; p=7.68*10^{-4}, session 3; p=2.10*10^{-6}, session 4; p=2.59*10^{-9}, session 5; p<10^{-10}, session 6; p=9.61*10^{-5}, session 7). *Post hoc* multiple comparison with Scheffé correction indicated that, in all individual sessions, the first lap was included in all pairs of laps that were significantly different. These results suggest that the formation of theta sequences can be rapidly achieved by single-trial experience.

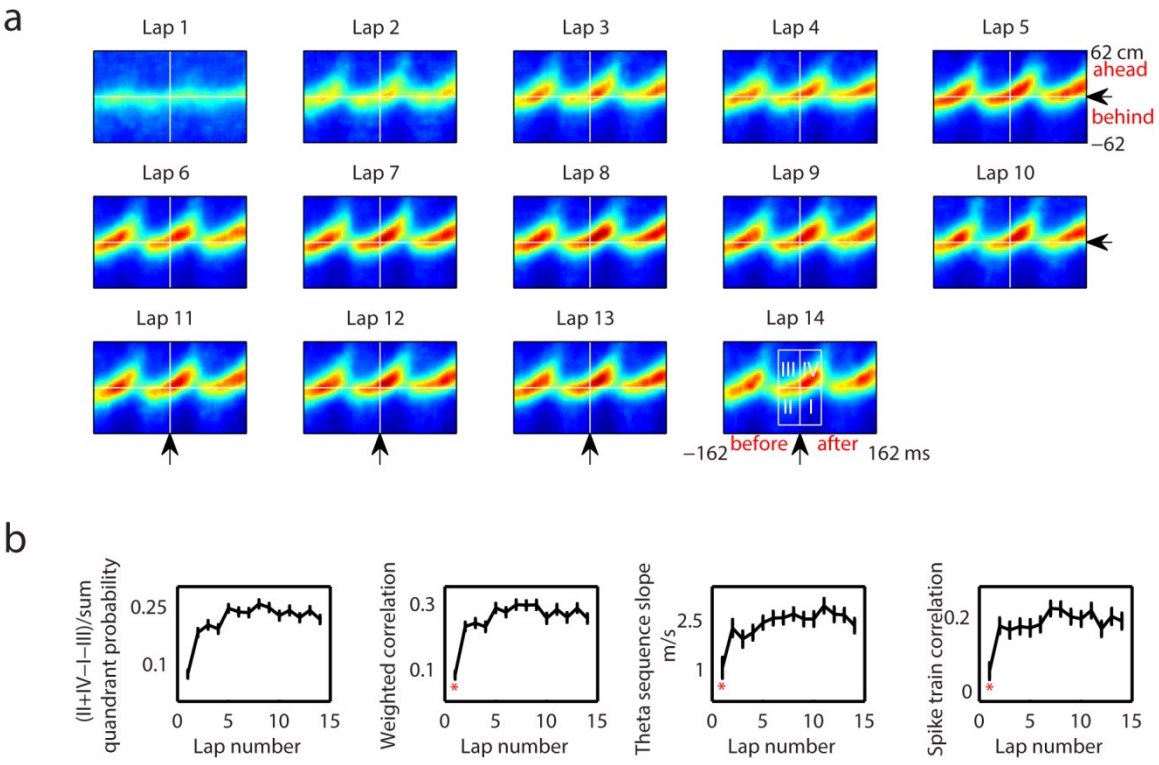

Figure 2. Theta sequence structure emerged immediately after the first experience on novel track using whole session decoding.

a) Averaged decoded probabilities over 125 cm centered by the animal's current running position, aligned by the animal's current running direction during 325 ms centered by the mid-time point of theta sequence for each lap. Color scale is the same as in Figure 1a. **b)** Theta sequence strength changed significantly between the first lap and the following laps. First panel, Probability of (II+IV-I-III)/(I+II+III+IV) Quadrant in a 100 cm and ½ theta cycle window centered by the animal's current running position and the mid-time point of theta sequence on different laps. Second panel, Weighted correlations between time and decoded positions across laps. Third panel, Theta sequence slopes across laps.

Fourth panel, Spike train correlations across laps. *lap that was included in all significant pairs of laps at 0.05 level.

3.3.2.1 The rapid development of theta sequences was not due to place field instability

Previous literature has reported that the ensemble code of hippocampal neural firing upon entering a novel environment is initially less robust and takes minutes to stabilize (Wilson and McNaughton, 1993), which raises a problem for the decoding algorithm I have used because the lack of sequential structure in the decoded probabilities during the first lap could simply result from the utilization of an inaccurate ensemble code based on spikes from the whole recording session ("whole session decoding"). I therefore implemented a second decoding algorithm using place fields calculated only from spikes that occurred during the lap being decoded ("single-lap decoding") to obtain a more faithful representation of theta sequences on each lap.

I tested the accuracy of single-lap decoding on the short sequence-decoding timescale (20 ms), which is different from the behavioral timescale (approximately seconds) over which place fields were generated, so that accuracy was not a trivial consequence of data overfitting. Indeed, single-lap decoding largely increased the accuracy of position estimation, especially on the first lap (Figure 3a,b). When comparing the decoded probabilities for the animal's current position, single-lap decoding (Figure 3b, blue) yielded a significantly higher probability ($p<10^{-10}$, Wilcoxon rank sum test) than whole session decoding (Figure 3b, black), and largely decreased the variability of decoded probabilities between laps (sum of squares of between-laps variability: $7.85*10^{11}$ versus $3.42*10^{12}$, single-lap versus whole session decoding). This variability

can be further decreased by controlling overall firing rate between different laps (Figure 3b, green; sum of squares of between-laps variability: $5.05*10^{11}$).

The rapid development of theta sequences after the first lap was preserved when reconstructing theta sequences using single-lap decoding (Figure 3c). More importantly, the decoded probabilities concentrated at the animal's current location on the first lap, suggesting a complete lack of sequential structure that was not due to an inaccurate representation of space from place cell activities. When quantifying the strength of theta sequences under single-lap decoding, all three methods based on decoding demonstrated a negative acceleration curve of theta sequence strength with the number of running laps, with near-zero theta sequence strength only on the first lap (Figure 3d, first to third panel). Spike train correlation between spike timing and place cell peak firing positions defined by single-lap place fields increased dramatically after the second lap (Figure 3d, fourth panel). There were statistically significant differences of theta sequence strength between different laps under all four methods (Kruskal-Wallis test: $H_{(13)}=169.93$, $p<10^{-10}$ for probability differences, Figure 3d, first panel; $H_{(13)}=160.39$, $p<10^{-10}$ for weighted correlation, Figure 3d, second panel; $H_{(13)=}75.95$, $p<10^{-10}$ for theta sequence slope, Figure 3d, third panel; $H_{(13)}=84.51$, $p<10^{-10}$ for spike train correlation, Figure 3d, fourth panel). *Post hoc* multiple comparisons with Scheffé correction indicated the first lap as the source of significant difference under the first three measurements of theta sequence strength, whereas the spike train correlation of both the first and second lap were significantly different with some of the later laps. The utilization of single-lap decoding suggested that the rapid development of theta sequences was not due to place field

instability (Wilson and McNaughton, 1993); further, because this decoding algorithm is based on single-lap unidirectional place fields that were calculated using spikes only from the current lap and the current running direction (see Methods), the decoded results should be unaffected by progressive changes in place field directionality (Frank et al., 2004). Also, when the data were divided by animals' running directions, clear sequential structure was absent on the first lap in both directions (probability differences measurement of theta sequence strength for one running direction: 0.04 ± 0.01 versus 0.15 ± 0.00, mean ± SEM of the first lap versus all the following laps combined; for the other running direction: 0.06 ± 0.02 versus 0.20 ± 0.00). Because single-lap decoding was more accurate and less variable than whole session decoding, I continued to use single-lap decoding in all the following analyses.

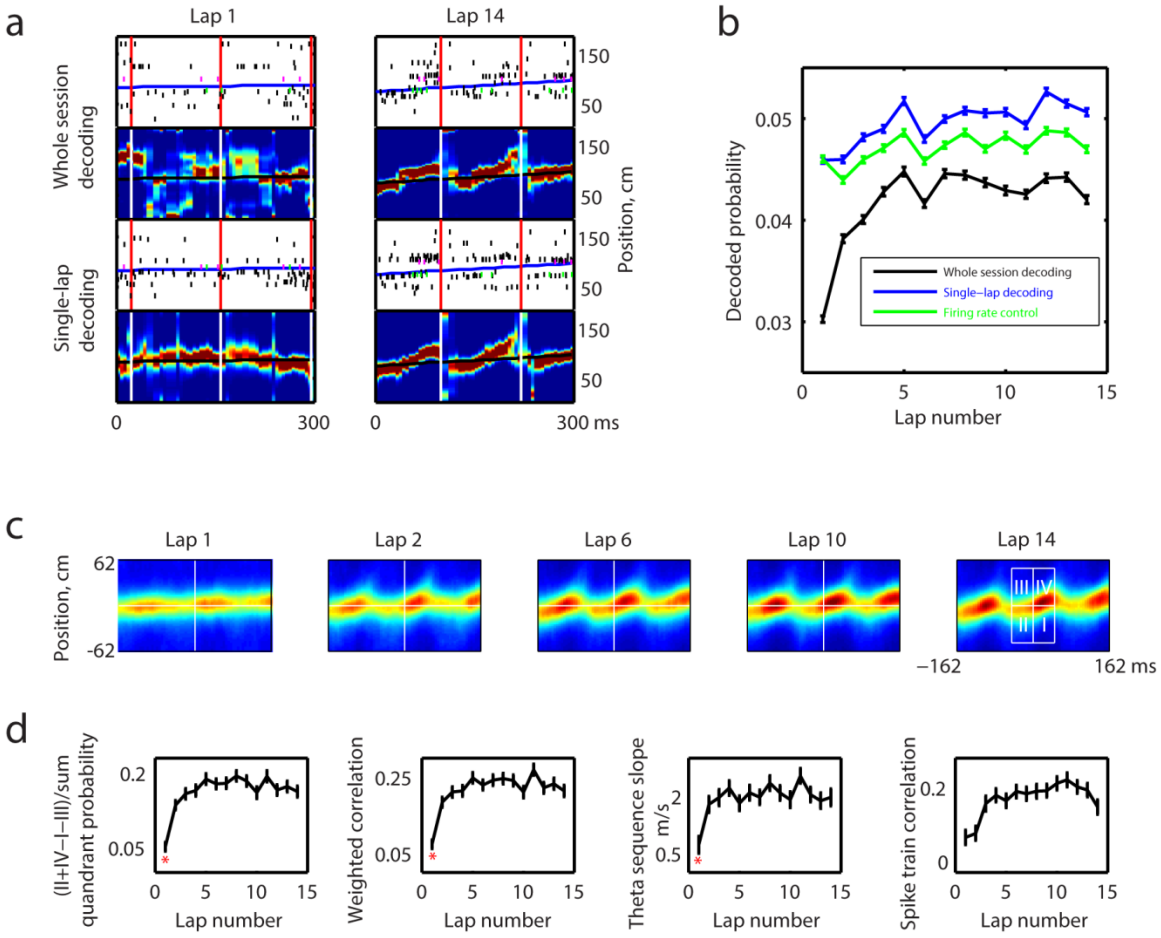

Figure 3. Single-lap decoding was more accurate than whole session decoding and preserved the rapid development of theta sequences.

a) Examples of 300 ms spike train (black bars) and decoding using whole session decoding and single-lap decoding in Lap 1 and Lap 14. The spikes were ordered, respectively, by cells' peak firing position in whole session place field or single-lap place field. Blue line in spike train and black line in decoding indicate the animal's current running location. The beginning and end of theta sequences were indicated as white (in decoding) or red bars (in spike train). Magenta and green bars represent spikes from two cells. Color scale is the same as in Figure 1a. **b)** Averaged decoded probabilities (decoded

window of 20 ms moving with 5 ms step) on the animal's current running locations between different laps. Black represents whole session decoding. Blue represents single-lap decoding. Green represents firing rate controlled data. **c-d)** Same as in Figure 2 using single-lap decoding. * and color scale as in Figure 2.

3.3.2.2 The rapid development of theta sequences was not due to other novelty-based changes in intrinsic hippocampal function or in behavior

Being exposed to a novel environment not only alters place field stability but also several other aspects of hippocampal function and behavior. Changes include decreases in theta frequency (Jeewajee et al., 2008b), increases in theta power (Penley et al., 2013), a suppression of interneuron activities (Wilson and McNaughton, 1993; Frank et al., 2004; Nitz and McNaughton, 2004), an elevation of pyramidal cell activities (Nitz and McNaughton, 2004) and a decrease in exploration speed (Mehta et al., 2002; Frank et al., 2004; Jeewajee et al., 2008b; Penley et al., 2013). Further, these changes co-vary, so that part of the variability in theta rhythm and neuronal activities can be explained by variation in exploration speed (Vanderwolf, 1969; Whishaw and Vanderwolf, 1973; McNaughton et al., 1983; Slawinska and Kasicki, 1998). In our recordings, the running speed of the animals increased in later laps as expected (Pearson's linear correlation coefficient $r=0.07$, $p=1.40*10^{-7}$; Figure 4a, fourth panel), co-occurring with an increased place cell overall firing rate (Pearson's linear correlation coefficient $r=0.04$, $p=9.57*10^{-4}$; Figure 4a, third panel), an increased instantaneous theta frequency (Pearson's linear correlation coefficient $r=0.09$, $p<10^{-10}$; Figure 4a, second panel) and a decreased normalized theta peak amplitude (Pearson's linear correlation coefficient $r=-0.07$, $p=2.94*10^{-8}$; Figure 4a, first panel). To examine whether the observed decrease in theta sequence strength on the first lap can be explained by novelty-based changes in intrinsic hippocampal function or the animal's speed of locomotion (Maurer et al., 2012), I correlated theta sequence strength with peak theta amplitude (Figure 4b, first column), instantaneous theta frequency (Figure 4b, second column), place cell firing rate (Figure

4b, third column), or animal's running speed (Figure 4b, fourth column). Under all four quantification methods, theta sequence strength in the laps after the first (Figure 4b, black line) correlated significantly with theta peak amplitude, theta frequency (with the exception of two methods), place cell firing rate (with the exception of one method), and the animal's running speed; yet no significant correlation was detected between theta sequence strength on the first lap with any of the variables (Figure 4b, gray line). Further, the specific theta amplitudes, theta frequencies, place cell firing rates, and exploration speeds associated with the strongest theta sequences during later laps were associated with little indication of theta sequence structure during the first lap. I also randomly subsampled the spikes on each lap to control for the variability of overall firing rates between laps (Figure 5a, b). Firing rate controlled results preserved the observation of theta sequence development, indicating that the novelty-based change in overall firing rate was not sufficient to account for the progressive change observed in theta sequence structure. I further verified the results by subsampling theta cycles on subsequent laps to match the same speed profile as on the first lap (Figure 5c, d). The above data suggest that the rapid emergence of theta sequence structure after the first lap cannot be explained by lap-by-lap variability of neural activities, such as theta rhythm, firing rate and the animal's running speed.

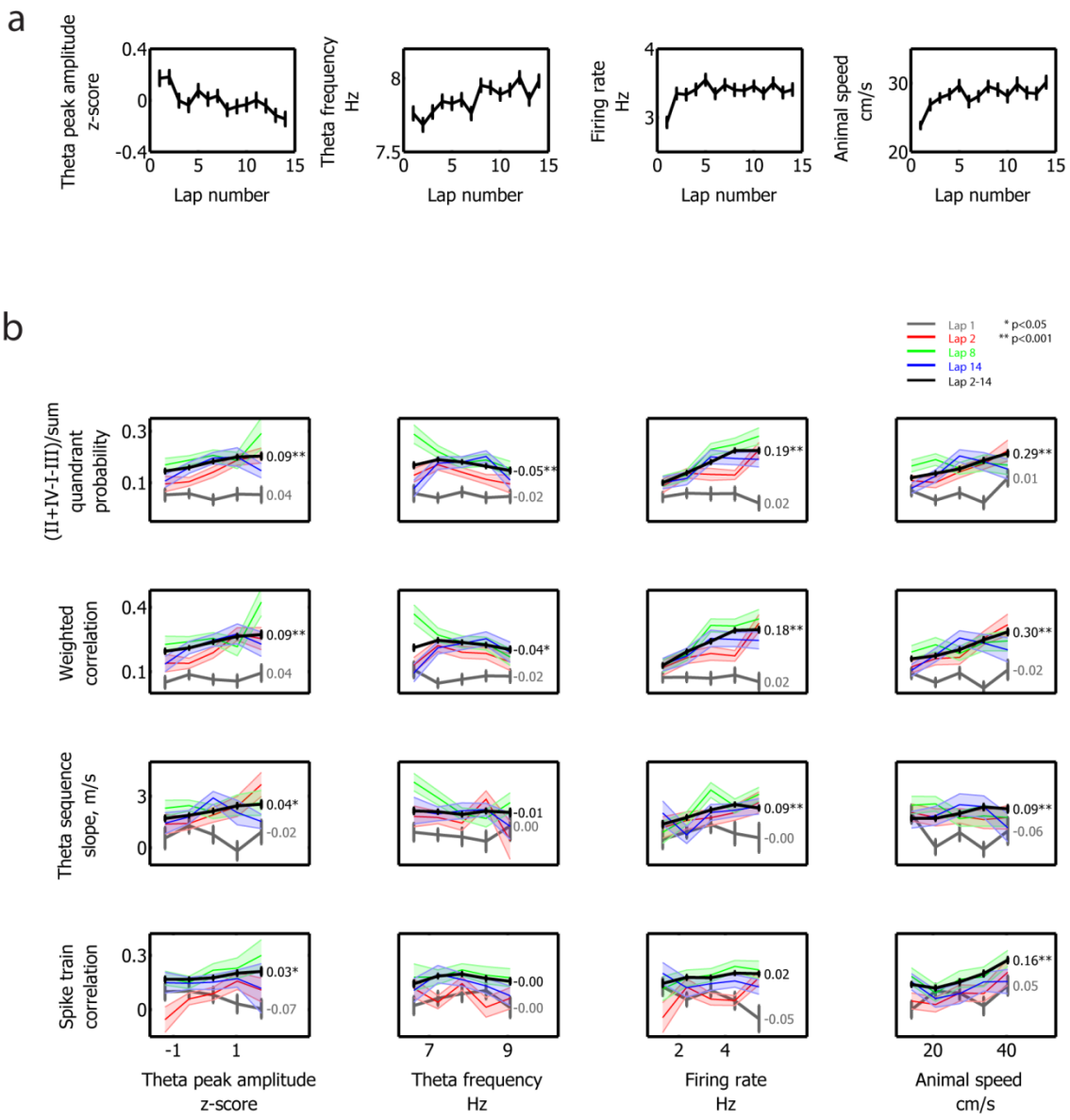

Figure 4. The variability of theta peak amplitude, theta instantaneous frequency, overall firing rate, and the animal's running speed between laps was not sufficient to account for the emergence of theta sequence structure after the first lap.

a) Lap-by-lap changes of z-scored theta peak amplitude (first panel), instantaneous theta frequency (second panel), place cell overall firing rates (third panel), and the animal's

running speed (fourth panel). **b)** Relationship between the above variables (four columns) and theta sequence strength under four different quantification methods (rows). Gray represents lap 1. Red represents lap 2. Green represents lap 8. Blue represents lap 14. Black represents lap 2-14. Shaded area and error bar indicate SEM. Text represents correlation value. *$p<0.05$. **$p<0.001$.

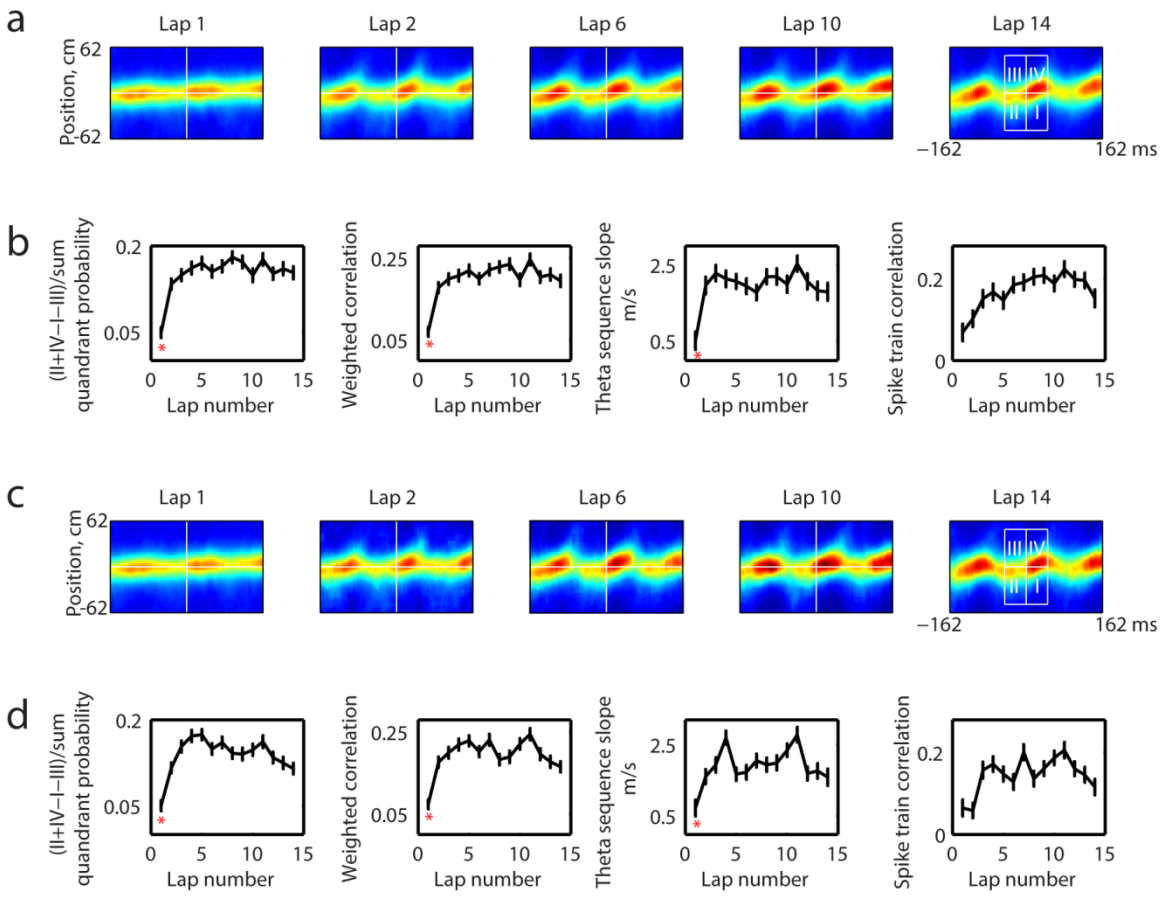

Figure 5. Control of place cell firing rate and the animal's running speed for the development of theta sequences.

a-b) Same as in Figure 2, firing rate control. **c-d)** Same as in Figure 2, data controlling for the animal's running speed. * and color scale as in Figure 2.

3.3.3 Individual place fields demonstrated strong phase precession on the first experience on a novel track

Several models of theta sequences propose that the sequential firing patterns emerge as a natural consequence of phase precession within individual place cells (Skaggs et al., 1996); thus I asked whether phase precession was also absent on the first lap of a novel track. In contrast to previous studies (Okeefe and Recce, 1993; Skaggs et al., 1996; Huxter et al., 2003; Dragoi and Buzsaki, 2006), where phase precession was quantified using spikes pooled across multiple traversals (Figure 6a, top), I examined phase precession on a lap-by-lap basis, to provide a better representation of temporally structured events (Schmidt et al., 2009). Individual place fields, despite a wide variability in single-lap firing rates and place field sizes, demonstrated strong phase precession during the first lap on the novel track (Figure 6a, bottom). The speed of the phase advancement varied between place cells (Figure 6a, blue line/text) and was dependent on both the phase range of the spikes and the size of place fields (Huxter et al., 2003). Of 139 stable place fields, 59 showed strong phase precession with phase-position correlation < -0.5 on the first lap, which was significantly greater than predicted by chance (Monte-Carlo $p<2.00*10^{-4}$, see Methods; Figure 6b, top). The phase-position correlation remained strong for the following laps (mean r = -0.48) and, strikingly, was constant between lap 1 and subsequent laps (Kruskal-Wallis test: $H_{(13)}=16.48$, p=0.22, Figure 6b, bottom, black). Thus phase precession appeared to be a pre-existing property of hippocampal place cells. Examining further the properties of single-lap phase precession, no significant difference between laps was observed in its slope (Kruskal-Wallis test: $H_{(13)}=9.18$, p=0.76; Figure 6c, first panel, black) or phase range (circular

Kruskal-Wallis test, p=0.48; Figure 6c, third panel, black), although there may have been a trend in phase offset (circular Kruskal-Wallis test, $p=9.36*10^{-2}$; Figure 6c, second panel, black). Similar to place cell overall firing rate (Figure 4a, third panel), the in-field firing rate for the group of 139 stable place fields also increased with running experiences (Pearson's linear correlation coefficient between mean in-field firing rate and running laps: r=0.09, $p=6.09*10^{-5}$; between peak in-field firing rate and running laps: r=0.10, $p=5.46*10^{-6}$; Figure 6c, fourth panel.); I therefore implemented the same firing rate control as in theta sequence quantifications for phase precession (see Methods). Firing rate controlled results revealed no significant difference across laps for phase-position correlation (Kruskal-Wallis test: $H_{(13)}=22.24$, $p=5.18*10^{-2}$; Figure 6b, bottom panel, gray), phase precession slope (Kruskal-Wallis test: $H_{(13)}=7.79$, p=0.86; Figure 6c, first panel, gray) or phase range (circular Kruskal-Wallis test, $p=6.93*10^{-2}$; Figure 6c, third panel, gray). However, under firing rate control, a significant difference across laps was observed in phase offset (circular Kruskal-Wallis test, $p=3.46*10^{-2}$; Figure 6c, second panel, gray), which will be further examined in the next section. Taken together, these data indicate that the observed absence of theta sequences on the first lap of a novel track cannot be explained by a similar lack of phase precession within individual neurons, suggesting instead a circuit-level explanation.

A previous study has reported single-lap phase precession becomes stronger (Mehta et al., 2002) as a result of asymmetric place field expansion with increased experience. I also observed a significant shift of place filed location to the direction that the animal is running from (Figure 6d, first panel; Pearson's linear correlation coefficient,

one-tailed, r=-0.09, $p=5.05*10^{-5}$), yet I failed to replicate the increase of place field size (Figure 6d, second panel; Pearson's linear correlation coefficient, one-tailed, r=-0.02, p=0.86), and the development of asymmetric place fields with experience (Figure 6d, third panel, skewness: Pearson's linear correlation coefficient, one-tailed, r=0.07, p=0.99; Figure 6d, fourth panel, FRAI, r=0.08, p=0.99). Similar conflicting results have been reported by other groups (Huxter et al., 2003; Lee et al., 2004; Schmidt et al., 2009). However, these studies, like ours, defined place field boundaries through firing rate thresholds, which might affect the precision of measurements of place field shape such as skewness if a portion of the place field tail was excluded by the boundaries. Nonetheless, my results demonstrated strong individual neuronal phase precessions throughout the recording session, whose strength were not affected by the progressive change of place field locations.

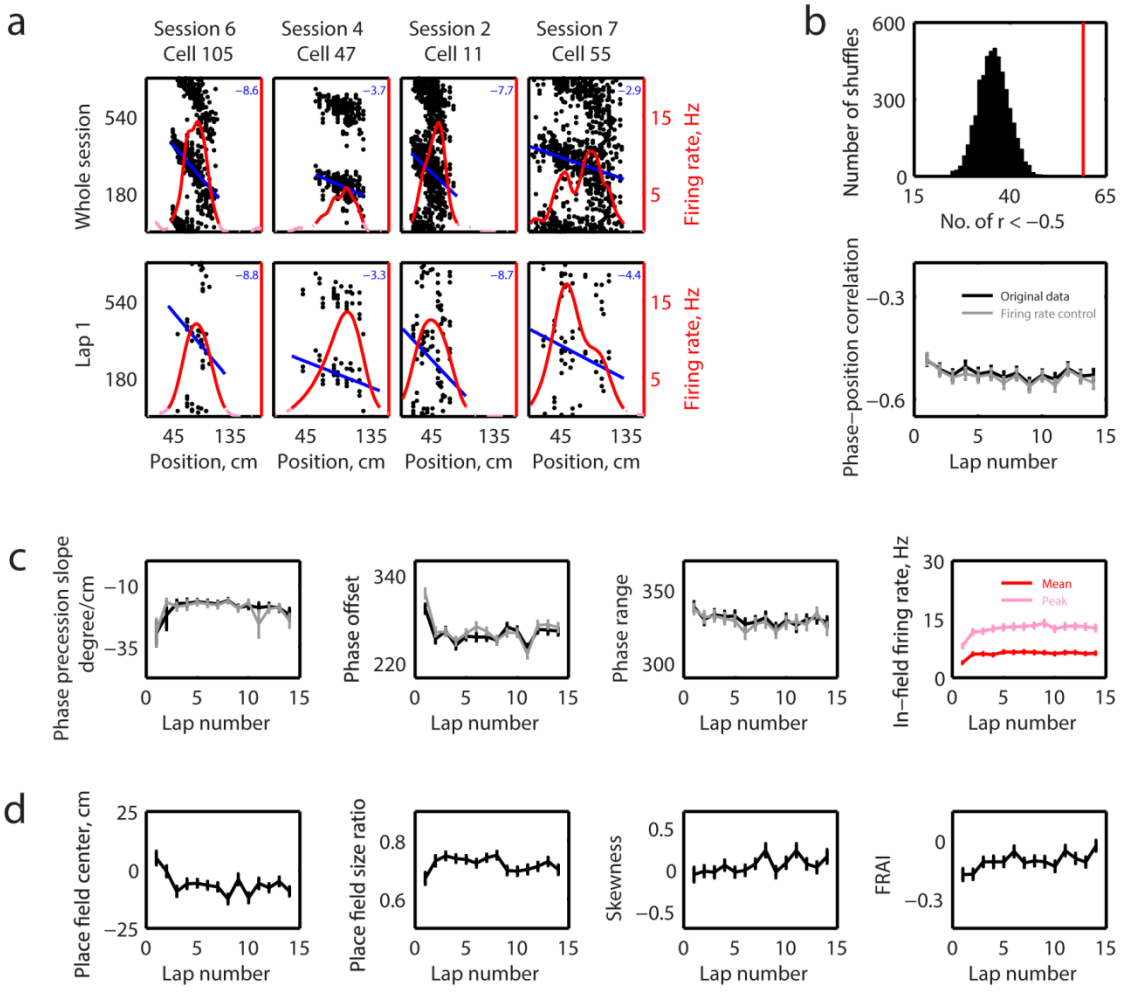

Figure 6. Individual place field demonstrated strong phase precession on the first experience on a novel track.

a) Phase precession from four different place cells. Each spike has been plotted out twice on the corresponding theta phase and the phase plus 360 degrees for visualization purpose. Top, spikes from the whole session; bottom, spikes during the first lap; only spikes within the boundary of whole session place field or single-lap place field are shown. Red solid line indicates firing rate > 1 Hz. Red dashed line indicates firing rate < 1 Hz. Blue line indicates fitted line of phases with positions. Text on the upper right

corner indicates the fitted slope. **b)** Top, Distribution of number of strong phase precessions (r<-0.5) from 5000 shuffles of 139 stable place fields. 59 place fields on the first lap demonstrated strong phase precession (red line). Bottom, Pearson's linear correlations between animal's running positions and shifted theta phases of emitted spikes across laps. Black represents original data. Gray represents firing rate control. **c)** Phase precession slope (first panel), phase offset (second panel), phase range (third panel), in-field mean (red) and peak (pink) firing rate (fourth panel) of 139 stable place fields across laps. **d)** Place field center of mass shift (first panel), ratio of size change (second panel), skewness (third panel) and FRAI (fourth panel) across laps in reference to the whole session place field.

3.3.4 The phase offset of phase precession became more synchronized among individual neurons after the first experience on novel track

Having demonstrated that the presence of phase precession does not necessarily result in population-level theta sequences, I next addressed the neural mechanism underlying this apparent dissociation between the two phenomena. Firstly I verified that the absence of theta sequences on the first lap was not driven by a portion of place fields possessing weak phase precession on the first lap. Previously, I demonstrated that the average strength of phase precession was constant across laps (Figure 6b, bottom). I further reconstructed theta sequences using only the subset of place fields that possessed strong phase precession (phase-position correlation $r<-0.5$) on the first lap; also, to be consistent with the firing rate criterion of examining single-lap phase precession, I excluded place fields with peak firing rates <5 Hz in this analysis. The reconstruction based on the subset of place fields again revealed no clear sequential structure on the first lap, yet theta sequence strength immediately after the first lap was largely unaffected (Figure 7a,b). This control analysis indicates that weak single-lap phase precession does not explain the observed absence of theta sequences on the first lap, further suggesting instead a circuit-level explanation for the dissociation between phase precession and theta sequences. An example of this dissociation can be seen in Figure 3a, where the spikes from two place cells (magenta and green) independently precess through three consecutive theta cycles during both the first and the fourteenth traverse of the same environment by the animal, yet the overall temporal relationship between the two neurons changes on different trials.

One explanation that accounts for the absence of theta sequences on the first lap despite the presence of phase precession is that while each individual neuron undergoes phase precession, each place cell initially precesses through a different phase range of the theta cycle, leading to a lack of structured sequence. Experience-dependent changes in hippocampal circuitry may subsequently serve to coordinate place cells, aligning them to the same phase offset to produce coherent theta sequences. Consistent with this hypothesis, I observed that the phase offset on the first lap was widely distributed and not significantly different from a uniform distribution (Figure 7c, first polar plot, $p=0.14$, Rayleigh test for circular uniformity), whereas on subsequent laps, the phase offset distribution was more concentrated and significantly different from a uniform distribution (Figure 7c, second to fifth polar plot, $p<6.07*10^{-8}$ for lap 2 to lap 14, circular uniformity test). The length of the resultant vector of phase offsets after the first experience was more than three times larger than that of the first lap (Figure 7c, red), indicating a larger variability of phase offset on the first lap. I obtained similar results when controlling for firing rate variance between different laps (Figure 7c, green), and also when I restricted my analysis only to place fields that demonstrated strong phase precession on each lap (Figure 7c, black). I next examined whether there was larger phase offset variability for cells recorded from different recording sites than for those from the same recording site. Within-sites place field pairs demonstrated significantly smaller phase offset variability in single-lap phase precession than between sites place field pairs (resultant vector length of single-lap phase offset of place field pairs, mean ± SEM: 0.78 ± 0.00 versus 0.71 ± 0.00, within-sites versus between sites; $p<10^{-10}$, Wilcoxon rank sum test; Figure 7d, left). Further, the decrease of single-lap phase offset variability with experience was more

predominant for between-sites than within-sites pairs (Pearson's linear correlation coefficient: within-sites, $r=0.027$, $p=1.94*10^{-2}$; between sites, $r=0.031$, $p=2.78*10^{-10}$). The decrease of phase offset variability among place fields could not be explained by either the theta phase deviation among different recording sites, as has been previously reported (Lubenov and Siapas, 2009; Patel et al., 2012), or by the spike modulation depth (Carr et al., 2012) by theta oscillation. No progressive changes of theta phase deviation (Figure 7d, middle, black line; circular Kruskal-Wallis test, $p=0.71$) or its variability (Figure 7d, middle, red line; Pearson's linear correlation coefficient $r=-0.16$, $p=0.58$) were observed, and the spiking of cells with stable place fields was theta-modulated to a similar extent throughout experience (Figure 7d, right; Pearson's linear correlation coefficient $r=-0.15$, $p=0.60$). Together, these data suggest that, upon exposure to a novel environment, individual neurons initially exhibit distinct phase offsets that rapidly become synchronized through early experience (Figure 8). Further, this rapid synchronization may involve macroscopic coordination of neural activity between different regions of the hippocampus.

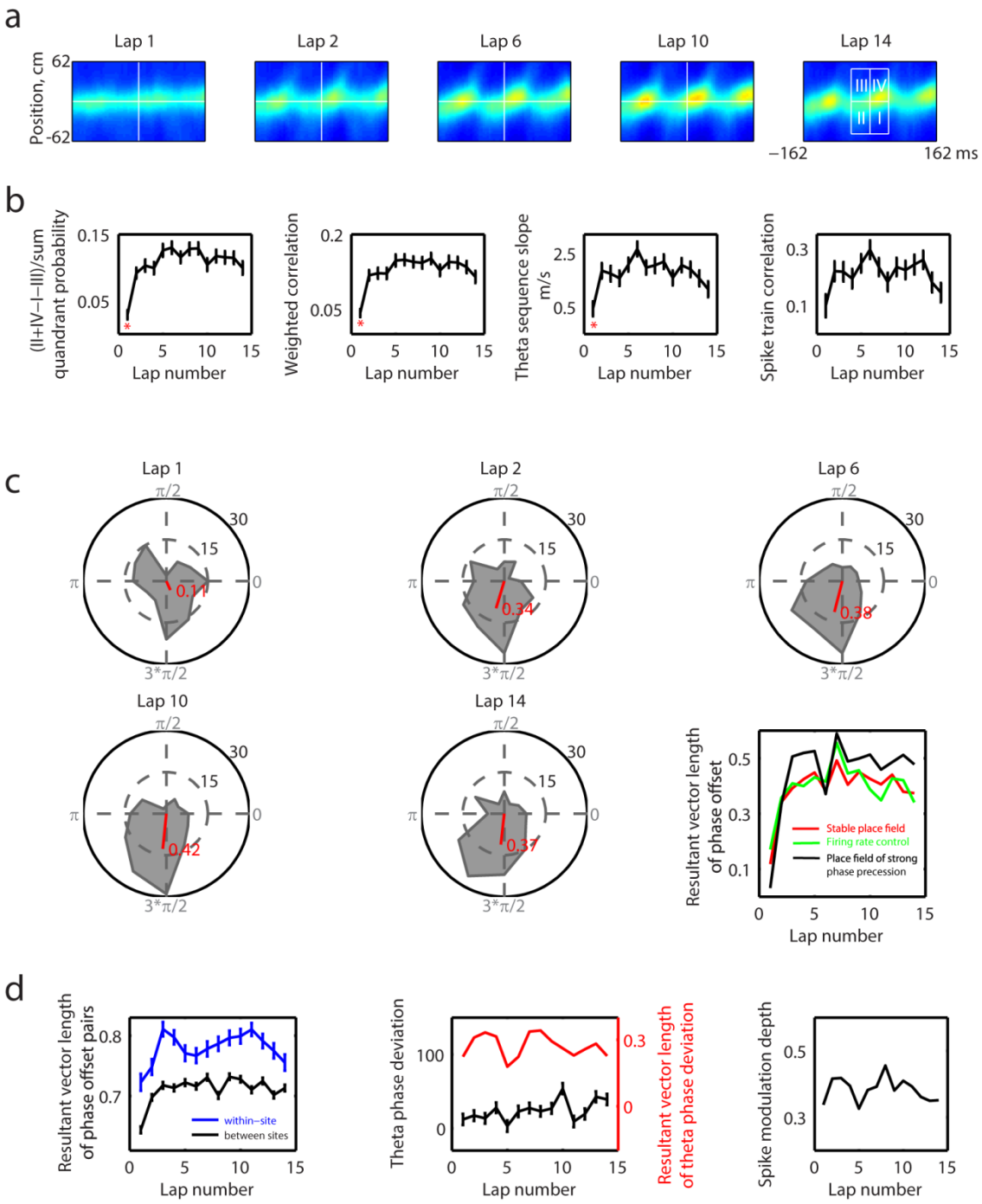

Figure 7. The phase offset of phase precession became more synchronized among individual neurons after the first experience on novel track.

a-b) Reconstructed theta sequences using the subset of place cells that possessed strong first-lap phase precession preserved the rapid development of theta sequences. Plots are the same as in Figure 2, 3 and 5. **c)** Phase offset distribution of 139 place fields in lap 1 (first row, left), lap 2 (first row, middle), lap 6 (first row, right), lap 10 (second row, left) and lap 14 (second row, middle). Gray represents angles. Black represents scales of histogram. Red represents resultant vectors. Right (second row), Resultant vector length of phase offset of 139 stable place fields between different laps (red); firing rate control (green); place fields with strong phase precession (black). **d)** Left, Resultant vector length of phase offset of 531 place field pairs within recording sites (blue) and 2870 place field pairs between recording sites (black). Middle, Theta phase deviation from 89 recording sites (black) and the resultant vector length of the phase deviations (red) across laps. Right, spike modulation depth of cells with stable place fields by theta oscillation. * and color scale as in Figure 2.

3.4 Discussion

I have demonstrated that ensemble-level theta sequences develop rapidly with experience, in contrast to individual neuronal phase precession that occurs without prior experience in the current environment. A previous study has reported that single-lap phase precession becomes stronger with increased experience (Mehta et al., 2002). However, their study used the same phase offset to quantify phase-position correlation for all laps, which according to our data, would produce a weak correlation for the first lap because the phase offset among individual neurons was most widely distributed on the first lap compared with other laps (Figure 7c). Here I quantified phase-position correlation lap-by-lap using single-lap phase offset, such that trial-by-trial variability of neural activities can be taken into account (Schmidt et al., 2009). In addition, the finding of Mehta et al.'s on phase precession development was proposed to be a neuronal read-out of the asymmetric expansion of place fields during early experience (Mehta et al., 2000), but this asymmetry has not been replicated in my study or in other groups' reports (Huxter et al., 2003; Lee et al., 2004; Schmidt et al., 2009).

Complementary to my findings, Cheng and Frank (2008) investigated how experience shapes hippocampal theta sequences and phase precession across days, and reported both stronger phase precession and higher spiking coordination between pairs of place cells during theta oscillations for familiar days compared to novel days. These results are in accordance with the notion of experience-dependent changes to hippocampal networks, but they do not address the possibility of rapid plasticity on the timescale of individual running laps or the possibility of a dissociation between phase

precession and theta sequences, which in our data is revealed by the separate examination of laps. Particularly striking is the fact that, although theta sequences are wholly absent during the first lap, they require only that first lap of experience to develop. It is likely also that my direct measurement of sequences across large numbers of cells enhances the resolution of these effects over the use of pairwise correlation measures (Cheng and Frank, 2008).

In order to accurately examine progressive changes of neuronal activities on the timescale of individual running laps upon exposure to novel environments, I implemented a decoding algorithm based on single-lap experience. The traditional method of pooling spikes across multiple experiences of the same environment helps to increase the signal-to-noise ratio of position estimation under the assumption that a stable population code has already been established. However, in a novel environment, the neuronal representation of space is not stable (Wilson and McNaughton, 1993; Frank et al., 2004) and undergoes progressive changes, such as place field center of mass shift or the development of place field directionality (Mehta et al., 2000; Frank et al., 2004; Lee et al., 2004), which limit the utilization of whole session decoding. As I demonstrated from our data, single-lap decoding naturally characterized neuronal spatial representation with equal accuracy on each individual lap and represented more accurate estimation than whole session decoding. It is also reasonable to believe that the accuracy should increase with the number of place cells that are simultaneously being recorded. Moreover, the algorithm of single-lap decoding is potentially more relevant to the online computations performed by the brain areas downstream of the hippocampus (Schmidt et al., 2009).

Contrary to the long-standing hypothesis that individual neuronal phase precession necessarily results in population-level theta sequences (Skaggs et al., 1996), our data demonstrate the absence of theta sequences on the first traversal of a novel linear track despite strong phase precession among individual place cells, further supporting the notion that phase precession and theta sequence may be dissociable (Dragoi and Buzsaki, 2006; Foster and Wilson, 2007). This is particularly striking with single-lap decoding, for which position is as strongly decoded as on other laps, but unlike subsequent laps is static throughout the theta cycle. Possible explanations to account for phase precession's insufficiency to evoke theta sequences on the first lap include the variability of firing rates between different laps, the variability between place field sizes and shapes, and the variability of the exact timing of spikes between different neurons. The first two explanations are unlikely because controlling for the number of emitted spikes on each lap yielded similar results (Figure 6b, grey), and only place fields that were stable throughout the recording session were used (see Methods). The third explanation is the most likely because I have demonstrated that the phase offset of phase precession for individual neurons becomes more synchronized after the first lap, indicating a decrease in the variability of the exact timing of spikes between different neurons with experience (Figure 7c). Note that this change is compatible with the possible trend that I observed in overall phase offset (Figure 6c, second panel). Moreover, it is possible that, in addition to a reduction in the variability of phase offsets, there may be a reduction in the variability of phase slope/range (Figure 6c, first and third panels), which my analyses did not fully extract but might also serve to bind cells together in sequences. It is also possible that more complex changes in the spiking time relationships between neurons beyond the

alignment of phase precession properties might have contributed to the development of theta sequences. Taken together, my findings suggest that the first experience of running along a novel linear track modulates the timing of firing of different neurons, to increase the temporal coordination between neurons in the following laps.

My results have implications for the mechanisms underlying the formation of theta sequences. It has previously been proposed that the sequential firing structure of theta sequences could simply arise from spike phase precession of independent neurons driven by a common theta pacemaker (pacemaker models, e.g. the dual-interference model; Okeefe and Recce, 1993; Skaggs et al., 1996); alternatively, it might require a strengthened temporal coordination among specific hippocampal cell assemblies reinforced by experience. My results suggest that the latter is the case, as I observed a rapid formation of theta sequence structure during early experience. One candidate mechanism is synaptic plasticity because it is well established that increasing the coupling strength between oscillating neurons can lead to strong phase synchronization (Breakspear et al., 2010). Further, the formation of sequence structure that I observed was associated with increased spiking coordination between anatomically distributed groups of neurons, suggesting the possibility of macroscopic coordination across the hippocampus. It remains unknown how this coordination integrates with other features of hippocampal macroscopic organization that have been reported, such as the traveling wave of theta along the septotemporal axis of the hippocampus (Lubenov and Siapas, 2009; Patel et al., 2012), or progressive differences in spatial coding properties along this

axis (Kjelstrup et al., 2008) and along the proximodistal axis of CA1 (Henriksen et al., 2010).

It is widely believed that experience-driven plastic changes in hippocampus underlie many learning and memory processes (Morris et al., 1982; Morris et al., 1986; Whitlock et al., 2006). Although it may take more than 10 minutes to develop a stable population code for a novel square arena (Wilson and McNaughton, 1993), and up to 3 d for a place field to fully develop its directionality on a novel linear arm (Frank et al., 2004), I have reported a very rapid process of formation for theta sequences, almost exclusively happening within the first experience (on average a few seconds of running on the novel linear track), when other neural activities were still undergoing progressive changes. This one-trial dramatic change of hippocampal sequential firing structure does not only support the notion of fast learning in the hippocampus but also indicates an important role of theta sequences in early spatial learning.

In summary, my results suggest that hippocampal neural networks may undergo rapid plasticity during experience, to acquire predictive representations of the immediate future in the form of theta sequences. This rapid development of theta sequences only requires a single experience and is achieved by synchronizing experience-independent temporal coding across individual neurons (Figure 8).

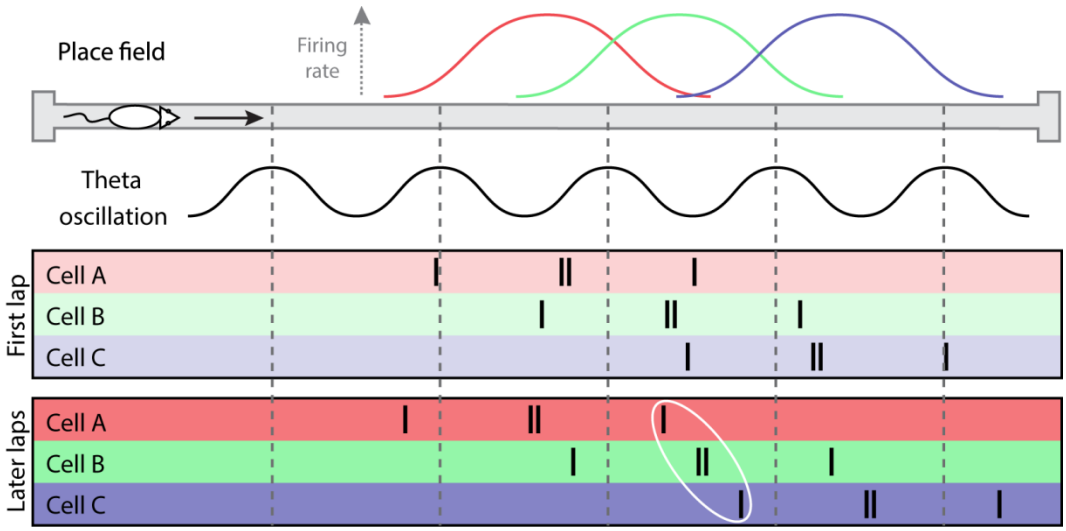

Figure 8. Model of theta sequence development.

Phase precession of individual neurons initially exhibit distinct phase offsets (first lap) but rapidly become synchronized after experience (late laps).

Chapter 4 — Trajectory events across hippocampal place-cells require previous experience

4.1 Introduction

Hippocampal replay is a phenomenon that occurs mainly during sharp-wave/ripple (SWR) events in the hippocampal LFP, in both awake and sleep states, in which place-responsive neurons (place cells) are active in precise sequences (Wilson and Mcnaughton, 1994; Lee and Wilson, 2002; Foster and Wilson, 2006; Diba and Buzsaki, 2007a; Karlsson and Frank, 2009a). Sequences can reflect previous behavioral trajectories (Lee and Wilson, 2002). They can also reflect future behavioral trajectories to remembered goal locations (Pfeiffer and Foster, 2013), and SWR disruption studies point to a necessary role for hippocampal replay in both the retrieval and consolidation of memory (Girardeau et al., 2009a; Ego-Stengel and Wilson, 2010; Jadhav et al., 2012a). More generally, the formation and retrieval of place-cell sequences may critically support the well-established hippocampal roles in navigation (Olton and Samuelson, 1976b; O'Keefe and Nadel, 1978b), and episodic memory (Scoville and Milner, 1957b; Gaffan, 1994a; Steele and Morris, 1999; Wood et al., 1999).

The standard interpretation of replay is that sequential activation of place cells arises as a consequence of the sequential ordering imposed on place cells by behavioral experience as an animal moves around (Suzuki, 2006; Miller and Wilson, 2008; Carr et al., 2011). Hence replay has been interpreted as a possible mechanism for the retrieval and/or consolidation of hippocampal dependent memories (Suzuki, 2006; Miller and

Wilson, 2008; Carr et al., 2011; Sadowski et al., 2011). However, it was recently reported that neuronal sequences recorded before experience matched the sequential order in which neurons responded subsequently (Dragoi and Tonegawa, 2011, 2013). This preplay was reported to occur on the same temporally condensed timescale as replay. The interpretation of this result was that the hippocampus utilizes pre-existing temporal sequences to structure the recruitment of cells during behavior. However, an unexpected corollary is that there is no reason to distinguish replay and preplay. Thus, the observation of preplay challenges the notion that replay sequences are learned from experience (Dragoi and Tonegawa, 2014).

In order to investigate the dependence of place-cell sequences on experience, we developed an experimental approach combining several features. Firstly, we focused on exploration of novel environments, since novelty promotes both synaptic plasticity and learning. Secondly, we focused on the simple behavior of running on linear tracks, as this hippocampus-independent behavior reliably drives place field responses and offline place-cell sequences (see, for example, Lee and Wilson, 2002; Foster and Wilson, 2006). Lastly, we used high density recording methods in order to maximize the number of units recorded across multiple environments, and across multiple days, to probe the contribution of place cell sequences to memory formation.

4.2 Methods

4.2.1 Subjects and experiment overview

Please refer to "Experiment protocol and subjects" and "Surgery and data acquisition" in chapter 2 for general information. In this study, a total of 4 male Long Evans rats (4-6 months old) were included. A recording day began with a 1 h pre-sleep session, which was followed by running on a novel linear track during run 1. Afterwards rats slept or remained at quiet rest during sleep session 2 for a period of 45 min. Rats ran on two more novel linear tracks during runs 2 and 3 for a period of 30-45 min each. The recording day ended with a long late sleep or quiet rest session of at least 2 h duration. All tracks were equally novel at the time of recording, and rats did not experience the same track twice. All group analyses were based on seven recording sessions from rats except for Sleep 1, where eight sessions from four rats were used.

4.2.2 Quantification of place fields and position reconstruction

Position was linearized and binned into 2.5 cm bins. Directional place fields were calculated as the number of spikes fired in a particular position bin and running direction divided by the time spent in that bin, smoothed with a Gaussian kernel with a s.d. of 5 cm, and identified when the peak firing rate of the pyramidal cell along the position bins was no less than 1 Hz. The place field size was defined as the total area of position bins where the firing rates were no less than 1 Hz. Sparsity was calculated as a measure of

spatial selectivity, to determine how diffuse the place cell firing was along the linear track as follows:

$$\text{Sparsity} \quad = \quad < f >^2 \ / \ < f^2 >$$

where f is the firing rate, and the expectations are calculated across all positions. Place cell average firing rate were calculated as the mean firing rate across all the position bins for each cell (Figure 11b). Place cell remapping index was defined as the Pearson linear correlation coefficient between place cell's peak firing positions on the current running track and the cell order from either the same or a different track (Figure 11c; for example, 1->3 denotes place cells on track 3 ordered by the firing order of the same cell on track 1). Position reconstruction from activity of these place fields is described as in chapter 2. In this chapter, a time window of 250 ms was used to estimate the rat's position on a behavioral timescale. A time window of 20 ms was used to estimate position during candidate population events. Position reconstruction error during the run was defined as the distance between the animal's current location and the peak decoded position in each 250 ms decoded time bin while the speed of the animal is more than 5 cm/s. Chance level of reconstruction error was determined by performing the same calculation except substituting the peak decoded positions with random positions.

4.2.3 Place cell ensemble activity analysis

Place cell ensemble activity was examined during stopping periods where the speed of the animal was less than 5 cm/s. Candidate population events were identified

during periods of increased spike density with peaks > 3 s.d. above the mean in the smoothed histogram (Gaussian kernel, s.d. of 10 ms). Start and end boundaries for each candidate population event were defined where the smoothed histogram crossed the mean. Only candidate events with 100 to 500 ms duration were included in the study.

Spike correlation of each candidate event was calculated as the Spearman's rank order correlation between the time of spikes and the ranked peak firing positions of the corresponding place cells. Because there were two running directions along a linear track and place cells are direction selective, I calculated spike correlations using two templates of place cell-ranked peak firing positions, each corresponding to a running direction. A small portion of candidate events (15 of 9803 in sleep 1) was excluded because the place cells that emitted spikes during those events had the same peak firing positions, and consequently real number correlation values could not be obtained from them. The shuffled data were created through randomly shuffle cell identities for 5000 times. The absolute values of spike correlations between original and shuffled datasets were compared, either when combing two values from both templates (Figure 9d, top) or only used the maximum value (Figure 9d, bottom), and the statistical significance for this comparison was evaluated using Levene's test, one-tailed Wilcoxon rank-sum test, one-tailed Kolmogorov-Smirnov test and Monte Carlo P-values. Monte Carlo P-values were calculated as $(n + 1)/(r + 1)$, where r is the total number of shuffled data sets and where n is the number of shuffled data sets that produced a number of correlated events greater than or equal to the number produced by the actual data, and where correlated events were defined as events with absolute spike correlation greater than the testing

threshold. For robustness, three testing thresholds were used, with values equal to 0.5, 0.6 or 0.7. The same quantification on down sampled place cells was done by randomly choosing 15 place cells for each recording session (Figure 12a) or by choosing place cells that had L_{ratio} equal to or less than the median value (Figure 12b, c).

Sequential structure of candidate events was estimated through the decoded posterior probabilities with six different measurements. (i) Weighted correlation is as described in chapter 2. (ii) Maximum jump distance was defined as the maximum distance between peak decoded positions in neighboring decoded time windows for each candidate event normalized by the length of the track. The decoded slope (iii) and replay score (iv) were defined as described in (Davidson et al, 2009): the likelihood (R) that the decoded candidate event (duration of n time bins) is along the fitted line with slope V and starting location ρ was calculated as the averaged decoded probability in a 30 cm vicinity along the fitted line as follows:

$$\mathrm{R}(\mathrm{V},\rho) = \frac{1}{\mathrm{n}}\sum_{\mathrm{k}=0}^{\mathrm{n}-1} \mathrm{P}_{\mathrm{r}}(|\mathrm{pos} - (\rho + \mathrm{V}\cdot\mathrm{k}\cdot\Delta\mathrm{t})| \leq \mathrm{d})$$

Where Δt is the moving step of the decoding time window (20 ms), and the value of d was empirically set to 15 cm for small local variations in slope. (For those time bins k when the fitted line would specify a location beyond the end of the track, the median probability of all possible locations was taken as the likelihood). To determine the most likely slope for each candidate event, I densely sampled the parameter space of V and ρ to find the values that maximize R. (v) Sharpness was defined maximum decoded

posterior probability for each candidate event. (vi) Position occupancy was defined as the set of peak posterior probability positions across all time bins in all events.

Trajectory events were defined as candidate events that obtained both strong weighted correlation ($corr$) and small maximum jump distance (dis) in the decoding (green stars in Figure 3-7, $corr > 0.6$ & $dis < 0.4$, $corr > 0.7$ & $dis < 0.4$, $corr > 0.7$ & $dis < 0.3$). To determine whether significant number of trajectory events can be observed under different conditions, I calculated the number of candidate events that passed both correlation and jump distance thresholds under all combinations, and compared them with the distribution of numbers from 5000 shuffled data sets that were generated through column-cycle shuffle (Davidson et al., 2009), which was done by circularly shift posterior probabilities of each decoded time bin by a random distance. The Monte-Carlo P-value was calculated as $(n + 1)/(r + 1)$, where r is the total number of shuffles and n is the number of shuffles that produce greater than or equal to the number of trajectory events that the meet the criteria compared to the actual data. I subsequently represented P-values under all combinations of two thresholds in a color-coded matrix (significance matrix), where a P-Value below 0.05 was considered significant and marked in red. To validate the detection thresholds for trajectory events, I generated two different control datasets as follows: (i) Poisson simulation: the spike train for each place cell was generated under a homogeneous Poisson process, with the firing rate for each cell given by the mean firing rate across all candidate events; and (ii) time swap: the posterior probability distribution of every 20 ms decoded time bins were randomly swapped with each other within each candidate event. Trajectory events should

be absent in the control datasets, as both of them theoretically lack temporal sequential structures (Figure 14).

4.3 Results

To investigate the role of experience in the encoding and retrieval of spatial memory, we applied high density electrophysiological recording techniques while animals engaged in exploration of three novel spatial environments in succession. A miniaturized microdrive holding 40 independently adjustable tetrodes (160 channels) was implanted in four rats, with tetrodes targeted bilaterally to dorsal hippocampal area CA1. Across multiple recording days, spike data, local field potentials and behavioral position data were collected, and on average 61 (SEM = 4.6) putative excitatory hippocampal neurons with place fields were isolated for each recording epoch (Foster and Wilson, 2006). Each recording day (Figure 9a) began with a rest period ("sleep 1") followed by exploration of a novel track ("run 1"), immediately after which followed a second rest period ("sleep 2"), followed by two additional novel tracks ("run 2" and "run 3"), and a final rest period ("sleep 3"). In the current dissertation, only data recorded in Sleep 1 and three running epochs are included. For each track, firing rate as a function of position was calculated for each active unit to define its place field for that track. Comparison across tracks demonstrated that place cells completely remapped from track to track (Figure 9b, 10, 11c), while running speeds and firing rates were the same for all three tracks (Figure 11a, b).

4.3.1 Absence of temporally sequenced events prior to experience

Candidate population events were identified as periods of increased spike density across all recorded units (Figure 9c), restricted to times when the animal's speed was below 5 cm/s (see Methods). Of candidate events, 86% occurred when the animal was at the top or bottom fifth of the track, which was where the animals tended to pause to consume food, groom, rest and turn around. Previous reports of preplay used measures of the correlation within candidate events between the times of spikes and the rank-ordered place field positions of the cells that produced them, as measured during subsequent behavioral testing. Therefore, I initially examined the same measure (Spearman's rank order correlation; see Methods). The histogram of correlations for sleep 1 candidate events was compared to the histogram for 5000 shuffled data sets, normalized by the number of shuffles (Figure 9d). However, there were two alternative methods in the implementation of this procedure, and I considered both. Because there were two running directions on the track, and given the directionality of place cells on the linear track, therefore there were two separate templates available to calculate a rank correlation for each candidate event.

In the first method, I considered both directional templates, generating 2 x the number of candidate events for the actual data and 2 x 5000 x the number of candidate events for the shuffles. The histograms of the actual data and of the shuffles normalized by the number of shuffles were both unimodal and centered on zero, and appeared to completely overlap (Figure 9d). I evaluated the similarities of the two histograms with four different statistical tests. I first confirmed that the absolute values of the correlations

in the actual data and the shuffled data came from distributions with equal variances (Levene's test of homogeneity of variance: p=0.44). I then determined that the absolute values of the correlations were no greater in the actual data than in the shuffled data (median: 0.174 versus 0.172; one-tailed Wilcoxon rank-sum test, p=0.08). Finally I assessed the flanks of the distributions of the absolute values of correlation between the actual data and the shuffled data. The actual data did not have longer tails that associate with greater absolute values of correlation than the shuffled data (one-tailed Kolmogorov-Smirnov test: p=0.122; Monte-Carlo P-value>0.1 with criteria of absolute correlation >0.5 or 0.6 or 0.7, see Methods).

In the second method, I considered only the directional template for each candidate event that maximized the absolute correlation. I likewise chose the best template for each shuffle. Thus there were 1 x the number of candidate events for the actual data, and 1 x 5000 x the number of candidate events for the number of shuffles. In this case both the actual and normalized shuffle histograms were bimodal, with peaks pushed away from zero, as a result of systematic maximization of the absolute correlation by selecting the template with the largest absolute value (Figure 9d). However, these histograms again appeared to overlap completely, and the absolute values were again statistically no greater in the actual data than in the shuffled data (median: 0.245 versus 0.258; one-tailed Wilcoxon rank-sum test, p=1) with equal variances (Levene's test of homogeneity of variance: p=0.77). The absolute values of correlation did not have longer tails in the actual data than in the shuffled data (one-tailed Kolmogorov-Smirnov test:

p=0.998; Monte-Carlo P-value>0.9 with criteria of absolute correlation >0.5 or 0.6 or 0.7, see Methods).

The above results demonstrate the importance of using matching procedures for actual and shuffled data because the shapes of the distribution differed greatly depending on the method. With neither method did I observe, as in the original reports (Dragoi and Tonegawa, 2011, 2013), a bimodal actual distribution and a unimodal shuffle distribution, with numbers of events equal to 1 x the number of candidate events and 1 x the number of shuffles x the number of candidate events, respectively. These numbers suggest that, in the original preplay papers, a choice of template was made for each event, but the unimodal shuffle distribution is inconsistent with this procedure. I conducted several further tests on our data to control for possible deviations from the original reports. my results were not changed when the numbers of cells were subsampled to match the numbers of cells in the original reports (Figure 12a). Furthermore, while it might be argued that poor cluster quality might account for my negative finding through the introduction of noise, I in fact determined that the great majority of the units were well clustered, using the L-ratio test (Sleep 1: 435of 442, 98%, Figure 12b; see Methods). I additionally subsampled from the population to include only those cells with an L-ratio less than or equal to the mean value, with no change in the result (Figure 12c).

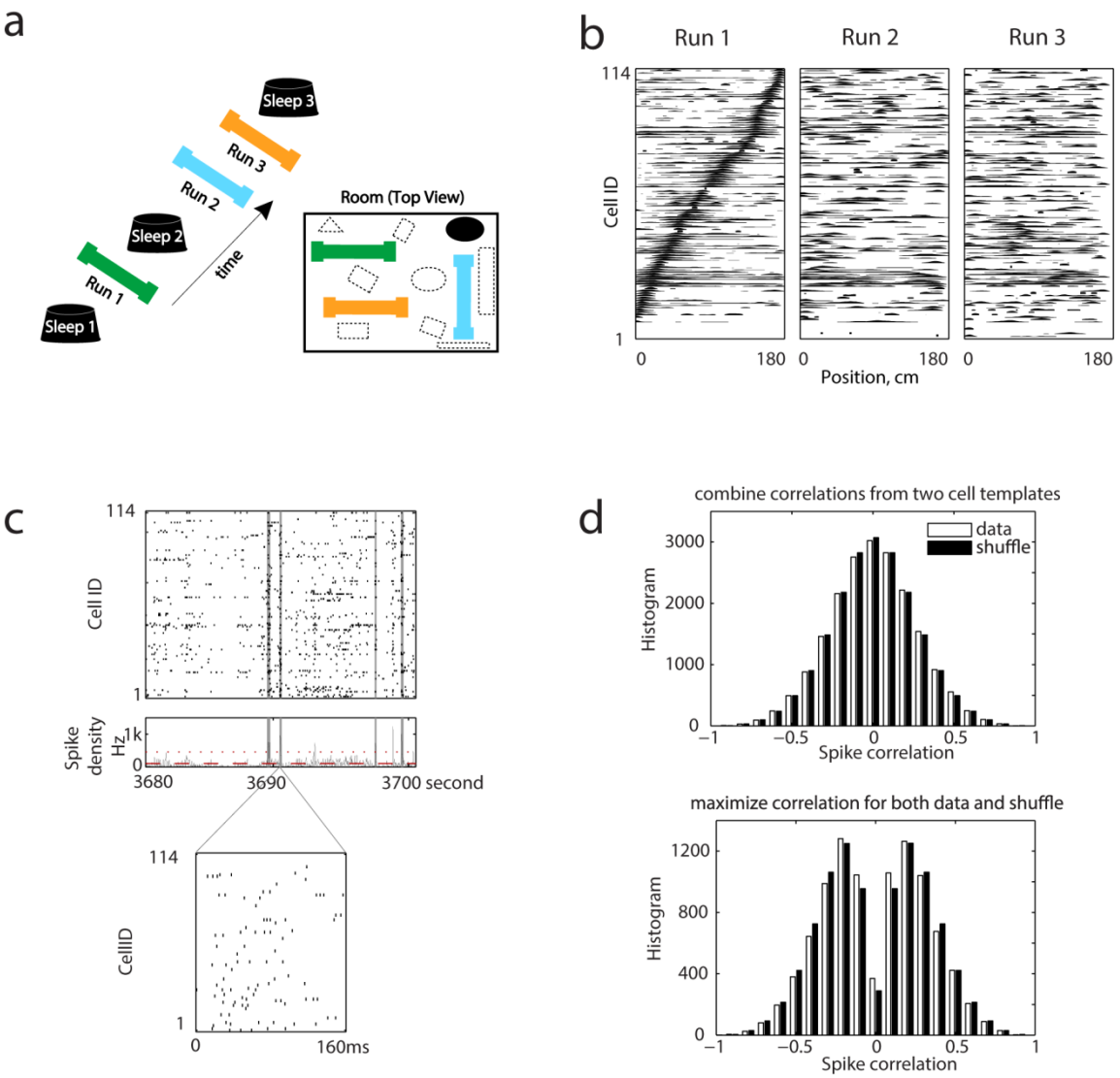

Figure 9. There are no sequentially structured events prior to experience.

(a) Experimental protocol. Left, timeline; bottom right, recording room layout. (b) Place field rate maps of 114 place cells from one session arranged by their peak firing positions on Track1. (c) Raster plot (top) and spike density (middle) of 114 simultaneously recorded place cells of a candidate event during Sleep 1. Red dotted line and dashed line represent respectively the thresholds for detecting candidate events and for defining their

boundaries. Gray shaded areas represent the time window of candidate events. Bottom plot, spikes emitted during a candidate event shown at expanded time scale. (d) Distribution of spike correlations of 9803 candidate events during Sleep 1. Open bars indicate spiking events versus the original place fields templates; filled bars indicate spiking events versus 5000 shuffled templates scaled down 5000 times. Top, both place fields templates in two running directions were included. Bottom, only the biggest absolute spike correlation resulted from two templates for each candidate event and shuffle were included.

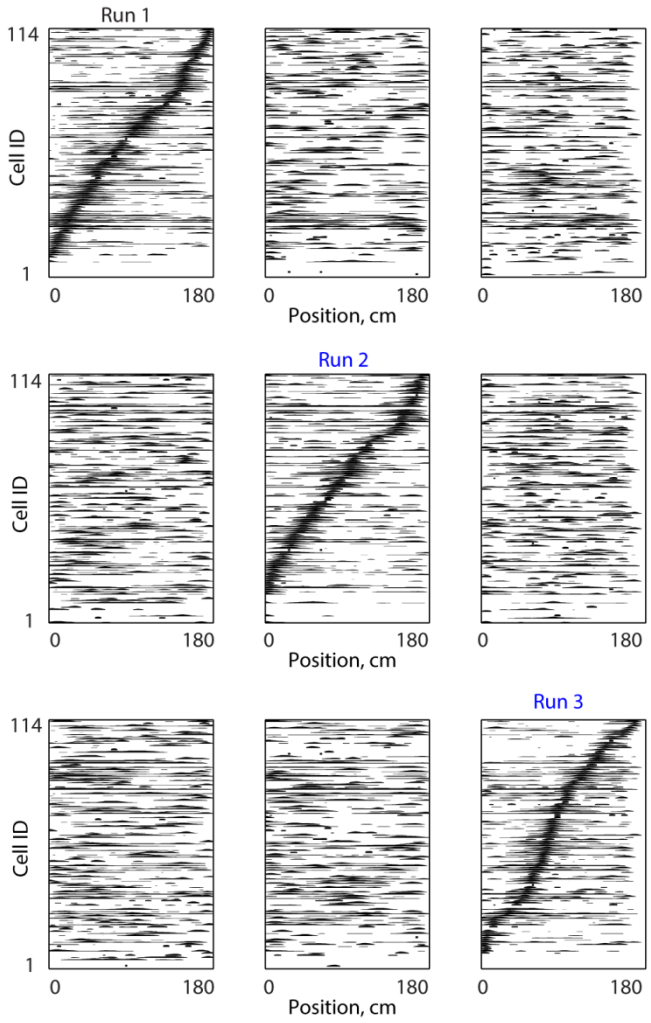

Figure 10. Place field rate maps for three different tracks.

Example of 114 place fields as they remap between three different tracks. The same 114 place cells are ordered by their peak firing positions on track 1 (1st row), track 2 (2nd row) and track 3 (3rd row) respectively.

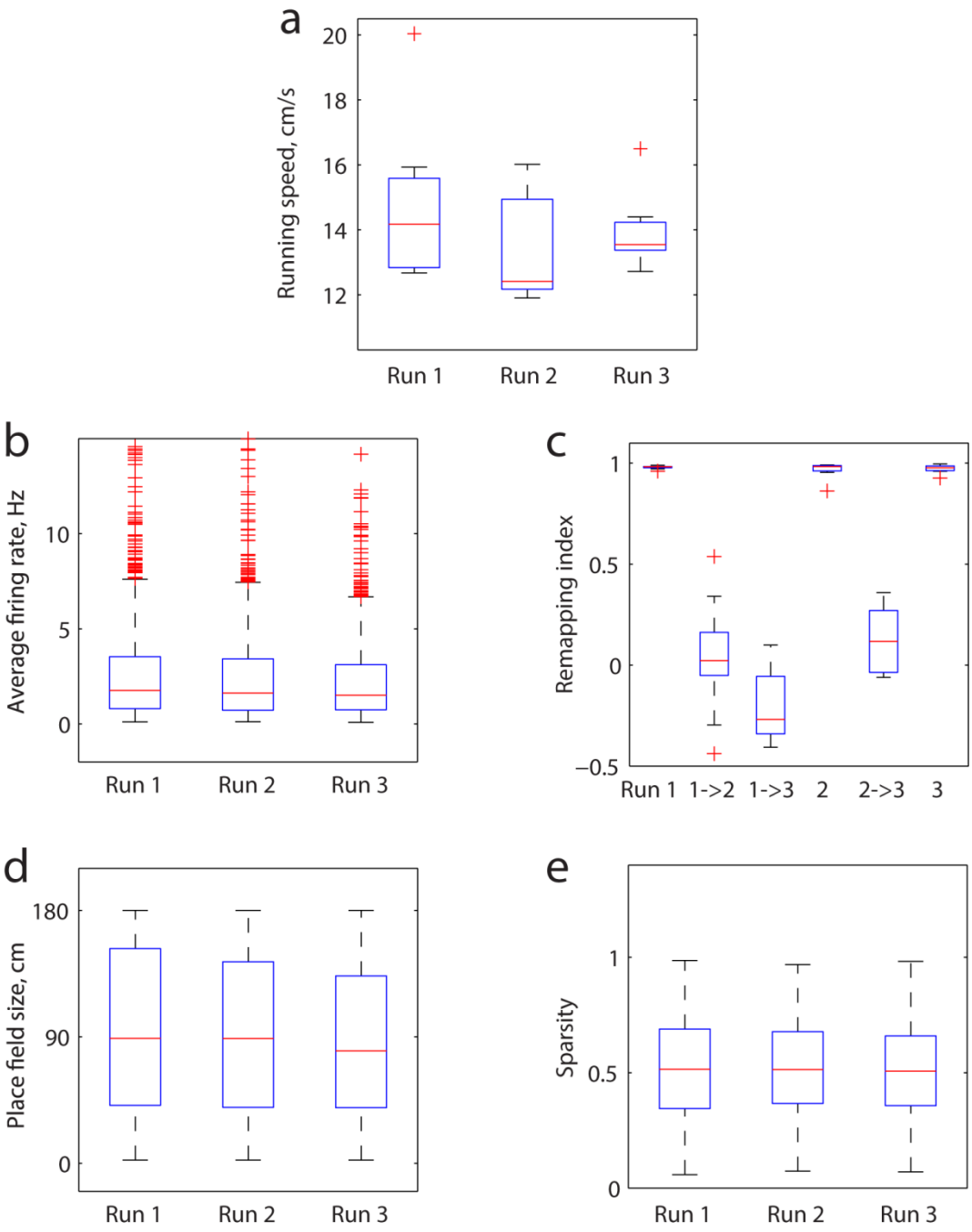

Figure 11. Animals' running speed and place field properties under different runs.

a) Animals' running speeds were not different between runs: Kruskal-Wallis test $H_{(2)}$=1.87, p=0.39. **b)** Place cell firing rates were not different between runs: Kruskal-

Wallis test $H_{(2)}$=4.98, p=0.08. **c)** Place cells remapped between different runs. Remapping index: Kruskal-Wallis test $H_{(2)}$=53.4, p=2.79*10-10. **d)** Place field size was not different between runs: Kruskal-Wallis test $H_{(2)}$=5.07, p=0.08. **e)** Place field sparsity was not different between runs: Kruskal-Wallis test $H_{(2)}$=1.16, p=0.56. The edges of the box are the 25th (q1) and 75th (q3) percentiles of the data. The red line in the box shows the median. Red crosses mark individual outliers that are larger than q3 + 1.5*(q3 – q1) or smaller than q1 – 1.5*(q3 – q1). The black whiskers extent to the most extreme data points not considering outliers.

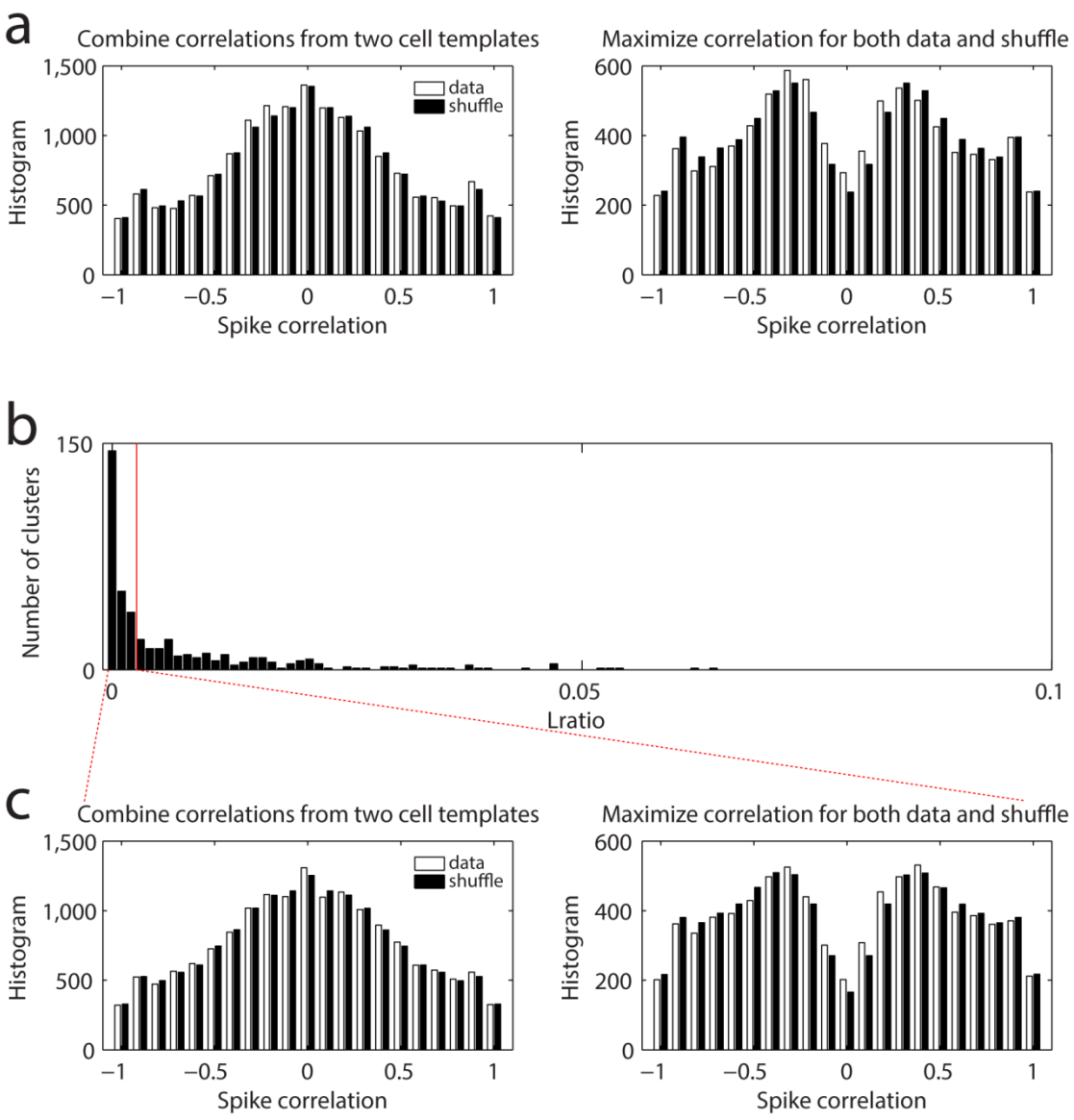

Figure 12. Structured events prior to experience are also absent with place cells randomly sampled or down-sampled by L_{ratio}.

a) Distribution of spike correlations of 8310 candidate events during sleep 1 after down-sampling to 15 cells. 15% candidate events in sleep 1 did not produce real number correlation after down-sampling cells thus were not included in the histogram. Open bars indicate spiking events versus the original place fields templates; filled bars indicate

spiking events versus 5000 shuffled templates scaled down 5000 times. Left, both place fields templates in two running directions were included (absolute correlation medians: 0.35 versus 0.36, data versus shuffle; one-tailed Wilcoxon rank sum test: p=0.75; one-tailed Kolmogorov-Smirnov test: p=0.81; Monte-Carlo P-value>0.4 with criteria of absolute correlation >0.5 or 0.6 or 0.7, see Methods). Right, only the biggest absolute spike correlation resulting from the two templates for each candidate event and shuffle were included (absolute correlation medians: 0.44 versus 0.47, data versus shuffle; one-tailed Wilcoxon rank sum test: p=1; one-tailed Kolmogorov-Smirnov test: p=1; Monte-Carlo P-value=1 with criteria of absolute correlation >0.5 or 0.6 or 0.7, see Methods). **b)** Histogram (bin size=0.001) of for 442 manually clustered, putative excitatory units in Sleep 1. Red line indicates the median value. **c)** Distribution of spike correlations of 8051 candidate events during Sleep 1 after sub-sampling cells that have an equal to or lower than the median value. 18% candidate events in sleep 1 did not produce real number correlation after sub-sampling cells thus were not included in the histogram. Open and filled bars are as described in **a)**. Left, same as in **a)**; absolute correlation medians: 0.36 versus 0.36, data versus shuffle; one-tailed Wilcoxon rank sum test: p=0.40; one-tailed Kolmogorov-Smirnov test: p=0.60; Monte-Carlo P-value>0.1 with criteria of absolute correlation >0.5 or 0.6 or 0.7. Right, same as in **a)**; absolute correlation medians: 0.48 versus 0.50, data versus shuffle; one-tailed Wilcoxon rank sum test: p=1; one-tailed Kolmogorov-Smirnov test: p=1; Monte-Carlo P-value=1 with criteria of absolute correlation >0.5 or 0.6 or 0.7.

4.3.2 Trajectory events observed after experience

4.3.2.1 Neuronal representation after experience is more "trajectory-like" than prior to experience

Given the absence of structure during Sleep 1 that anticipated the subsequent ordering of place fields on the track, I hypothesized that experience led to the establishment of new structure in the activity of place cells during population spiking events. To better analyze this structure, I applied Bayesian position decoding (Davidson et al., 2009) (see Methods) to candidate events divided into non-overlapping 20ms time bins, and examined the properties of the decoded position posterior probabilities within each candidate event for both sleep 1 and run 1 (Figure 13). Note that both sets of decoded events used the same cells, with the same place fields (those measured during Run 1), in order to understand how the structure of activity changed as a function of experience. I first visualized, for one session, the best positively and negatively correlated candidate events, for sleep 1 (Figure 13a) and for run 1 (Figure 13b). The structure of the events differed strikingly between the two epochs, with sleep 1 events exhibiting no discernible patterns while run 1 events exhibited clear line-like depictions of trajectories from one end of the track to the other. I then quantified, for all the sleep 1 and run 1 candidate events from all sessions (Figure 13c)., six different measures of sequence structure: (i) the weighted correlation, defined as Pearson's product-moment correlation weighted by the decoded posterior probability (Wu and Foster, 2014) (see Methods); (ii) the maximum jump distance within each event between two successive estimates of peak

position; (iii) the slope of the best linear fitted trajectory of the posterior probabilities (Davidson et al., 2009); (iv) the replay score (Davidson et al., 2009), which measures concentration of posterior probability within a line depicting a direct trajectory along the entire track; (v) the sharpness, defined as the amount of posterior probability concentrated near the peak; and (vi) the position occupancy, defined as the set of peak posterior probability positions across all time bins in all events. These quantifications revealed systematic differences in structure between sleep 1 and run 1 candidate events. The apparently small differences in slope and position occupancy suggested that it was not because sleep 1 events represented static locations that they failed to produce correlated events. More strikingly, I found that Run1 events were more correlated (positively or negatively), had smaller jumps, and were more sharply defined and more concentrated around the linear path along the track. A unifying account of these factors is that they are all properties of the depiction of trajectories through space, and so I hypothesized that Run 1 candidate events encoded trajectories along the track whereas sleep 1 candidate events did not.

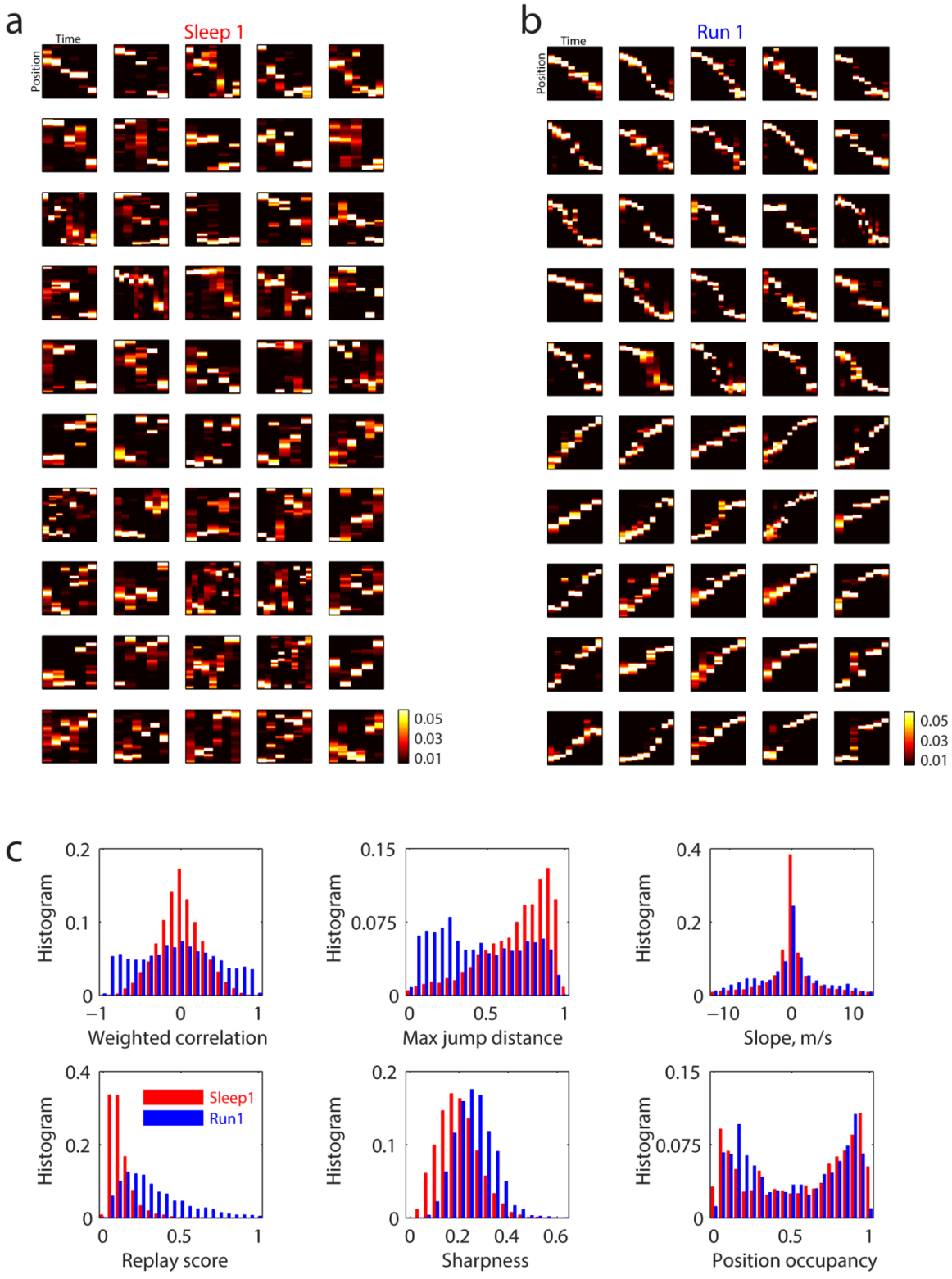

Figure 13. Position depiction within candidate events during sleep 1 and run 1.

a) Top 25 positively and top 25 negatively correlated events of track 1 during sleep1 using the same 114 cells as in Figure1. Each subplot is the decoding of a candidate event, with the y axis representing position and spanning the full length of the track (1.8 m), and the x axis representing time, with each pixel is 20 ms wide. The scale of decoded posterior probabilities is shown in the color bar. **b)** Top 25 positively and top 25 negatively correlated events of track 1 during run 1 using the same 114 cells from Figure1. Scales are the same as in **a**. **c)** Quantifications of 9818 candidate events during sleep 1 and 4438 candidate events during run 1. Median ± SEM, sleep 1 versus run 1: 0.17 ± 0.00 versus 0.40 ± 0.00 for absolute weighted correlation, 0.75 ± 0.00 versus 0.43 ± 0.00 for maximum jump distance, 1.25 ± 0.07 versus 2.5 ± 0.06 for absolute slope, 1.00 ± 0.00 versus 0.27± 0.00 for replay score, 0.19± 0.00 versus 0.26± 0.00 for sharpness, 0.61± 0.00 versus 0.51± 0.00 for position occupancy, all with $p<10^{-10}$, Wilcoxon rank-sum test.

4.3.2.2 Quadrant analysis of trajectory events

To test statistically the hypothesis of trajectory depiction for different tracks in different conditions, I developed an analysis that measured events in terms of the two strongest differentiating factors, correlation and jump distance, and varied them independently (Figure 14). Specifically, I considered all combinations of two thresholds, one on the weighted correlation, and one on the maximum jump distance, and asked how many candidate events passed both thresholds, and compared this number to the distribution of numbers for 5000 shuffled data sets (using the column cycle shuffle, see Methods). This comparison yielded a matrix of significance values for Sleep 1 (left matrix) and Run 1 (right matrix) events (Figure 3a). Whereas neither threshold by itself separated sleep 1 and run 1, except for very high values of the correlation threshold, the joint application of correlation and jump distance thresholds defined a quadrant-shaped region, where sleep 1 events were highly nonsignificant and run 1 events were highly significant (green box, Figure 14a). I defined these events as "trajectory events".

I further considered the result that, for large regions corresponding to application of a single threshold (the upper left and lower right portions of the matrix), there were significant numbers of events for Sleep 1. Given the absence of sequential structure observed from the spike train analysis of the previous section, I speculated that these significant zones of the matrix might correspond to spurious significance, that is, structure that was not indicative of pre-existing spatial or temporal arrangement of place fields, but rather corresponded to alternative sources of non-uniformity. To test this hypothesis, I generated data sets for which temporal structure was either absent by

construction or removed, but in which other forms of structure were preserved. First, I hypothesized that non-uniformity in firing rates might have given rise to significance. Therefore, I created Poisson spike trains for each cell for each sleep 1 candidate event, using for each cell the firing rate averaged across all candidate events (Figure 14b, left). The resulting matrix bore a remarkable similarity to the actual sleep 1 matrix (Figure 14a, left), particularly with respect to the lower-right correlated region, suggesting that the non-uniform distribution of firing rates might alone account for the pattern of significance in the sleep 1 data. Second, I hypothesized that non-uniformity in the distribution of place fields might have given rise to significance. Therefore I generated shuffled candidate events, in which the time bins within each event were swapped randomly, while preserving, within each time bin, the distribution of posterior probabilities across positions (Figure 14b, right). This shuffle also produced a similar pattern of significance to the actual sleep 1 data. Together these analyses suggested that, when using Bayesian decoding, spurious events were likely to be found if analyzed using thresholds on either correlation or maximum jump distance alone. Notably, the quadrant defining trajectory events was insignificant in both randomized data sets, supporting my contention that the joint application of these thresholds was a robust method for measuring temporally structured activity across place cell populations.

Finally, the same pattern of results was observed for subsequent runs (Figures 14c and d), in which activity in either sleep 1 (left), or runs 2 or 3 respectively (right), was analyzed using the templates from the respective runs. These data demonstrate the complete absence of trajectory depiction in sleep 1 for any of the three subsequent tracks.

I further considered a trio of specific threshold pairs close to the boundary of the trajectory quadrant (green stars in Figure 14), that allowed us both to check the sensitivity of the quadrant boundary, and to sample from that part of the quadrant with the least stringent constraints and hence the greatest number of data points. In the next chapter I used the same trajectory quadrant analysis, specifically, the trajectory events were detected under the criteria that the absolute correlation is more than 0.6, and the maximum jump distance is less than 40 percent of the track (the green star closest to the quadrant boundary in Figure 14).

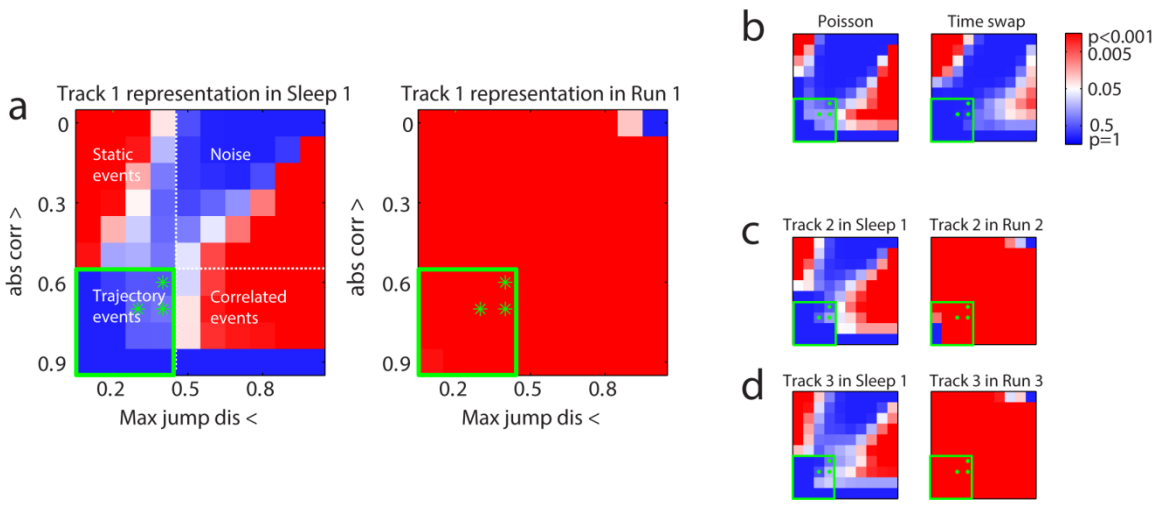

Figure 14. Trajectory events are found only after experience.

a) Significance matrix under parameter space of absolute weighted correlation and maximum jump distance. No significant trajectory events (lower left quadrant) of track 1 experience were detected during sleep 1, but were present during run 1. **b)** Significance matrix of control datasets (see Methods) of track 1 representation in Sleep 1 generated by Poisson simulation (left) and time swap (right). **c) and d)** Significance matrix of track 2 and track 3 representation in sleep 1 and the current run epoch. Color bar in **a** gives probability values for all matrices: blue values, insignificant ($p>0.05$); red values, significant ($p<0.05$); white, $p=0.05$.

4.4 Discussion

I have investigated the experience dependence of offline place cell sequences. Previously, these sequences have been reported both following experience (replay) and also preceding any experience (preplay). The conceptual challenge of preplay is that, if the sequences pre-exist, then replay, as measured in the hippocampus, cannot be interpreted as evidence of learning or memory formation. However, I found no evidence for the existence of preplay sequences, using similar quantification methods to the original reports (Dragoi and Tonegawa, 2011, 2013) but with much larger numbers of simultaneously recorded units. Following the preplay literature (Dragoi and Tonegawa, 2013), I have tested for preplay in multiple subsequent environments, with the same result. To further understand these data, I took advantage of the large number of cells recorded simultaneously and recently developed decoding methods to measure the fine spatio-temporal structure of both pre-experience and post-experience events. These methods revealed that post-experience events were better correlated, less jumpy, more sharply defined and more linear; I have summarized these findings with the designation "trajectory events". Thus, in contrast to the original reports that may not have had the cell counts to resolve such differences, I found that experience results in a dramatic reorganization of place cell activity, to reflect the contingencies between places in the experienced environment that define behavioral trajectories.

These findings have implications for the mechanism by which hippocampal cells acquire place fields. If preplay sequences dominated, then any given place cell would potentially have to become associated to any arbitrary set of inputs, reflecting the input to

the hippocampus at the location where the cell has been "pre-ordained" to fire by virtue of its order within the preplay sequence. By contrast, recent studies suggest that the input to all hippocampal cells is spatially modulated (Lee et al., 2012), in accordance with a model whereby place cells begin with a place field and learn the contingencies between places, expressed as sequences, only through experience. Furthermore, I recently dissociated place field responses including intact phase precession during the first run in a novel environment, from theta sequences emerging later (Feng et al., 2015). Our present data strongly support such a model, since I find no evidence for a pre-existing temporal order for place cells. This model also fits the subtle effects of NMDA receptor antagonism that have previously been reported (Kentros et al., 1998; Ekstrom et al., 2001), as will be discussed further in chapter 6.

I have used decoding methods to extract structure from offline events and developed a comprehensive method by which the significance of events is tested against a matrix of threshold values for two parameters (correlation and jump distance) simultaneously. I find a quadrant within the matrix defined by minimum thresholds on each parameter that consistently differentiated between pre-experience and post-experience events, and I interpret this quadrant as a measure of "trajectory events". This matrix analysis comes with some important caveats. First, very loose and very tight constraints both make significance less likely in the top right and bottom left far corners of the matrix, respectively. Second, apparent significance was measured in all conditions including pre-experience, for the top left and bottom right quadrants. This may seem puzzling, given the complete absence of structure detected using the spike-based

correlations, but Bayesian decoding is powerful at extracting structure, and my further analyses using random data suggest that these regions of significance likely reflect spurious effects of the decoding method. Given the utility of the decoding method for resolving fine structural changes in representation, it is important to develop robust methods for assessing significance. I propose my definition of the trajectory quadrant as one robust way to quantify the experience-dependent structure of decoded events. Robustness could potentially be increased further by adding a third parameter, such as sharpness.

Finally, we might consider what kind of information is acquired and encoded during the experience-dependent formation of trajectory events. It has been demonstrated that, provided the logical contingencies between locations in an environment are known or have at least been sampled, the hippocampus is capable of generating place cell sequences in an order that has never been experienced (Foster and Wilson, 2006; Diba and Buzsaki, 2007a; Davidson et al., 2009; Karlsson and Frank, 2009a; Gupta et al., 2010), and generating sequences that depict as-yet never experienced trajectories (Gupta et al., 2010; Pfeiffer and Foster, 2013) - in particular, novel paths to a remembered goal (Pfeiffer and Foster, 2013). Together these results raise the possibility that the encoding process for trajectory events may not consist of recording or reinforcing specific sequences of experience for veridical playback, but rather the learning of underlying contingencies in environments. In this sense, replay sequences might be thought of as constructive attempts to read out information from a learned cognitive map (O'Keefe and Nadel, 1978b), where the underlying contingencies are learned from experience and

stored in the synaptic matrix, but where specific retrieval events can be modified uniquely to suit the requirements of the current task. In this way, hippocampal replay provides a model system that can reconcile the mnemonic (Scoville and Milner, 1957b) and constructive (Hassabis et al., 2007) aspects of the brain's episodic memory system (Tulving, 2002a).

Chapter 5 — Mechanisms contributing to experience-dependent changes in the structure of hippocampal replay sequences

5.1 Introduction

The hippocampus is critical for navigational learning (O'Keefe and Nadel, 1978a; Morris et al., 1982) and episodic memory (Scoville and Milner, 1957a; Olton and Samuelson, 1976a; Gaffan, 1994b; Steele and Morris, 1999), both of which require rapid temporal encoding of relationships between events and/or locations. The mechanism underlying rapid encoding of information is thought to involve plasticity changes in the neural network driven by synaptic long-term potentiation (Morris et al., 1986; Whitlock et al., 2006), that can be induced by precisely controlled spike timing coordination (Hebb et al., 1994; Bi and Poo, 1998b; Zhang et al., 1998b; Wittenberg and Wang, 2006). In hippocampus, groups of place cells fire in compressed sequences corresponding to the current or previous behavior sequences during or following exploration. The former is named 'theta sequences' (Skaggs et al., 1996; Dragoi and Buzsaki, 2006; Foster and Wilson, 2007; Gupta et al., 2012), which are repetitive sequential firing among local place cells, and are accompanied by theta oscillations in hippocampal local field potentials (LFPs). The latter is termed 'replay' (Wilson and Mcnaughton, 1994; Lee and Wilson, 2002; Foster and Wilson, 2006; Pfeiffer and Foster, 2013), a compressed sequence that typically recruits a larger group of place cells than theta sequences, and which is co-occurring with sharp-wave-ripples (SWRs) during sleep, or periods of quiet wakefulness immediately after exploration. While theta sequences have been suggested

to play a role in inducing plasticity changes during early learning (Okeefe and Recce, 1993; Jensen and Lisman, 1996; Skaggs et al., 1996; Jensen and Lisman, 2005; Dragoi and Buzsaki, 2006; Foster and Wilson, 2007), and have been reported to develop with experience (chapter 3) (Feng et al., 2015), these issues are less well studied for hippocampal replay.

As discussed extensively in chapter 4, the current debate of the experience-dependence of hippocampal replay focuses on whether or not hippocampal "offline" place cell sequences exist prior to experience. Yet a more interesting topic of the relationship between hippocampal replay and experience: the progressive changes of hippocampal replay induced upon repeated exposures to the same environment, has never been directly addressed. Previous studies failed to address this question likely due to the challenge of accurately detecting replay from small number of simultaneously recorded neurons, or due to failure to precisely examine the spatial representation of replay in a fine timescale from noisy data. With the improvement of technology, recently our lab was able to record more than two hundred hippocampal place cells simultaneously, and utilized a Bayesian decoding algorithm to dissect the detailed spatial representation of hippocampal replay (Pfeiffer and Foster, 2013, 2015). In all of these studies, hippocampal replays are depicted as place cell sequences that represent distinct trajectories through space in the recording environment. I further introduced a robust quadrant analysis in chapter 4, where hippocampal replay is detected with threshold values for two parameters (correlation and jump distance). I named the hippocampal replay detected in my study as "trajectory events" because they fit the definition of "trajectory": better correlated, less

jumpy, more sharply defined and more linear compared with noise. In this chapter, hippocampal replays are frequently referred as "trajectory events" for consistency of terminology.

In this study, we used high density recording methods that allow both simultaneous recording of hundreds of hippocampal place cells, and the examination of ensemble activity within fine temporal scale, to probe the mechanisms underlying the generation of replay sequences and the contribution of hippocampal replay to memory formation. We focused on exploration of novel environments, since novelty promotes synaptic plasticity and learning (Wilson and McNaughton, 1993), as well as the instances of hippocampal replays (Foster and Wilson, 2006). We also focused on examining offline hippocampal place-cell sequences during the simple behavior of running on linear tracks, as this hippocampus-independent behavior reliably drives place field responses and offline place-cell sequences (e.g. (Lee and Wilson, 2002; Foster and Wilson, 2006)), and enables us to examine replays on a single-experience basis. By examining hippocampal replays from lap to lap, I was able to accurately capture the dynamics of the development of hippocampal replay during early learning, and thus provide insights for both the neuronal mechanism and physiological functionality underlying hippocampal replay.

5.2 Methods

5.2.1 Subjects and experiment overview

Please refer to "Experiment protocol and subjects" in chapter 2 for general information. In this study, seven adult male Long-Evans rats (4-6 months old) were food deprived and pre-trained on a linear track in the training room before implantation. Thirty-One recording sessions of animals running on novel linear tracks (180 cm in length; number of laps per session: 15 ± 0.79, mean ± SEM) in the recording room were included in this study. "Surgery and data acquisition" are as described in chapter 2.

5.2.2 Detection and quantifications of trajectory events

"Position reconstruction from activity of place cells" is as described in chapter 2. A decoding window size of 20 ms was used for replay detection. The detection of candidate events through population spike density is as described in chapter 4. Consistent with Chapter 4, replays of trajectory events were defined as candidate events that obtained both strong absolute weighted correlation ($corr$, see also chapter 2) and small maximum jump distance (dis, see chapter 4) in the decoding. Here I use $corr > 0.6$ & $dis < 0.4$ as the set of two thresholds (Silva et al., 2015). Duration of replay was defined by the length of spike density window (Figure 15d, 17a, 18a, 19a). The decoded slope (Figure 15e, 17b, 18b) was defined as described in (Davidson et al, 2009) and in chapter 4: The likelihood (R) that the decoded candidate event (duration of n time bins) is along the fitted line with slope (V) and starting location (ρ) was calculated as the averaged decoded probability in a 30 cm vicinity along the fitted line:

$$R(V,\rho) = \frac{1}{n}\sum_{k=0}^{n-1} P_r(|pos - (\rho + V \cdot k \cdot \Delta t)| \leq d)$$

where Δt is the moving step of the decoding time window (20 ms), and the value of d was empirically set to 15 cm for small local variations in slope (for those time bins k when the fitted line would specify a location beyond the end of the track, the median probability of all possible locations is taken as the likelihood). To determine the most likely slope for each candidate event, I densely sampled the parameter space of V and ρ to find the values that maximize R. To quantify the neuronal activity within individual events, place cell overall firing rate during each event was calculated as the total number of spikes emitted during the event, divided by the duration of the event and the total number of the active place cells across the recording session (Figure 19b). Percentage of cell recruitment for each event was calculated as the ratio of the active place cells in the current recording session that has emitted at least one spike during the event (Figure 19c). Spike number emitted by each cell was counted, and cell activation ratio for each cell was defined as the percentage of events that the cell fired at least one spike (Figure 19d).

5.2.3 Analysis of gamma rhythm and discretized spatial representation of trajectory events

LFP from the electrode with the highest theta signal-to-noise ratio during animals' running for each tetrode was analyzed. To examine the power and frequency of slow-gamma rhythm during candidate events, LFP from tetrodes on which excitatory hippocampal cells were recorded were averaged before being band-pass filtered between

25 and 50 Hz (Carr et al., 2012; Pfeiffer and Foster, 2015). The instantaneous gamma frequency was determined as the reciprocal of duration of each gamma cycle of the filtered signal (Figure 20d, black). Slow-gamma power was estimated as the smoothed absolute value of the Hilbert transform of the filtered signal (Gaussian kernel, SD = 85 ms). When comparing slow-gamma power during trajectory events between different laps, z-scored value was calculated for each individual recording session when pooling data together (Figure 20d, blue).

To capture the discretized spatial representation of trajectory events, posterior probabilities (see chapter 2) were calculated in a 20 ms time window advancing every 5 ms. Distances between the weighted means of the posterior probabilities of two consecutive decoding time frames (Figure 20a, black) were compared with hypothesized distances predicted by smooth trajectories, which are determined by the range of distance that the trajectory event traveled divided by the total number of decoding time frames minus one (Figure 20a, red). To quantify the phase-locking of decoded distance to slow-gamma (Figure 20b), the phase of the decoded distance between neighboring decoding time frames was calculated as the average phase of all the spikes that occurred within the 15 ms overlapping time window between the two consecutive time frames, whereas the phase of each spike was determined in reference to the gamma oscillation on the tetrode from which the spike was recorded. The peak of the oscillation was defined as 0°/360° and the mid-point of the descending phase was defined as 90°. To assess the modulation depth of this phase-locking between different laps, the average across-session neighboring decoding distance as a function of slow-gamma phase (similar as in Figure

20b) was calculated for each individual lap, and the modulation depth was calculated as the range of the mean decoding distance across gamma phase divided by the summation of the maximum and the minimum (Figure 20c). The spatial representations of trajectory events were segregated into discrete stationary epochs and movement epochs, where decoded distances between neighboring time frames less than or equal to 2.5 cm (1 spatial bin) were considered stationary, or otherwise considered moving. The duration of stationary and movement epochs were calculated separately (Figure 20d, e). The moving distance of a movement epoch was determined as the total range of position traveled within the time frames of its epoch (Figure 20g). A stationary and movement epoch pair is a "step" in the discretized spatial representations of trajectory events. The step size is the number of alternations between stationary and movement epochs in the spatial representations of each trajectory events (Figure 20h).

5.3 Results

Rats were trained to run on a novel linear track for several laps while stopping at each end to consume food between laps (lap number: 15 ± 0.79, mean ± SEM). Microdrives with tetrodes were implanted in the hippocampal dorsal CA1 region to record spike timings from a large number of cells simultaneously (7 rats, 31 sessions, 69 ± 2.82, mean ± SEM). Directional place fields were calculated, and used to decode spike trains for position estimation. Awake replays were identified during immobility as events of transiently high spike density across cells (Foster and Wilson, 2006; Pfeiffer and Foster, 2013), which have strong weighted correlation and small maximum jump distance

in the decoding (Figure 15a-c, see the criteria of trajectory events in Methods). Events of transiently high spike density during immobility that failed to satisfy both the correlation and continuity criteria of trajectory events, such as candidate events with weak weighted correlation and big maximum jump distance in the decoding, were identified as noisy events and were used as a control.

Because our animals ran on average 15 laps, I only looked at events that occurred before the fifteenth lap such that on average 191 trajectory events (summed across all 31 sessions) after each lap (SEM: 17.82) were included in the study. In a total of 14643 candidate events, 2675 events were identified as trajectory events. Although awake replays of trajectory events are events with strong weighted correlation and small maximum jump distance in the decoding, the degree to which the estimated positions are correlated with time in each event varies (Figure 15f, absolute weighted correlation: 0.80 ± 0.002, mean ± SEM), and the degree to which the spatial representation is continuous in each event varies (Figure 15e, maximum jump distance: 0.25 ± 0.002, mean ± SEM), suggesting that not all the events are identical. I next asked whether other properties of trajectory events, especially those that are independent of the two replay detection criteria, vary between individual events. I first noticed that the durations of trajectory events were different between individual events (Figure 16b, c, Figure 15b, c). The variation of the duration (Figure 15c, duration: 155 ± 0.84 millisecond, mean ± SEM) does not come from different animals or different recording sessions, rather it lies between individual events within the same session (Figure 16b, c). Even trajectory events that occurred close

in time (for example during the same stopping period, Figure 16 a-c) do not always have exactly the same duration.

Because trajectory events represent traversal of the linear track in their decoding, the differences of duration could come from the following two sources: 1) trajectory events with smaller duration traverse a shorter distance along the linear track in their decoding with a constant speed, in which case smaller duration reflects a spatially shorter sequence; 2) trajectory events with a smaller duration traverse the same distance along the track but with a faster speed in their decoding, in which case smaller duration reflects a temporally faster sequence. Our data strongly suggested the latter because the durations are different even for events that traverse equal length of the track. For example, Figure 16 includes eight different trajectory events from the same session with 2 to 3 folds differences in their durations, but their decoding all traverse from one end to the other end of the track. Note that the starting and ending time point of each trajectory event, as well as their duration, were defined purely based on population spike density, thus were completely independent of the decoded spatial representation of each event, and were not biased to result in neither spatially longer nor shorter sequence in decoding. My observations suggest that, the speed by which trajectory events traverse the positions along the track is not constant, as indicated differently in a previous report (Davidson et al., 2009). I hence directly measured the speed of trajectory events by calculating the slope in the decoding as in Davidson et al. (2009) (see Methods). As expected, the slope in the decoding demonstrated big variations among trajectory events (Figure 15e, slope: 6.28 ± 0.05 m/s, mean ± SEM). Also the duration and the slope of trajectory events are

negatively correlated (Pearson's linear correlation coefficient $r=-0.20$, $p<10^{-10}$), further supporting that the difference in duration is a reflection of the variations in the speed of trajectory events.

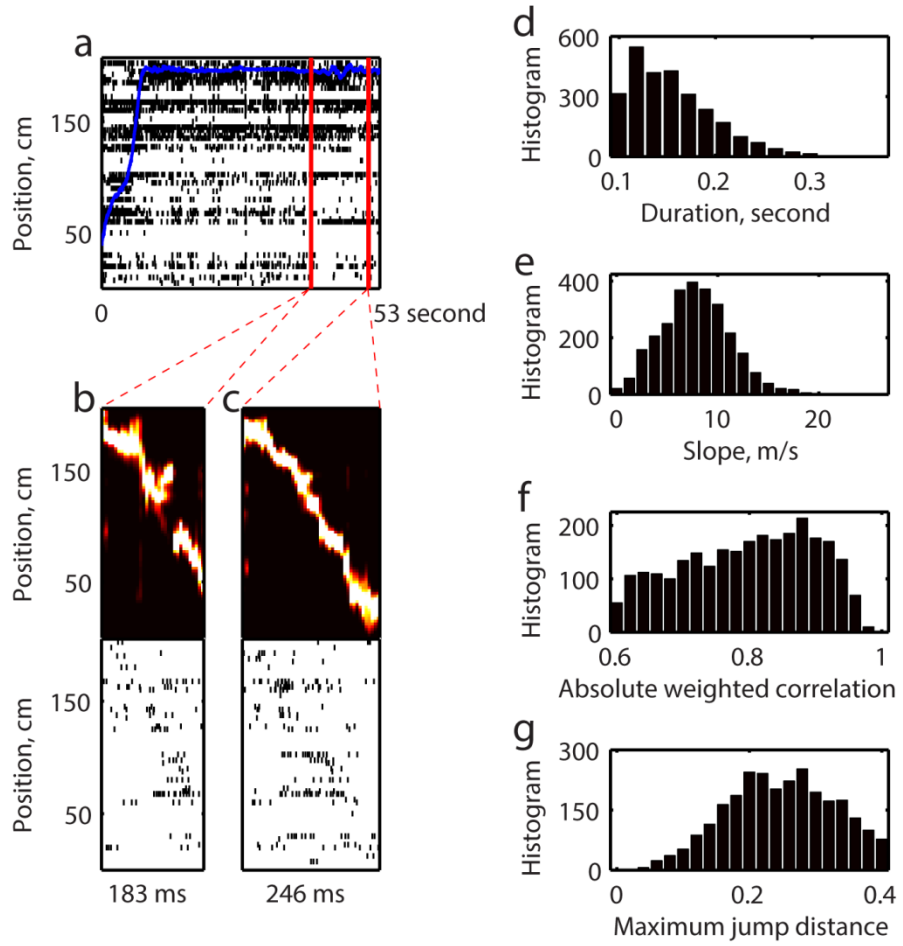

Figure 15. Hippocampal trajectory events.

a) Spikes (black bars) from 107 CA1 pyramidal cells ordered by place cells' peak firing positions along the track during 53 seconds of recording. Overlay blue line indicates the running trajectory of the animal. Red lines mark the occurrence of the two trajectory events shown in b and c. **b) and c)** Two example trajectory events. Top, trajectory events constructed from raw spikes (probability estimates were color scaled). Bottom, Spikes (black bars) ordered by place cells' peak firing positions along the track in the corresponding time window of each trajectory event. **d-g)** Histograms of duration,

absolute slope, absolute weighted correlation and maximum jump distance of 2675 trajectory events.

5.3.1 Sequential activation of hippocampal place cells during replay slows down with experience

Next I asked whether the differences of the propagation speed of trajectory events are inherent or modulated by external factors such as experience. To examine the change of speed of replay with experience, I grouped the detected trajectory events according to the number of prior experiences (running laps) that the animal had acquired of the environment. As reported previously (Foster and Wilson, 2006), significant replays emerged during early experience, that is, immediately after the first running lap on a novel linear track (Monte Carlo P-values $2*10^{-4}$, Figure 16), and were continuously present during the following resting periods (Figure 16). Interestingly, when comparing trajectory events on different laps, I found that the speed at which replay traversed the track slowed down with increased running experience, reflected by a decrease in the slope of hippocampal replay (Figure 17b, Pearson's linear correlation coefficient r=-0.14, $p<10^{-10}$), and an increase of the duration of replay (Figure 17a, Pearson's linear correlation coefficient r=0.10, $p=8.41*10^{-8}$). Surprisingly, the correlation between estimated position and time during replay was not different between different laps (Figure 17c, Pearson's linear correlation coefficient $r=3.52*10^{-4}$, p=0.99), suggesting the temporal coordination between spike timings are equally strong between different laps. Maximum jump distance, however, decreased with increased experience, suggesting a more continuous spatial representation in later replay (Figure 17d, Pearson's linear correlation coefficient r=-0.09, $p=3.26*10^{-6}$). I used candidate events with weak correlation and large maximum jump distance in the decoding as control datasets, because they are by definition similar transiently increased population activity but do not represent

trajectories of the current environment, and consequently should not be modified by the current experience. As expected they yielded significantly smaller durations, slopes, correlations and significantly bigger maximum jump distances than trajectory events. These candidate events did not demonstrate a change of duration (Figure 18a, Pearson's linear correlation coefficient r=0.003, p=0.79) and weighted correlation (Figure 18c, Pearson's linear correlation coefficient r=0.003, p=0.81) between different laps. However, they demonstrated a weak but significant decrease of slope (Figure 18b, Pearson's linear correlation coefficient r=-0.04, $p<4.8*10^{-3}$) and maximum jump distance (Figure 18d, Pearson's linear correlation coefficient r=-0.03, p=0.02). This significance may likely be driven by a small fraction of replays that had failed to pass my detection threshold, because of inherent experimental limitations in my ability to measure replay, given that the number of neurons recorded represents only a tiny fraction of the total network. Nevertheless, the drastic changes of trajectory events on the duration, slope and maximum jump distance were not preserved in the control datasets, leading to my conclusion that the progressive change of propagation speed of trajectory events is a result of increased experience of the current environment.

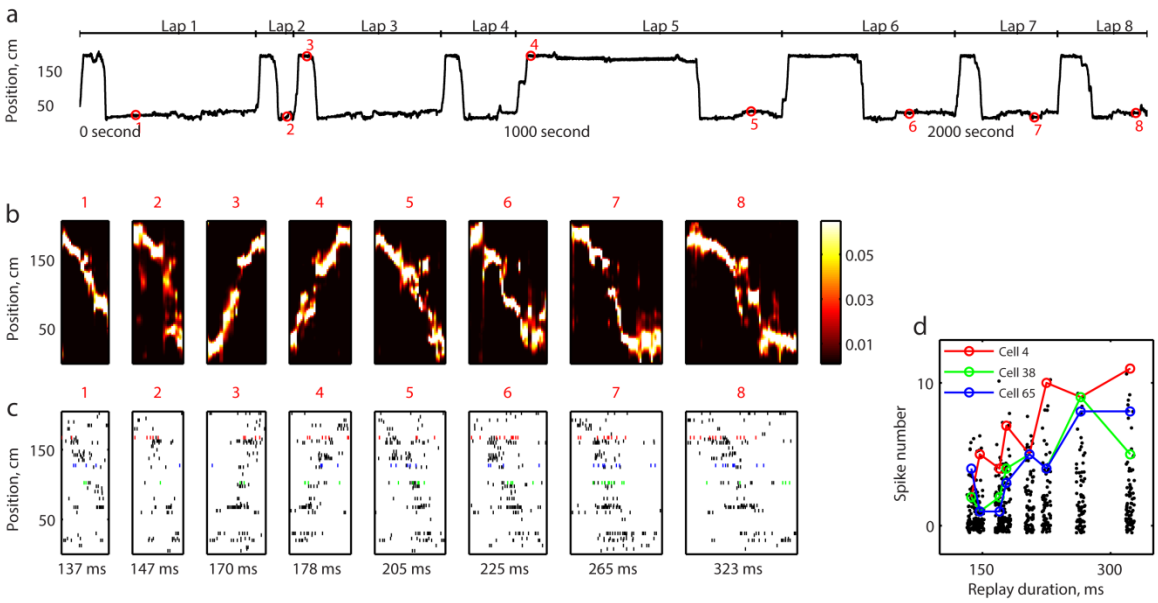

Figure 16. Replay examples during the first eight running laps in a session.

a) Running trajectory of the first eight laps of the animal. Red circles mark the time of occurrence of the example trajectory events in b) and c). Top tick bars mark the start and end of each lap. **b)** Decoding of the eight example trajectory events. Colorbar on the right indicates the scale of probability estimates. **c)** Spikes (black bars) ordered by place cells' peak firing positions along the track in the corresponding time window of each example trajectory events. Red, green and blue are spikes from three different cells. **d)** Spike number for each cell for each trajectory event. Each black dot indicates the number of spikes emitted by a single cell during an example trajectory event. Red, green, blue mark the same example cells as in c). Jitter was added to the duration for eight replays for visualization purposes.

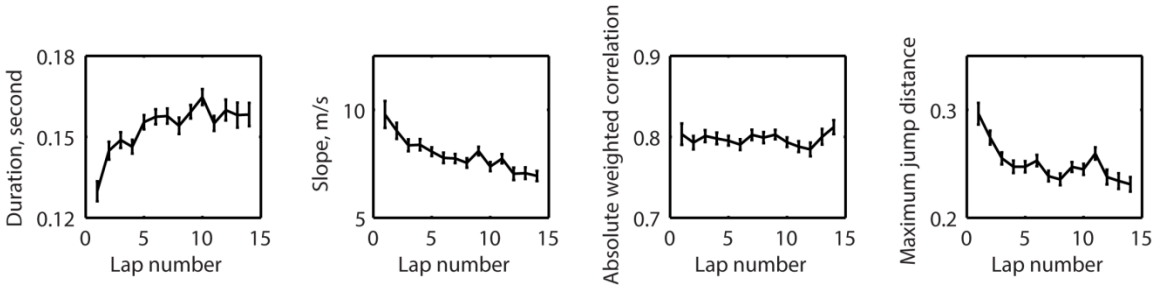

Figure 17. Progressive changes of trajectory events between different laps.

Duration (1st panel), absolute slope (2nd panel), absolute weighted correlation (3rd panel), maximum jump distance (4th panel) for trajectory events in the first 14 laps.

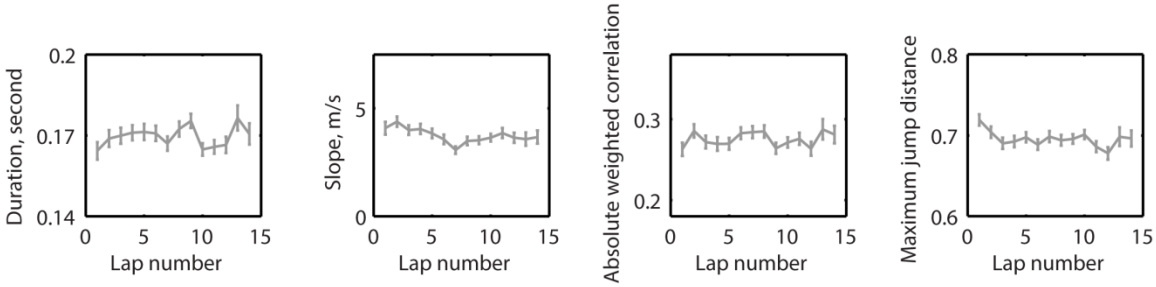

Figure 18. Properties of control events between different laps.

Duration (1st panel), absolute slope (2nd panel), absolute weighted correlation (3rd panel), maximum jump distance (4th panel) for control events in the first 14 laps.

5.3.2 The firing rates and recruitment of hippocampal pyramidal cells during trajectory events are stable throughout experience

Next I examined the dynamics of the spiking activities of individual pyramidal cells during trajectory events. I started with overall firing rates, because an increased propagation speed of replay sequences may result from an increase in overall firing rates of pyramidal cells, as predicted by simple sequence-generation models such as synfire chains (Wennekers and Palm, 1996). However, our data indicated a constant overall firing rate throughout experience (Figure 19b, Pearson's linear correlation coefficient r=-0.001, p=0.96), despite the propagation speed of hippocampal replay decreasing with experience. The average number of spikes emitted by each cell was in proportion to the duration of the trajectory events (Figure 19a, Pearson's linear correlation coefficient r=0.58, $p<10^{-10}$), hence the same pyramidal cell emitted more spikes for trajectory events that occurred late in experience and longer in duration, than for trajectory events that occurred early in experience and shorter in duration (see example cells in Figure 16c-d)

I then asked if the constant overall firing rates co-occur with a stable recruitment of hippocampal place cells for each trajectory event. All place cells were actively participating in trajectory events throughout the session, but different trajectory events recruited different subsets of place cells, as on average 41% of hippocampal place cells were active in each trajectory event (SEM 0.24%). However, the percentage of cell recruitment in each trajectory event did not change with increased experience (Figure 19c, Pearson's linear correlation coefficient r=0.027, p=0.16), that is, pyramidal cells have an equal probability to be active in late replays when the duration is longer, compared with

early replays when the duration is shorter. I also looked at individual cells, and asked if an individual pyramidal cell became more or less active with increased experience (Figure 19d). Only a small fraction of pyramidal cells demonstrated significant changes in activation ratio with experience (217 out of 2142 increased activation ratio, 139 out of 2142 decreased activation ratio; Figure 19d, red bar), whereas the majority of them did not show a significant modulation of activation ratio with experience (Figure 19d, white bar). Taken together, our data suggested that overall firing rate and recruitment of hippocampal place cells during trajectory events are intrinsically determined and are independent of the speed of self-generated sequences.

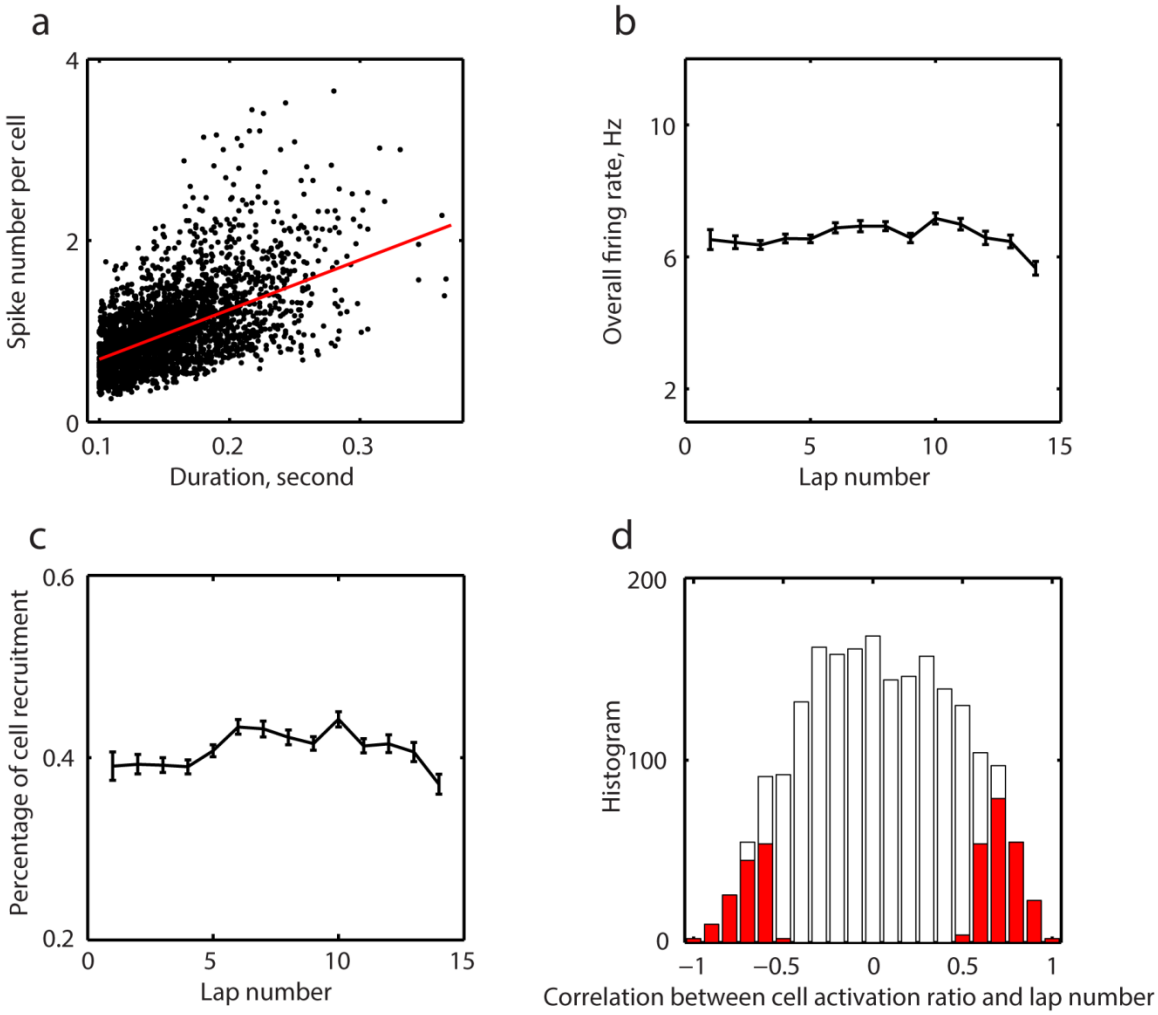

Figure 19. The firing rates and recruitment of hippocampal pyramidal cells are constant throughout experience.

a) Spike number per cell is proportional to the duration of trajectory events. Each dot is a trajectory event. Spike number per cell is the average spike number emitted by the pyramidal cells for each trajectory event. Overall firing rate **b)** and percentage of cell recruitment **c)** stay constant throughout experiences. **d)** Histogram of the correlation between the activation ratio and the lap number for each cell. Red bar indicates significant correlations.

5.3.3 The discretized spatial representation of hippocampal trajectory events is modulated by slow-gamma and experience

My observation of stable place cell firing rate under different speeds of hippocampal replay suggests that a simple sequence-generation model, e.g. synfire chains, is not sufficient for replay generation. Neural network models purely based on heteroassociative connections fail to explain my observation that replay slows down with experience, due to the following two reasons: 1) theoretical work has shown that, sequences of patterns that are stored based on weights reflecting correlations between different patterns ("heteroassociation") suffer from unsustainability, because any noise leads to divergence in subsequent patterns (Sompolinsky and Kanter, 1986); 2) weights between different patterns increase with experience according to the spike-timing-dependent plasticity rule, leading to an increase in the propagation speed of sequences (Zhang, 1996), which is the opposite of what I observed. All these evidence points to more complicated models of replay generation.

A recent publication in Science (Pfeiffer and Foster, 2015) suggested the generation of replay is composed of two components: firstly, autoassociative networks of recurrently excitable neurons store discrete memories as stable activity patterns (attractors) that can rapidly converge; secondly, heteroassociative connections between different autoassociative networks slowly transit patterns of activities between different attractors. This work also provided experimental evidence that the represented spatial trajectory of replay is discretized with segments of slow and fast movement, which, respectively, corresponds to the sharpening of attractors (autoassociation) and the

transitions between attractors (heteroassociation), and which are phase-locked to slow-gamma rhythm (25-50 Hz). Despite providing exciting insight for the current study, this report did not examine replays during early learning. Here I first asked whether replays in a novel environment also represent discretized spatial locations and are modulated by slow-gamma rhythm. And the next logical question I will address is how this hybrid model of autoassociative and heteroassociative neural networks could explain the change of propagation speed of hippocampal replay with experience.

To examine the discretized spatial representation in each replay, I re-decoded the sequence in a finer time scale (time window of 20 ms, moving every 5 ms) and compared the decoded positions between neighboring overlapping time bins. I replicated the finding that decoded trajectories are alternating between immobility and rapid movement, as the decoded moving distances between consecutive decoding frames (Figure 20a, black) can be much smaller (in which consecutive decoding frames represented the same location), or much bigger (in which consecutive frames represented a sequential path of unique positions) than would be predicted by smooth trajectories (Figure 20a, red). I also observed a modulation of decoded moving distance with slow-gamma, with peak moving distance phase-locked to the trough of gamma (Figure 20b). The depth of modulation stayed constant throughout experience (0.027 ± 0.0047, mean ± SEM). Furthermore, I did not observe any progressive changes of instantaneous gamma frequency nor gamma power during trajectory events induced by increased experience (Figure 20d, Pearson's linear correlation coefficient: instantaneous gamma frequency, $r=-8.64*10^{-10}$, p=0.96; z-scored gamma power, r=0.0035, p=0.86).

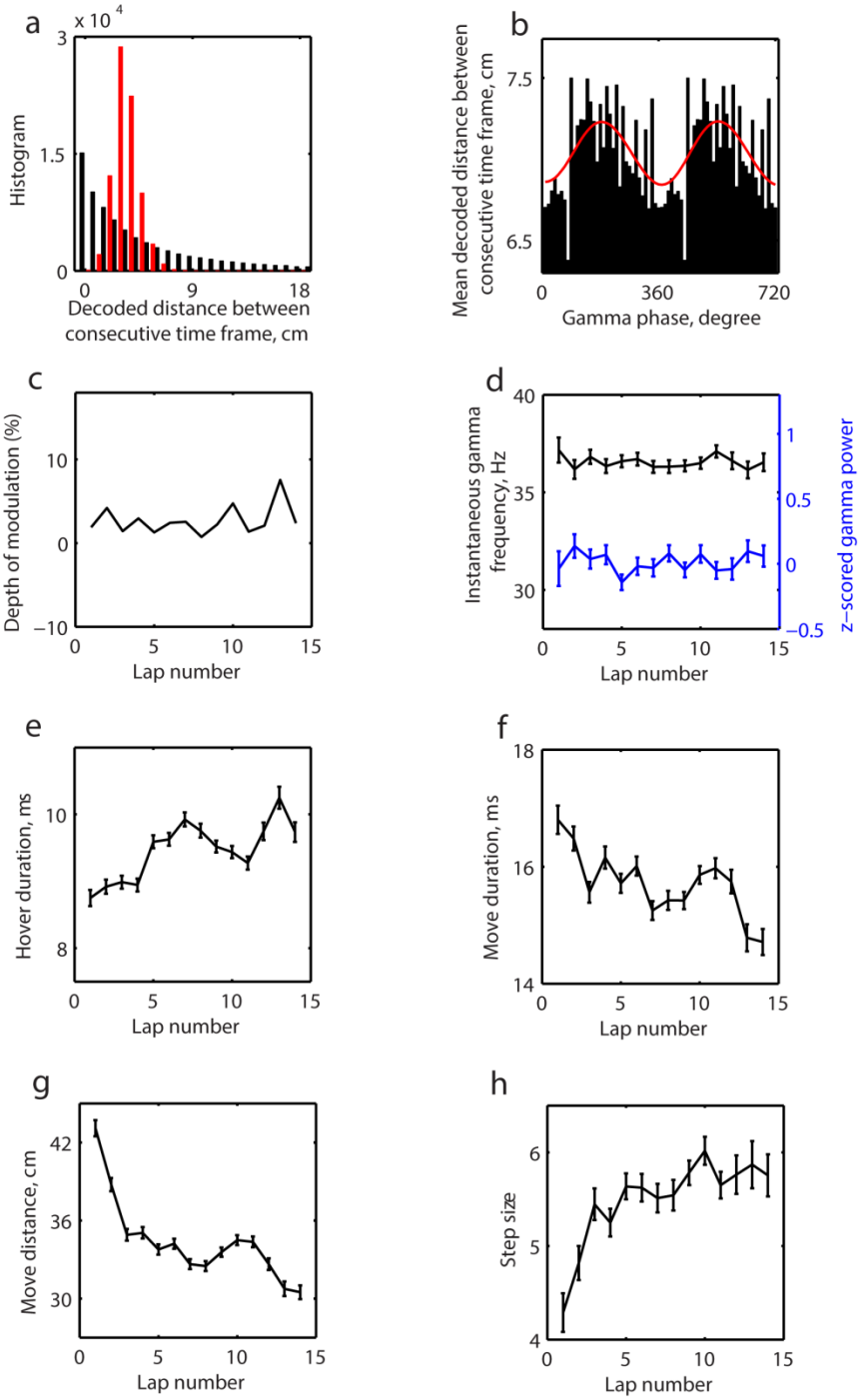

Figure 20. The development of discretized spatial representations of replay with experience.

a) Probability histogram (bin size = 0.9 cm) of distance between neighboring overlapping decoded time bins for all trajectory events. Predicted distances (red) based on hypothesized smooth trajectory. Observed (black) versus predicted populations are significantly different (Kolmogorov-Smirnov test, $P < 10^{-10}$). **b)** For all sessions, across-session neighboring decoded distance as a function of slow-gamma phase (bin size =10 degree) for all trajectory events. Red line indicates the smoothed average. **c)** Depth of modulation of the average neighboring decoded distance by slow gamma oscillation is constant with experience. **d)** Instantaneous gamma frequency and z-scored gamma power is constant with experience. **e)** Hover duration increases with experience. **f)** Move duration decreases with experience. **g)** Move distance decreases with experience. **h)** Step size increases with experience.

I next asked how this discretized spatial representation of replay changes with experience. Firstly I segmented the discretized spatial representation into several stationary epochs (referred to as "hover" in later text and figures) and movement epochs (referred to as "move" in later text and figures), and calculated the duration of each epoch separately. I have showed that the duration of trajectory events increased with experience, thus it is possible that the increase of duration is reflected in either the duration of the stationary epoch, or of the movement epoch, or of both (Figure 21a). However, I have also demonstrated that the transition between stationary and movement epochs is phase-locked to gamma rhythm. The duration increase of either "hover" or "move" should correlate with an increase of the duration of each gamma cycle, and a decrease of the frequency of slow gamma oscillations (Figure 21a). Because gamma frequency is constant throughout experience, increase of duration in both "hover" and "move" is unlikely; rather, the duration of "hover" and "move" has to be constant or change in different directions (for example, hover duration increases while move duration decreases, or vice versa; Figure 21b). Indeed, when looking at the duration of "hover" and "move" on different running laps, the former increased with experience (Figure 20e, Pearson's linear correlation coefficient, $r=0.03$, $p<10^{-10}$), whereas the latter decreased (Figure 20f, Pearson's linear correlation coefficient, $r=-0.02$, $p<6.18*10^{-10}$), and the gross increase of "hover" duration precisely matched the gross decrease of "move" duration. Because the change of duration in "hover" and "move" counterbalanced each other, the increased duration of hippocampal replay has to be reflected by an increased number of alternations (referred to as "step size" in later text and figure) between stationary and movement epochs (Figure 21c). And because the spatial representation of all my detected replays is

restricted to the length of the track, the distance of movement during each “move” segment has to decrease in proportion to the increased number of alternating segments (Figure 21c). Indeed, our data fits all the above predictions and demonstrated a decreased move distance and an increased step size with experience (Figure 20g, move distance, Pearson's linear correlation coefficient, $r=-0.06$, $p<10^{-10}$; Figure 20h, step size, Pearson's linear correlation coefficient, $r=0.1$, $p=2.02*10^{-7}$); additionally, the product of move distance and step size matched the total length of the track.

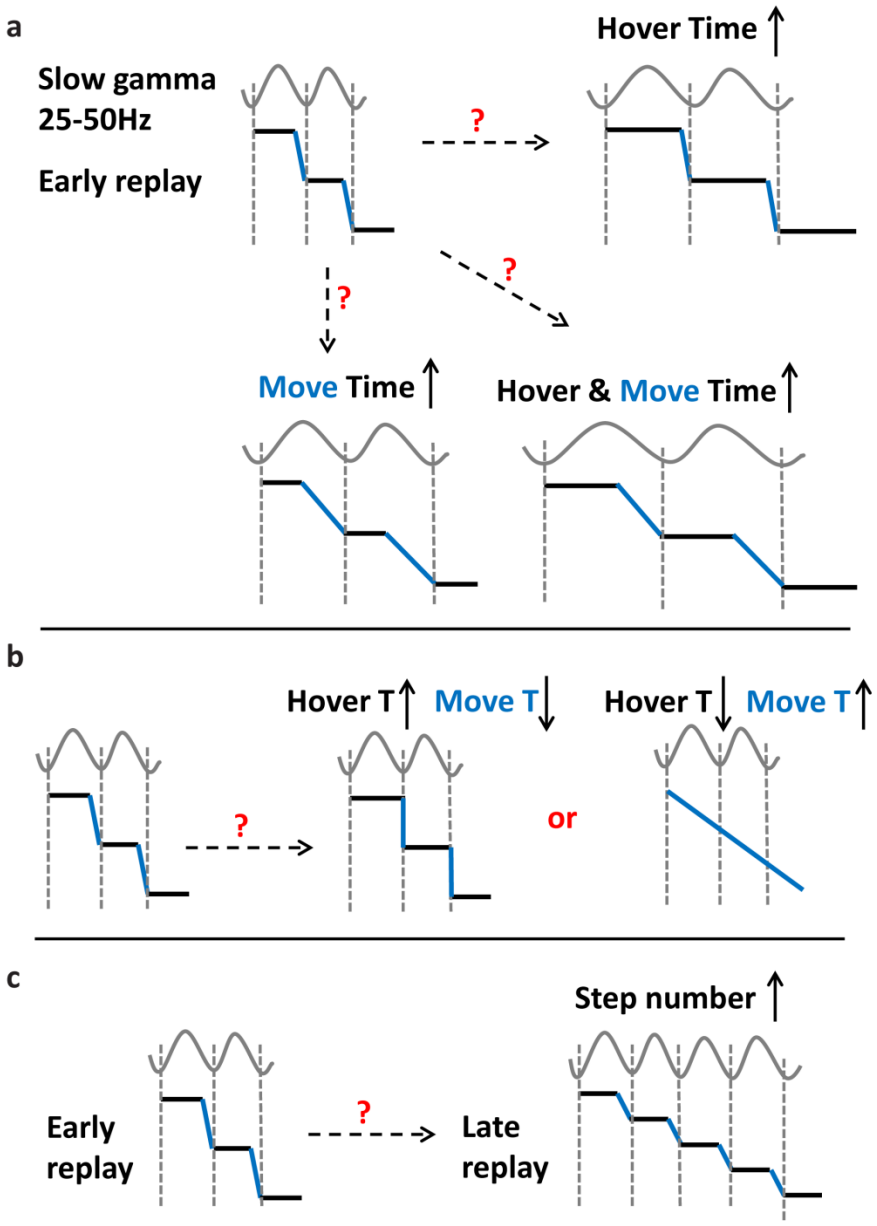

Figure 21. Hypotheses of how the discretized spatial representations of trajectory events change with experience.

a) If the spatial representations of replay in a novel environment are discretized with alternating static ("hover") and rapid movement ("move") segments and phase-locked to slow gamma, then the duration increase of each or both segments can result in the change

of speed of replay. However, these scenarios predict a decrease in gamma frequency. **b)** A counterbalanced duration change of "hover" and "move" segments leads to an unchanged gamma frequency. In the extreme case, replay will either depict a perfect step-wise trajectory or a perfect smooth trajectory. **c)** Alternatively, an increased number of alternating steps of "hover" and "move" can result in a decrease of replay speed, without prerequisites of changes in gamma frequency or the duration of "hover"/"move".

Overall, our data fits the prediction of the slow-gamma governed hybrid model of autoassociative and heteroassociative neuronal networks. I not only reported that the spatial representation in replays are discretized and phase-locked to slow gamma during early learning, but also provided physiological evidence that different discretized segments change differently with experience, corresponding to their respective neural networks. With learning, the synaptic connections in both autoassociative and heteroassociative neuronal networks strengthened. As a result the "attractors" are more stable and difficult to "escape" (reflected in an increase of duration of "hover"), and the transitions between different "attractors" become faster (reflected in a decrease of the duration of "move"). With strengthened synaptic connections between neurons, more "attractors" emerged (more autoassociative networks become stable), resulting in a more discretized and detailed spatial representation of replay (reflected in the increase of alternations between static and movement epochs).

5.4 Discussion

Examining hippocampal neural activities during the initial stage of learning is critical for understanding the neural mechanisms underlying learning and memory. Although progressive changes in run-time place cell activities have been reported, such as the development of place field skewness (Mehta et al., 2002), and of theta sequences across place cells (Feng et al., 2015), this is the first report of a progressive change in the trajectory structure of replay sequences. And unlike other plasticity changes that can complete rapidly, for example within minutes, the trajectory structure of replay

progressively changes throughout, and potentially beyond, the first fourteen experiences, which can occur during the time frame of half an hour or more, depending on the animal's running speed and the behavioral task.

Previous studies have examined spike reactivations of place cells during early learning, but never directly examined the modulation of experience on the spatial trajectories represented in these spike reactivations. For example, Cheng and Frank (2008) reported spiking between novel arm cells during reactivation was more precisely timed than that of familiar arm cells. This result can be related with ours; because I have reported a faster propagation speed of replay during early learning, with the implication that place cells with overlapping place fields have tighter temporal relationship in their spiking sequences. However, because Cheng and Frank (2008) did not examine the spatial representations of these spike reactivations and did not distinguish trajectory events from other candidate events, their results are not specific to hippocampal replay. An alternative trivial explanation of their results can be the higher ratio of trajectory events to candidate events in novel versus familiar environments, as suggested by previous studies (Foster and Wilson, 2006). Only trajectory events, but not other candidate events, are equipped with a precisely controlled temporal order of spike timings between neurons, so a higher percentage of trajectory events in the candidate events pool will naturally produce tighter averaged temporal relationships, between neurons across all the candidate events in novel versus familiar environments. In contrary, my study examined trajectory events exclusively; further I examined fast plasticity

changes on a lap-by-lap basis, which provides more detailed information than examining between days as in Cheng and Frank (2008).

Sequential run-time place cell activities such as hippocampal theta sequences has been suggested to play a role in driving plasticity during the initial stage of learning, but they are not the only type of spiking sequences that exist during early experience. I have shown that hippocampal replays occurred immediately after the first running experience, and the progressive change of the represented trajectory occurred on the level of single experiences. Hippocampal replay propagated faster during initial learning, indicating a tighter temporal relationship between place cells with overlapping place fields during spike reactivation associated with novelty, which is well suited to induce synaptic plasticity in the hippocampal-cortical network. Hippocampal replay is less compressed in the temporal domain when there is less to be learned (for example in a familiar environment), and contains more discrete locations in its represented space when the animal is highly experienced. The more detailed spatial representation of replay during late experience may reflect the process of learning (for example, an individual is able to remember every bus stop when he/she gets familiar with the bus route); similarly, and pending experimental proof, the more temporally compressed and coarse spatial representation of trajectory events during early experience may be consistent with the notion that during the initial stage of learning, critical events, such as important landmarks in this experiment, are the first to be learned.

In addition to providing insights into the function of replay, our data may also be informative about the mechanisms underlying replay generation. In particular, these

results are inconsistent with certain models of neuronal sequence generation, such as synfire chains (Wennekers and Palm, 1996), or dynamical attractor models without dynamic inhibition (Samsonovich and McNaughton, 1997; Tsodyks, 1999), which predict that the speed of sequence transmission during replay should correlate positively with firing rate, or positively with synaptic strength between place cells representing adjacent locations in space (Zhang, 1996). Instead I have reported a decreased propagation speed of replay with experience, coupled with constant place cell firing rates and a more detailed structure of trajectory events. The first of such report of discretized spatial representation in replay is from a recent Science article (Pfeiffer and Foster, 2015), where the authors proposed the following mechanism: the attractor produced by the autoassociative networks within CA3 recurrent synapses (Lisman, 1999) oscillates its strength between high levels of activity (focusing the neural representation on a "unit" of information, such as a single location in space) and low levels of activity (weakening the attractor dynamics to allow transition to a different unit) at the slow-gamma frequency; whereas the heteroassociative network with connectivity between other hippocampal areas and CA3 enables the transition between different attractors at the switch of slow-gamma. My results provided further support to this theory from the perspective of plasticity-induced changes during early learning, with the following evidence: 1) slow gamma with a constant frequency governs the discretized structure of trajectory events at all learning stages, in that each discretized "unit"- a pair of stationary and movement epochs – is constant in total duration that corresponds to a slow-gamma cycle; 2) the decrease of the propagation speed of replay is due to the increase of discretization of the structure of trajectory events, which is consistent with the notion that more attractors

become stable within CA3 recurrent network with increased experience; 3) under the same notion, neural activity "lingers" longer over group of place cells representing the same location before propagating to the next neural group in replay during late experience; 4) the strengthening of heteroassociative connections between other hippocampal areas and CA3 neurons with increased experience speeds up the transition between neural groups that represent different locations, hence counterbalancing the increased time of "linger" within groups. Overall, my study highlights the importance of slow-gamma rhythm and multiregional hippocampal loop in learning and memory.

In conclusion, hippocampal replays undergo rapid plasticity with experience, and may play a role in the initial formation of spatial memories; the change of propagation speed of place cell activations during replay is independent of firing rate, and may reflect internal changes of hippocampal neural network.

Chapter 6 — Summary and implications

6.1 Summary and discussions of the functional role of hippocampal place cell sequences

The hippocampus has long been suggested to function as a cognitive map (O'Keefe and Nadel, 1978a), where unique locations of the space are stored in different place cells, and together they allow an individual to acquire, store, recall and decode information about the relative locations to guide future behavior. This dissertation focuses on a particular pattern of hippocampal place cell activities, the place cell sequences, which we hypothesize are the "carrier" of episodic memories. I am particularly interested in the phase of early learning, and investigated how learning and increased experience modulate these place cell sequences.

I have presented two different types of hippocampal place cell sequences, theta sequences (chapter 3) and hippocampal replay (chapter 4 and 5). These two types of place cell sequences have many similarities and differences. First, by definition, both are patterns of activities from groups of hippocampal place cells that possess temporally compressed, precisely controlled, spike timing relationships between individual cells. However, theta sequences and hippocampal replay occur under different behavior and brain states. Theta sequences are short place cell sequences, which recruit small numbers of locally activated place cells under the "theta" brain state, during an animal's active exploration. In contrast, hippocampal replays are "offline" long sequences, which recruit a larger population of neurons co-occurring with sharp-wave ripples.

In this dissertation, I have discovered many new features of theta sequences and hippocampal replay from the perspective of their experience-dependent development (Figure 22). Four key aspects of the new features are now summarized: (i) neither theta sequences nor hippocampal replay can exist prior to experience; (ii) a very brief exposure to a new environment, such as a single running experience on a linear track, is sufficient to induce both theta sequences and hippocampal replay; (iii) the strength of theta sequences stay constant once established, whereas hippocampal replay is continuously modulated by individual experiences; (iv) the development of theta sequences may require macroscopic organization of place cells between different regions of hippocampus; similarly, the progressive change of hippocampal replay is modulated by global slow-gamma oscillation across the dorsal CA1 area of hippocampus.

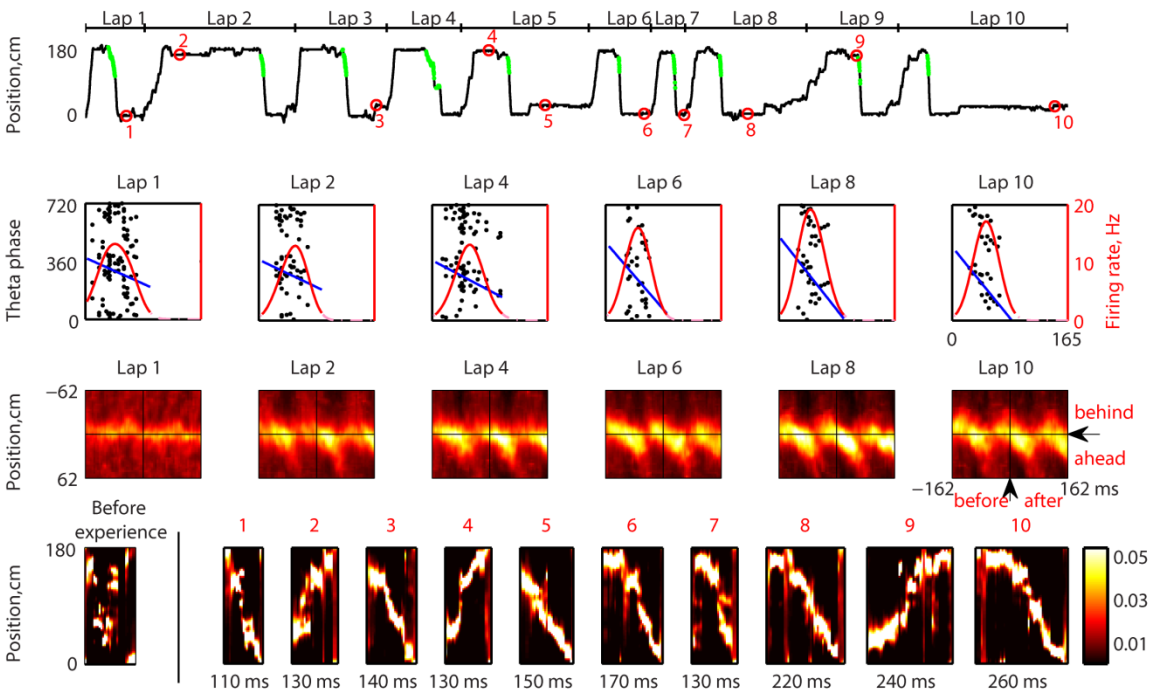

Figure 22. Individual neuronal phase precession, theta sequences and hippocampal replay with different levels of experience.

First row, running trajectory of the first ten laps of the animal. Red circles mark the time of occurrence of the example trajectory events shown in bottom row. Green dots mark the time of occurrence of the spikes from the example cell shown in 2nd row. **Second row**, phase precession of an example place cell during lap 1, 2, 4, 6, 8 and 10. Each spike has been plotted out twice on the corresponding theta phase, and the phase plus 360 degrees, for ease of visualization. Red solid line, firing rate more than 1 Hz; red dashed line, firing rate less than 1 Hz. Blue line, fitted line of phases with positions. **Third row**, theta sequences from the same session. Averaged decoded probabilities over 125 cm centered by the animal's current running position, aligned by the animal's current running direction during 325 ms centered by the mid-time point of theta sequence for lap 1, 2 , 4, 6, 8 and 10. **Fourth row**, examples of hippocampal replays. No trajectory events were

observed prior to experience (the first example). The remaining examples are decoding of the ten trajectory events marked in 1st row. Colorbar on the right indicates the scale of probability estimates.

Theta sequences and hippocampal replays share similar functions. They have been suggested to be important in early learning, particularly in encoding episodic memory (Foster and Knierim, 2012), because the precise spike timing relationship between neighboring place cells in both types of sequences adheres to the spike-timing-dependent plasticity (STDP) rule (Feldman, 2012), and is well suited to promote plasticity.

This dissertation provides further evidence for the above functional role of place cell sequences, as I have demonstrated that both theta sequences and hippocampal replay develop very rapidly with learning, and persist throughout the early learning experience. Notably, both theta sequences and hippocampal replays developed exclusively from a single experience, in the time scale of seconds, indicating the hippocampal neuronal network undergoes a rapid and efficient plasticity change during early learning. This plasticity change contrasts with the experience-independence of individual neuronal phase precession. This evidence further supports that, it is the order of activities between individual neurons, not the activity of independent neurons, which is being learned and stored, in the weights matrix of synaptic connections within the hippocampal neuronal network, which reflects the encoding of episodic memory.

More broadly, the functional roles of hippocampal place cell sequences support the hippocampus as a model system for cognitive processes involving episodic memory. I have demonstrated in this dissertation that the formation of hippocampal place cell sequences requires experience, however hippocampal place cell sequences are not exclusively a function of experience, as they are not always “faithful” or “stereotyped”

playbacks of past experiences. Even in an environment as simple as the linear track, I have observed variability among individual theta sequences, and among individual hippocampal replays, which cannot be explained by experience, for example the spatial representations of hippocampal replays occurred after the same degree of running experience are not "exact" copies (chapter 5). Notably, even though animals' running behavior on a linear track is very stereotyped, (they do not tend to stop in the middle of the track), different locations along the track are selectively expressed as static representations in different replays (chapter 5).

Furthermore, previous reports have demonstrated that the hippocampus can generate place-cell sequences in an order that has never been experienced (Foster and Wilson, 2006; Diba and Buzsaki, 2007a; Davidson et al., 2009; Karlsson and Frank, 2009a; Gupta et al., 2010), and sequences that depict not yet experienced trajectories (Gupta et al., 2010; Pfeiffer and Foster, 2013), in particular, novel paths to a remembered goal (Pfeiffer and Foster, 2013). The trajectories depicted by theta sequences have also been suggested to reflect goal locations (Johnson and Redish, 2007; Gupta et al., 2012; Wikenheiser and Redish, 2015).

My new observations, combined with previous reports, raise the possibility that the encoding of hippocampal place cell sequences is an active learning process of the spatial structure in the environment, and the reactivation of hippocampal place cell sequences might function as an information retrieval process from the stored cognitive map to guide future behavior and decision making.

6.2 Discussions of the neural mechanisms and computational models of hippocampal place cell sequences

This dissertation also suggests interesting neural mechanisms underlying the generation of hippocampal place cell sequences. Classical Hebbian STDP (spike-timing-dependent Plasticity) supports learning of temporal sequences (Abbott and Blum, 1996; Blum and Abbott, 1996; Rao and Sejnowski, 2001a, b), because sequential activation of neurons drives LTP (Long-Term-Potentiation) at synapses in the forward direction and LTD (Long-Term-Depression) in the reverse direction, consequently creating directional connections. These asymmetric synaptic connections within hippocampal recurrent networks, once properly triggered, can generate learned sequences in the form of theta sequences (such as those triggered by the activation of local place cells), or hippocampal replay (such as those triggered by changes of global inhibition in the neuronal network during SWRs events). With repeated occurrence of theta sequences and hippocampal replays, the asymmetric synaptic connections further strengthened in the direction of the sequence propagation, thus resulting in more robust retrieved sequences.

However, in this dissertation, I report a divergence of STDP rule. As I have shown in chapter 3, during the initial experience, the activities of place cells with overlapping place fields follow their behavior order, but the exact spike timing within each theta cycle was initially disorganized. This observation violates the STDP rule, which requires that presynaptic neurons fire in close temporal proximity, but prior to, the postsynaptic neurons to drive LTP (Feldman, 2012). Nevertheless, my results suggested that under this violation, neighboring place cells were still able to form strengthened

synaptic connections to the direction that the animal is running from after the first experience, to subsequently induce organized spike timing in each theta sequence, or in spontaneous "offline" hippocampal replay sequences.

This apparent divergence of the STDP rule would be puzzling if one neglects the distinctive influence of neuromodulators on STDP rules. Specifically, neuromodulatory systems can influence STDP rules by acting via dopaminergic, noradrenergic, muscarinic, and nicotinic receptors, which can change the threshold for plasticity induction (Pawlak et al., 2010). In particular, a recent study has reported that dopamine increased the sensitivity and decreased the temporal contrast of STDP in hippocampal synapses in vitro (Zhang et al., 2009). Under the presence of dopamine, normally ineffective weak stimuli with fewer spike pairs, or with larger temporal delay between the spike pair, can induce significant LTP. Most strikingly, dopamine can convert the stimuli pair that would normally result in LTD into inducing LTP.

If this phenomenon holds true *in vivo*, place cells with overlapping place fields can form strengthened synaptic connections in the direction that the animal is running, despite the disorganized spike timing of individual neurons within each theta cycle. More experiments are required to directly test this hypothesis, for example to test if a dopamine antagonist prevents the generation of theta sequences in a novel environment; nevertheless such a hypothesized mechanism is not unlikely. The hippocampus receives reward-related information from dopamine-releasing ventral tegmental area (VTA) neurons (Schultz, 2000), and studies have reported novelty-induced activities of dopaminergic neurons in VTA (Lisman and Grace, 2005), as well as dopamine-receptor-

dependent, novelty-induced sensitivity increase of LTP at hippocampal CA1 synapses (Li et al., 2003). Taken together, a neural mechanism that links both STDP and reward-mediated learning may play a role in the generation of hippocampal place cell sequences.

When discussing the molecular mechanisms of synaptic plasticity, NMDA receptors need to be considered. The NMDA receptors have long been identified as a key mechanism underlying many forms of synaptic plasticity (Malenka and Bear, 2004), and have been implicated directly in the formation of hippocampal dependent memories (Morris, 1989; Shapiro and Caramanos, 1990; Steele and Morris, 1999).

In this dissertation, I did not include findings that the development of hippocampal replay depends on the activity of the NMDA receptors, which, together with the content in chapter 4 is a paper published in Nature Neuroscience (Silva et al., 2015). My collaborator Dr. Delia Silva and I reported that the blockage of NMDA receptors prevented the generation of hippocampal replay of a new environment, whereas replays of previously learned environments were intact, and remarkably can be preserved as long as some 5 h after the initial experience. Thus, the NMDA receptors were required for the encoding, but not retrieval, of hippocampal trajectory events, which is consistent with previous literature (Morris, 1989; Shapiro and Caramanos, 1990; Bannerman et al., 1995; Steele and Morris, 1999). We also reported a discrepancy in the effect of NMDA receptor blockade on individual place cells and place cell sequences, further suggesting that ensemble-level place cell sequences, not individual neurons, reliably predict memory function.

This dissertation further provides insights on computational models of the generation of hippocampal place cell sequences. In chapter 3, I extensively discussed how the "pace-maker" model and "ensemble" model lead to different predictions of the experience dependence of individual neuronal phase precession and/or ensemble-level theta sequences, and provided direct experimental evidence that phase precession and theta sequences are dissociable phenomena which may correspond to different computational models. In chapter 4, I focused on the experience-dependence of hippocampal replay, and reported an absence of pre-configured sequences prior to experience. This discovery is of great importance to the field because demonstrating that hippocampal replay is a learned sequence aligns with its role in encoding and retrieving episodic memory.

In chapter 5, I examined the relationship between the propagation speed of hippocampal place cell sequences and individual neuronal activities, and demonstrated a discrepancy that would not be expected by classic computational models. Specifically, if the generation of hippocampal place cell sequences is purely based on the directional connections between neurons induced by synaptic plasticity, as discussed in chapter 5, it is expected that the propagation speed of hippocampal place cell sequences positively correlates with the activity level of individual neurons. However, I reported a decreased speed of the sequence propagation, which is independent of place cell firing rates. Furthermore, according to the STDP rule, the directional connections should be strengthened with both increased experience and repetitive occurrence of hippocampal place cell sequences. These strengthened directional connections should lead to speeding

up of the sequence, as opposite to my observation of a decrease in speed. All these elements of evidence suggest that heteroassociative neural networks are not sufficient for the generation of hippocampal place cell sequences. Thus in chapter 5, I introduced a hybrid model of hetero- and auto-associative neural networks, which involves the hippocampal CA3 recurrent network ("autoassociation") and other feed-forward networks ("heteroassociation"), to account for the progressive changes of the speed of hippocampal replay that I observed.

6.3 Future experiments

The current dissertation thoroughly examined the experience-dependence of hippocampal place cell sequences, and asked how learning modulates the neuronal activities in these sequences. My discoveries support that hippocampal place cell sequences are the result of learning, and are themselves "carriers" of episodic memories. More experiments can be done to further enrichment this conclusion.

For example, chapter 3 and 5 focus on examining progressive changes of hippocampal place cell sequences while the animal is awake but not during sleep. One interesting experiment is to quantify the minimum amount of experience that is required to induce hippocampal replay during the subsequent sleep. We know that a single experience is sufficient to induce awake hippocampal replay, but is it also sufficient to induce subsequent sleep replay? To address this, animals might be immediately picked up and placed into sleep box after a single running lap (or traverse) of the novel linear track. After an extended sleep session, animals can be placed back on the same linear track and

allowed to run for a sufficient number of laps for reliable place field reconstruction. One can first ask if a single running experience can induce subsequent sleep replay; if not, how many individual experiences are required? One can also ask whether the occurrence of awake SWRs events or awake hippocampal replays, or the presence of a reward, is a prerequisite for the generation of subsequent sleep replay. Further, in our Nature Neuroscience paper we have demonstrated sleep replays can be observed approximately 5 h after the first experience of a novel environment (Silva et al., 2015), thus it will be interesting to know if a single exposure to the environment can also induce sleep replay into extended hours.

In addition to further testing how rapidly or efficiently experience can induce hippocampal place cell sequences under different conditions, more experiments can be designed to further address the functional roles of hippocampal place cell sequences in episodic memory. I have discovered that the spatial representation of hippocampal replays are composed of extended static representations of different locations which can be modulated by experience. But I do not know whether those static representations of locations correspond to particular landmarks, or to locations of cognitive importance to the animal. This question may be addressed by carefully manipulating the local or distal cues in the environment.

Furthermore, as discussed before, we hypothesized hippocampal replay is a cognitive "readout" of the learned spatial structure/contingency of the environment. It will be interesting to examine the dynamics of spatial representations of hippocampal replay upon changing of the contingency of the environment. For example, removing a

small barrier in a maze may not change much of the overall spatial structure, but may create a "short-cut" that may be of important behavioral relevance for the animal. If our hypothesis that the hippocampal replays encode spatial contingency rather than "videotape" previous experiences holds true, this "short-cut" trajectory should be reflected in the spatial representation of the subsequent hippocampal replay.

6.4 Other general discussions

Beyond supporting the functionality of hippocampal place cell sequences in episodic memory, this dissertation has revealed the existence of rich dynamics between individual sequences. It has been known that hippocampal replay may represent different trajectories in the environment (Davidson et al., 2009; Pfeiffer and Foster, 2013), and here I reported for the first time that the details in the trajectories can be different even when they traverse the same distance of space (chapter 5). I have reported that the richness in the details of the trajectory is correlated with experience, yet we still do not know what governs the minor differences between trajectory events that happened after acquiring the same amount of experience (for example Figure 15 b and c). Similarly, I reported small variations between the strength of individual theta sequences in chapter 3.

All these observations suggest that the generation of hippocampal place cell sequences is a dynamic process. Interestingly, other perspectives of neuronal activities during hippocampal place cell sequences are incredibly robust. For example, the firing rates of place cells during hippocampal trajectory events are constant, regardless of the duration of the reactivations. Trajectory events recruit different place cells between

different reactivations, yet the percentage of cell recruitment is constant. All these lines of evidence suggest that a precisely-configured hippocampal neuronal network is behind the functionality of hippocampal place cell sequences in episodic memory. Overall, it is important that the hippocampal neuronal activity is maintained in balance between variations and consistency, which enables both flexibility and robustness of the memory functionality of hippocampus.

The hippocampus is not acting by itself when generating place cell sequences. As discussed in chapter 1, the hippocampus has extensive connections with many other brain areas, and together they carry sophisticated cognition and behavior. It has been reported that the sensory cortex was co-activated during hippocampal SWRs events, for example neurons in visual cortex were "replaying" the same experience as hippocampal place cell sequences (Ji and Wilson, 2007). Interestingly, external stimulation from sensory cortex can bias "offline" reactivation of hippocampal place cell sequences (Bendor and Wilson, 2012). Together these results suggest that the hippocampus and sensory cortex are acting together for the functionality of memory consolidation. It has also been reported that neurons in subcortical areas such as ventral striatum are theta-modulated, and demonstrated robust phase precession relative to the hippocampal theta rhythm, co-occurring with hippocampal theta sequences (van der Meer and Redish, 2011). Because the ventral striatum is important in encoding information regarding rewards, its interactions with the hippocampus during the theta brain wave suggest that these regions contribute together to the learning and expression of associations between places and rewards, which is important for future decision-making.

Finally, all three projects discussed in this dissertation, the development of theta sequences with experience (chapter 3), the dependence of hippocampal replays on experience (chapter 4), and the progressive changes of hippocampal replays induced by experience (chapter 5), required extensive data analysis. Many of the key findings are supported by the robust analytical methods I developed, which can be generalized to address other questions in studies using similar single-unit recording techniques. For example, single-lap decoding improved decoding accuracy during early learning, and was used in reconstructing the theta sequence structure in chapter 3. Although this method was developed for a control analysis to exclude potential confounding factors, such as the instability of place cells in a novel environment, it might be generally useful for "instantaneous" decoding when a stable spatial representation from ensemble place cells is difficult to achieve, for example when the environment is constantly changing. Under the circumstances that a stable ensemble code is established for the environment, single-lap decoding may still be useful in revealing small modulations of neuronal activities by individual experiences. For instance, if we are interested in examining whether a particular running experience can affect hippocampal replay, single-lap decoding can produce reliable probability estimates of the represented spatial trajectories, with the large number of place cells we simultaneously recorded.

Another powerful method I developed is the quadrant analysis for hippocampal trajectory events (chapter 4). Not all the candidate events depict trajectories of the current environment (in our data less than 20% of candidate events are trajectory events), therefore it is critical to develop a reliable and accurate method for the detection of

trajectory events. By carefully comparing the neuronal activities before and after experience, I identified two quantification methods – absolute weighted correlation, and maximum jump distance - that best captured the differences of spatial representations of ensemble place cells before and after experience. Furthermore, instead of choosing a single detection threshold for each of the quantification methods, I searched the parameter space extensively, and achieved a visualization of the Monte-Carlo significance matrix, which demonstrated distinctive patterns between before and after experience, and between NMDA-receptor-antagonist treated animals and control animals. I also verified the quadrant analysis by generating control data sets from both homogeneous Poisson simulations and randomly swapping the time windows of the decoding. Even though this quadrant analysis was built on a rich dataset (abundant SWRs in a novel environment), and a powerful neuron decoder (large number of simultaneously recorded cells), this method should be of general guidance to the field for how to reliably identify hippocampal trajectory events.

To conclude, in this dissertation I investigated the neural substrate of learning and memory, in the form of hippocampal place cell sequences, examined their formation and progressive changes with experience, and discussed the underlying neuronal mechanism. This dissertation should contribute significantly to the field of hippocampal functionality and its neurobiology basis.

References

Abbott LF, Blum KI (1996) Functional significance of long-term potentiation for sequence learning and prediction. Cereb Cortex 6:406-416.

Abbott LF, Nelson SB (2000) Synaptic plasticity: taming the beast. Nat Neurosci 3 Suppl:1178-1183.

Andersen P, Morris R, Amaral D, Bliss T, O'Keefe J (2006) The hippocampus book: Oxford University Press, USA.

Bannerman DM, Good MA, Butcher SP, Ramsay M, Morris RG (1995) Distinct components of spatial learning revealed by prior training and NMDA receptor blockade. Nature 378:182-186.

Bear MF, Malenka RC (1994) Synaptic plasticity: LTP and LTD. Curr Opin Neurobiol 4:389-399.

Bendor D, Wilson MA (2012) Biasing the content of hippocampal replay during sleep. Nat Neurosci 15:1439-1444.

Berens P (2009) CircStat: A MATLAB Toolbox for Circular Statistics. J Stat Softw 31:1-21.

Best PJ, White AM, Minai A (2001) Spatial processing in the brain: the activity of hippocampal place cells. Annu Rev Neurosci 24:459-486.

Bi GQ, Poo MM (1998a) Synaptic modifications in cultured hippocampal neurons: dependence on spike timing, synaptic strength, and postsynaptic cell type. J Neurosci 18:10464-10472.

Bi GQ, Poo MM (1998b) Synaptic modifications in cultured hippocampal neurons: Dependence on spike timing, synaptic strength, and postsynaptic cell type. Journal of Neuroscience 18:10464-10472.

Blum KI, Abbott LF (1996) A model of spatial map formation in the hippocampus of the rat. Neural Comput 8:85-93.

Brandon MP, Bogaard AR, Libby CP, Connerney MA, Gupta K, Hasselmo ME (2011) Reduction of theta rhythm dissociates grid cell spatial periodicity from directional tuning. Science 332:595-599.

Breakspear M, Heitmann S, Daffertshofer A (2010) Generative models of cortical oscillations: neurobiological implications of the Kuramoto model. Front Hum Neurosci 4.

Burgess N, Barry C, O'Keefe J (2007) An oscillatory interference model of grid cell firing. Hippocampus 17:801-812.

Buzsaki G (1989) Two-stage model of memory trace formation: a role for "noisy" brain states. Neuroscience 31:551-570.

Buzsaki G (2002) Theta oscillations in the hippocampus. Neuron 33:325-340.

Buzsaki G, Leung LW, Vanderwolf CH (1983) Cellular bases of hippocampal EEG in the behaving rat. Brain Res 287:139-171.

Buzsaki G, Horvath Z, Urioste R, Hetke J, Wise K (1992) High-frequency network oscillation in the hippocampus. Science 256:1025-1027.

Carr MF, Jadhav SP, Frank LM (2011) Hippocampal replay in the awake state: a potential substrate for memory consolidation and retrieval. Nat Neurosci 14:147-153.

Carr MF, Karlsson MP, Frank LM (2012) Transient slow gamma synchrony underlies hippocampal memory replay. Neuron 75:700-713.

Cheng S, Frank LM (2008) New experiences enhance coordinated neural activity in the hippocampus. Neuron 57:303-313.

Colgin LL, Moser EI, Moser MB (2008) Understanding memory through hippocampal remapping. Trends Neurosci 31:469-477.

Corcoran KA, Desmond TJ, Frey KA, Maren S (2005) Hippocampal inactivation disrupts the acquisition and contextual encoding of fear extinction. J Neurosci 25:8978-8987.

Corkin S (2013) Permanent present tense: The unforgettable life of the amnesic patient: Basic books.

Csicsvari J, O'Neill J, Allen K, Senior T (2007) Place-selective firing contributes to the reverse-order reactivation of CA1 pyramidal cells during sharp waves in open-field exploration. Eur J Neurosci 26:704-716.

Davidson TJ, Kloosterman F, Wilson MA (2009) Hippocampal replay of extended experience. Neuron 63:497-507.

Diba K, Buzsaki G (2007a) Forward and reverse hippocampal place-cell sequences during ripples. Nat Neurosci 10:1241-1242.

Diba K, Buzsaki G (2007b) Forward and reverse hippocampal place-cell sequences during ripples. Nat Neurosci 10:1241-1242.

Dragoi G, Buzsaki G (2006) Temporal encoding of place sequences by hippocampal cell assemblies. Neuron 50:145-157.

Dragoi G, Tonegawa S (2011) Preplay of future place cell sequences by hippocampal cellular assemblies. Nature 469:397-401.

Dragoi G, Tonegawa S (2013) Distinct preplay of multiple novel spatial experiences in the rat. Proc Natl Acad Sci U S A 110:9100-9105.

Dragoi G, Tonegawa S (2014) Selection of preconfigured cell assemblies for representation of novel spatial experiences. Philos Trans R Soc Lond B Biol Sci 369:20120522.

Ego-Stengel V, Wilson MA (2010) Disruption of Ripple-Associated Hippocampal Activity During Rest Impairs Spatial Learning in the Rat. Hippocampus 20:1-10.

Ekstrom AD, Meltzer J, McNaughton BL, Barnes CA (2001) NMDA receptor antagonism blocks experience-dependent expansion of hippocampal "place fields". Neuron 31:631-638.

Feldman DE (2012) The Spike-Timing Dependence of Plasticity. Neuron 75:556-571.

Feng T, Silva D, Foster DJ (2015) Dissociation between the Experience-Dependent Development of Hippocampal Theta Sequences and Single-Trial Phase Precession. J Neurosci 35:4890-4902.

Ferino F, Thierry AM, Glowinski J (1987) Anatomical and Electrophysiological Evidence for a Direct Projection from Ammons Horn to the Medial Prefrontal Cortex in the Rat. Exp Brain Res 65:421-426.

Foster DJ, Wilson MA (2006) Reverse replay of behavioural sequences in hippocampal place cells during the awake state. Nature 440:680-683.

Foster DJ, Wilson MA (2007) Hippocampal theta sequences. Hippocampus 17:1093-1099.

Foster DJ, Knierim JJ (2012) Sequence learning and the role of the hippocampus in rodent navigation. Curr Opin Neurobiol 22:294-300.

Frank LM, Stanley GB, Brown EN (2004) Hippocampal plasticity across multiple days of exposure to novel environments. Journal of Neuroscience 24:7681-7689.

Fyhn M, Hafting T, Treves A, Moser MB, Moser EI (2007) Hippocampal remapping and grid realignment in entorhinal cortex. Nature 446:190-194.

Gaffan D (1994a) Scene-specific memory for objects: a model of episodic memory impairment in monkeys with fornix transection. J Cogn Neurosci 6:305-320.

Gaffan D (1994b) Scene-specific memory for objects: a model of episodic memory impairment in monkeys with fornix transection. J Cognitive Neurosci 6:305-320.

Gaiarsa JL, Caillard O, Ben-Ari Y (2002) Long-term plasticity at GABAergic and glycinergic synapses: mechanisms and functional significance. Trends Neurosci 25:564-570.

Giocomo LM, Zilli EA, Fransen E, Hasselmo ME (2007) Temporal frequency of subthreshold oscillations scales with entorhinal grid cell field spacing. Science 315:1719-1722.

Girardeau G, Benchenane K, Wiener SI, Buzsaki G, Zugaro MB (2009a) Selective suppression of hippocampal ripples impairs spatial memory. Nat Neurosci 12:1222-1223.

Girardeau G, Benchenane K, Wiener SI, Buzsaki G, Zugaro MB (2009b) Selective suppression of hippocampal ripples impairs spatial memory. Nat Neurosci 12:1222-1223.

Graf P, Schacter DL (1985) Implicit and explicit memory for new associations in normal and amnesic subjects. J Exp Psychol Learn Mem Cogn 11:501-518.

Gupta AS, van der Meer MA, Touretzky DS, Redish AD (2010) Hippocampal replay is not a simple function of experience. Neuron 65:695-705.

Gupta AS, van der Meer MAA, Touretzky DS, Redish AD (2012) Segmentation of spatial experience by hippocampal theta sequences. Nat Neurosci 15:1032-1039.

Hafting T, Fyhn M, Molden S, Moser MB, Moser EI (2005) Microstructure of a spatial map in the entorhinal cortex. Nature 436:801-806.

Harvey CD, Collman F, Dombeck DA, Tank DW (2009) Intracellular dynamics of hippocampal place cells during virtual navigation. Nature 461:941-946.

Hassabis D, Kumaran D, Vann SD, Maguire EA (2007) Patients with hippocampal amnesia cannot imagine new experiences. Proc Natl Acad Sci U S A 104:1726-1731.

Hebb DO, Martinez JL, Glickman SE (1994) The Organization of Behavior - a Neuropsychological Theory - Hebb,Do. Contemp Psychol 39:1018-1020.

Henriksen EJ, Colgin LL, Barnes CA, Witter MP, Moser MB, Moser EI (2010) Spatial representation along the proximodistal axis of CA1. Neuron 68:127-137.

Holt W, Maren S (1999) Muscimol inactivation of the dorsal hippocampus impairs contextual retrieval of fear memory. J Neurosci 19:9054-9062.

Hubel DH, Wiesel TN, LeVay S (1977) Plasticity of ocular dominance columns in monkey striate cortex. Philos Trans R Soc Lond B Biol Sci 278:377-409.

Huxter J, Burgess N, O'Keefe J (2003) Independent rate and temporal coding in hippocampal pyramidal cells. Nature 425:828-832.

Itskov V, Curto C, Pastalkova E, Buzsaki G (2011) Cell assembly sequences arising from spike threshold adaptation keep track of time in the hippocampus. J Neurosci 31:2828-2834.

Jadhav SP, Kemere C, German PW, Frank LM (2012a) Awake Hippocampal Sharp-Wave Ripples Support Spatial Memory. Science.

Jadhav SP, Kemere C, German PW, Frank LM (2012b) Awake Hippocampal Sharp-Wave Ripples Support Spatial Memory. Science 336:1454-1458.

Jay TM, Glowinski J, Thierry AM (1989) Selectivity of the Hippocampal Projection to the Prelimbic Area of the Prefrontal Cortex in the Rat. Brain Res 505:337-340.

Jeewajee A, Barry C, O'Keefe J, Burgess N (2008a) Grid Cells and Theta as Oscillatory Interference: Electrophysiological Data From Freely Moving Rats. Hippocampus 18:1175-1185.

Jeewajee A, Lever C, Burton S, O'Keefe J, Burgess N (2008b) Environmental novelty is signaled by reduction of the hippocampal theta frequency. Hippocampus 18:340-348.

Jensen O, Lisman JE (1996) Hippocampal CA3 region predicts memory sequences: accounting for the phase precession of place cells. Learn Mem 3:279-287.

Jensen O, Lisman JE (2005) Hippocampal sequence-encoding driven by a cortical multi-item working memory buffer. Trends Neurosci 28:67-72.

Ji DY, Wilson MA (2007) Coordinated memory replay in the visual cortex and hippocampus during sleep. Nat Neurosci 10:100-107.

Johnson A, Redish AD (2007) Neural ensembles in CA3 transiently encode paths forward of the animal at a decision point. Journal of Neuroscience 27:12176-12189.

Karlsson MP, Frank LM (2009a) Awake replay of remote experiences in the hippocampus. Nat Neurosci 12:913-918.

Karlsson MP, Frank LM (2009b) Awake replay of remote experiences in the hippocampus. Nat Neurosci 12:913-918.

Kentros C, Hargreaves E, Hawkins RD, Kandel ER, Shapiro M, Muller RV (1998) Abolition of long-term stability of new hippocampal place cell maps by NMDA receptor blockade. Science 280:2121-2126.

Kim JJ, Rison RA, Fanselow MS (1993) Effects of Amygdala, Hippocampus, and Periaqueductal Gray Lesions on Short-Term and Long-Term Contextual Fear. Behav Neurosci 107:1093-1098.

Kjelstrup KB, Solstad T, Brun VH, Hafting T, Leutgeb S, Witter MP, Moser EI, Moser MB (2008) Finite scale of spatial representation in the hippocampus. Science 321:140-143.

Lee AK, Wilson MA (2002) Memory of sequential experience in the hippocampus during slow wave sleep. Neuron 36:1183-1194.

Lee D, Lin BJ, Lee AK (2012) Hippocampal place fields emerge upon single-cell manipulation of excitability during behavior. Science 337:849-853.

Lee I, Rao G, Knierim JJ (2004) A double dissociation between hippocampal subfields: Differential time course of CA3 and CA1 place cells for processing changed environments. Neuron 42:803-815.

Levy WB, Steward O (1983) Temporal contiguity requirements for long-term associative potentiation/depression in the hippocampus. Neuroscience 8:791-797.

Li S, Cullen WK, Anwyl R, Rowan MJ (2003) Dopamine-dependent facilitation of LTP induction in hippocampal CA1 by exposure to spatial novelty. Nat Neurosci 6:526-531.

Lisman JE (1999) Relating hippocampal circuitry to function: recall of memory sequences by reciprocal dentate-CA3 interactions. Neuron 22:233-242.

Lisman JE, Grace AA (2005) The hippocampal-VTA loop: Controlling the entry of information into long-term memory. Neuron 46:703-713.

Lubenov EV, Siapas AG (2009) Hippocampal theta oscillations are travelling waves. Nature 459:534-539.

Luo AH, Tahsili-Fahadan P, Wise RA, Lupica CR, Aston-Jones G (2011) Linking Context with Reward: A Functional Circuit from Hippocampal CA3 to Ventral Tegmental Area. Science 333:353-357.

Malenka RC, Bear MF (2004) LTP and LTD: an embarrassment of riches. Neuron 44:5-21.

Maurer AP, Burke SN, Lipa P, Skaggs WE, Barnes CA (2012) Greater running speeds result in altered hippocampal phase sequence dynamics. Hippocampus 22:737-747.

McNaughton BL, Barnes CA, O'Keefe J (1983) The contributions of position, direction, and velocity to single unit activity in the hippocampus of freely-moving rats. Exp Brain Res 52:41-49.

Mehta MR, Quirk MC, Wilson MA (2000) Experience-dependent asymmetric shape of hippocampal receptive fields. Neuron 25:707-715.

Mehta MR, Lee AK, Wilson MA (2002) Role of experience and oscillations in transforming a rate code into a temporal code. Nature 417:741-746.

Miller EK, Wilson MA (2008) All my circuits: using multiple electrodes to understand functioning neural networks. Neuron 60:483-488.

Monaco JD, Rao G, Roth ED, Knierim JJ (2014) Attentive scanning behavior drives one-trial potentiation of hippocampal place fields. Nat Neurosci 17:725-731.

Morris RG (1989) Synaptic plasticity and learning: selective impairment of learning rats and blockade of long-term potentiation in vivo by the N-methyl-D-aspartate receptor antagonist AP5. J Neurosci 9:3040-3057.

Morris RG, Garrud P, Rawlins JN, O'Keefe J (1982) Place navigation impaired in rats with hippocampal lesions. Nature 297:681-683.

Morris RG, Anderson E, Lynch GS, Baudry M (1986) Selective impairment of learning and blockade of long-term potentiation by an N-methyl-D-aspartate receptor antagonist, AP5. Nature 319:774-776.

Moser EI, Kropff E, Moser MB (2008) Place cells, grid cells, and the brain's spatial representation system. Annu Rev Neurosci 31:69-89.

Muller RU, Kubie JL (1987) The Effects of Changes in the Environment on the Spatial Firing of Hippocampal Complex-Spike Cells. Journal of Neuroscience 7:1951-1968.

Muller RU, Bostock E, Taube JS, Kubie JL (1994) On the Directional Firing Properties of Hippocampal Place Cells. Journal of Neuroscience 14:7235-7251.

Nakazawa K, McHugh TJ, Wilson MA, Tonegawa S (2004) NMDA receptors, place cells and hippocampal spatial memory. Nat Rev Neurosci 5:361-372.

Nitz D, McNaughton B (2004) Differential modulation of CA1 and dentate gyrus interneurons during exploration of novel environments. J Neurophysiol 91:863-872.

O'Keefe J (1976) Place units in the hippocampus of the freely moving rat. Exp Neurol 51:78-109.

O'Keefe J (1979) A review of the hippocampal place cells. Prog Neurobiol 13:419-439.

O'Keefe J, Dostrovs.J (1971) Hippocampus as a Spatial Map - Preliminary Evidence from Unit Activity in Freely-Moving Rat. Brain Res 34:171-&.

O'Keefe J, Nadel L (1978a) The Hippocampus as a Cognitive Map. Behav Brain Sci 2:520-528.

O'Keefe J, Nadel L (1978b) The Hippocampus As A Cognitive Map. London: Clarendon.

Okeefe J, Recce ML (1993) Phase Relationship between Hippocampal Place Units and the Eeg Theta-Rhythm. Hippocampus 3:317-330.

Olton DS, Samuelson RJ (1976a) Remembrance of places passed: spatial memory in rats. J Exp Psychol Anim Behav Process 2:97-116.

Olton DS, Samuelson RJ (1976b) Remembrance of places past: spatial memory in rats. J Exp Psychol Anim Behav Process 2:97-116.

Patel J, Fujisawa S, Berenyi A, Royer S, Buzsaki G (2012) Traveling theta waves along the entire septotemporal axis of the hippocampus. Neuron 75:410-417.

Pawlak V, Wickens JR, Kirkwood A, Kerr JN (2010) Timing is not Everything: Neuromodulation Opens the STDP Gate. Front Synaptic Neurosci 2:146.

Penley SC, Hinman JR, Long LL, Markus EJ, Escabi MA, Chrobak JJ (2013) Novel space alters theta and gamma synchrony across the longitudinal axis of the hippocampus. Front Syst Neurosci 7:20.

Pfeiffer BE, Foster DJ (2013) Hippocampal place-cell sequences depict future paths to remembered goals. Nature 497:74-79.

Pfeiffer BE, Foster DJ (2015) PLACE CELLS. Autoassociative dynamics in the generation of sequences of hippocampal place cells. Science 349:180-183.

Phillips RG, Ledoux JE (1992) Differential Contribution of Amygdala and Hippocampus to Cued and Contextual Fear Conditioning. Behav Neurosci 106:274-285.

Pitkanen A, Pikkarainen M, Nurminen N, Ylinen A (2000) Reciprocal connections between the amygdala and the hippocampal formation, perirhinal cortex, and postrhinal cortex in rat - A review. Ann Ny Acad Sci 911:369-391.

Rao RP, Sejnowski TJ (2001a) Spike-timing-dependent Hebbian plasticity as temporal difference learning. Neural Comput 13:2221-2237.

Rao RP, Sejnowski TJ (2001b) Predictive learning of temporal sequences in recurrent neocortical circuits. Novartis Found Symp 239:208-229; discussion 229-240.

Rosenzweig ES, Ekstrom AD, Redish AD, McNaughton B, Barnes CA (2000) Phase precession as an experience independent process: hippocampal pyramidal cell phase precession in a novel environment and under NMDS-receptor blockade. Soc Neurosce Abstr 26:982.

Sadowski JH, Jones MW, Mellor JR (2011) Ripples make waves: binding structured activity and plasticity in hippocampal networks. Neural Plast 2011:960389.

Samsonovich A, McNaughton BL (1997) Path integration and cognitive mapping in a continuous attractor neural network model. Journal of Neuroscience 17:5900-5920.

Schmidt R, Diba K, Leibold C, Schmitz D, Buzsaki G, Kempter R (2009) Single-Trial Phase Precession in the Hippocampus. Journal of Neuroscience 29:13232-13241.

Schmitzer-Torbert N, Redish AD (2004) Neuronal activity in the rodent dorsal striatum in sequential navigation: separation of spatial and reward responses on the multiple T task. J Neurophysiol 91:2259-2272.

Schultz W (2000) Multiple reward signals in the brain. Nature Reviews Neuroscience 1:199-207.

Scoville WB, Milner B (1957a) Loss of recent memory after bilateral hippocampal lesions. J Neurol Neurosurg Psychiatry 20:11-21.

Scoville WB, Milner B (1957b) Loss of recent memory after bilateral hippocampal lesions. J Neurol Neurosurg Psychiatry 20:11-21.

Selden NRW, Everitt BJ, Jarrard LE, Robbins TW (1991) Complementary Roles for the Amygdala and Hippocampus in Aversive-Conditioning to Explicit and Contextual Cues. Neuroscience 42:335-350.

Shapiro ML, Caramanos Z (1990) Nmda Antagonist Mk-801 Impairs Acquisition but Not Performance of Spatial Working and Reference Memory. Psychobiology 18:231-243.

Shatz CJ (1992) The developing brain. Sci Am 267:60-67.

Silva D, Feng T, Foster DJ (2015) Trajectory events across hippocampal place cells require previous experience. Nat Neurosci 18:1772-1779.

Skaggs WE, McNaughton BL (1996) Replay of neuronal firing sequences in rat hippocampus during sleep following spatial experience. Science 271:1870-1873.

Skaggs WE, McNaughton BL, Wilson MA, Barnes CA (1996) Theta phase precession in hippocampal neuronal populations and the compression of temporal sequences. Hippocampus 6:149-172.

Slawinska U, Kasicki S (1998) The frequency of rat's hippocampal theta rhythm is related to the speed of locomotion. Brain Res 796:327-331.

Sompolinsky H, Kanter I (1986) Temporal Association in Asymmetric Neural Networks. Phys Rev Lett 57:2861-2864.

Squire LR (1992a) Memory and the Hippocampus - a Synthesis from Findings with Rats, Monkeys, and Humans. Psychol Rev 99:195-231.

Squire LR (1992b) Declarative and nondeclarative memory: multiple brain systems supporting learning and memory. J Cognitive Neurosci 4:232-243.

Squire LR (2004) Memory systems of the brain: a brief history and current perspective. Neurobiol Learn Mem 82:171-177.

Squire LR, Zola SM (1996) Structure and function of declarative and nondeclarative memory systems. Proc Natl Acad Sci U S A 93:13515-13522.

Steele RJ, Morris RG (1999) Delay-dependent impairment of a matching-to-place task with chronic and intrahippocampal infusion of the NMDA-antagonist D-AP5. Hippocampus 9:118-136.

Suzuki WA (2006) Encoding new episodes and making them stick. Neuron 50:19-21.

Thompson RF (1986) The Neurobiology of Learning and Memory. Science 233:941-947.

Toft PA (1996) The radon transform - theory and implementation. PhD thesis, Technical University of Denmark

Tsodyks M (1999) Attractor neural network models of spatial maps in hippocampus. Hippocampus 9:481-489.

Tsodyks MV, Skaggs WE, Sejnowski TJ, McNaughton BL (1996) Population dynamics and theta rhythm phase precession of hippocampal place cell firing: a spiking neuron model. Hippocampus 6:271-280.

Tulving E (1992) Memory systems and the brain. Clin Neuropharmacol 15 Suppl 1 Pt A:327A-328A.

Tulving E (2002a) Episodic memory: from mind to brain. Annual review of psychology 53:1-25.

Tulving E (2002b) Episodic memory: from mind to brain. Annu Rev Psychol 53:1-25.

Ulanovsky N, Moss CF (2007) Hippocampal cellular and network activity in freely moving echolocating bats. Nat Neurosci 10:224-233.

Ullman MT (2004) Contributions of memory circuits to language: the declarative/procedural model. Cognition 92:231-270.

van der Meer MA, Redish AD (2011) Theta phase precession in rat ventral striatum links place and reward information. J Neurosci 31:2843-2854.

Vanderwolf CH (1969) Hippocampal electrical activity and voluntary movement in the rat. Electroencephalogr Clin Neurophysiol 26:407-418.

Wennekers T, Palm G (1996) Controlling the speed of synfire chains. In: Artificial Neural Networks - ICANN 96, pp 451-456.

Whishaw IQ, Vanderwolf CH (1973) Hippocampal EEG and behavior: changes in amplitude and frequency of RSA (theta rhythm) associated with spontaneous and learned movement patterns in rats and cats. Behav Biol 8:461-484.

Whitlock JR, Heynen AJ, Shuler MG, Bear MF (2006) Learning induces long-term potentiation in the hippocampus. Science 313:1093-1097.

Wikenheiser AM, Redish AD (2015) Hippocampal theta sequences reflect current goals. Nat Neurosci 18:289-294.

Wilson MA, McNaughton BL (1993) Dynamics of the hippocampal ensemble code for space. Science 261:1055-1058.

Wilson MA, Mcnaughton BL (1994) Reactivation of Hippocampal Ensemble Memories during Sleep. Science 265:676-679.

Wittenberg GM, Wang SSH (2006) Malleability of spike-timing-dependent plasticity at the CA3-CA1 synapse. Journal of Neuroscience 26:6610-6617.

Wood ER, Dudchenko PA, Eichenbaum H (1999) The global record of memory in hippocampal neuronal activity. Nature 397:613-616.

Wu X, Foster DJ (2014) Hippocampal replay captures the unique topological structure of a novel environment. J Neurosci 34:6459-6469.

Yamaguchi Y, Aota Y, McNaughton BL, Lipa P (2002) Bimodality of theta phase precession in hippocampal place cells in freely running rats. J Neurophysiol 87:2629-2642.

Yartsev MM, Ulanovsky N (2013) Representation of three-dimensional space in the hippocampus of flying bats. Science 340:367-372.

Ylinen A, Bragin A, Nadasdy Z, Jando G, Szabo I, Sik A, Buzsaki G (1995) Sharp wave-associated high-frequency oscillation (200 Hz) in the intact hippocampus: network and intracellular mechanisms. J Neurosci 15:30-46.

Zhang JC, Lau PM, Bi GQ (2009) Gain in sensitivity and loss in temporal contrast of STDP by dopaminergic modulation at hippocampal synapses. Proc Natl Acad Sci U S A 106:13028-13033.

Zhang K (1996) Representation of spatial orientation by the intrinsic dynamics of the head-direction cell ensemble: a theory. J Neurosci 16:2112-2126.

Zhang K, Ginzburg I, McNaughton BL, Sejnowski TJ (1998a) Interpreting neuronal population activity by reconstruction: unified framework with application to hippocampal place cells. J Neurophysiol 79:1017-1044.

Zhang LI, Tao HW, Holt CE, Harris WA, Poo MM (1998b) A critical window for cooperation and competition among developing retinotectal synapses. Nature 395:37-44.

Curriculum Vitae

Ting Feng **12/6/2015**

Education

Ph.D.	2015	Neuroscience Mentors: David J. Foster, PhD	Johns Hopkins School of Medicine
M.S.	2009	Biomedical Engineering	Shanghai Jiao Tong University, China
B.S.	2007	Biomedical Engineering	Shanghai Jiao Tong University, China

Research Rotations

2010 Jun – 2010 Aug	Lab of Dr. Amy J. Bastian
2010 Jan – 2010 May	Lab of Dr. Steven S. Hsiao
2009 Sep – 2009 Dec	Lab of Dr. James J. Knierim

Research Publications

Delia Silva*, **Ting Feng***, David J. Foster. Trajectory events across hippocampal place- cells require previous experience. Nature Neuroscience, vol. 18, pp. 1772-1779, 2015. ***co-first author**.

Ting Feng, Delia Silva, David J. Foster. Dissociation between the experience-dependent development of hippocampal theta sequences and single-trial phase precession. Journal of Neuroscience, vol. 35, pp. 4890-4902, 2015.

Yu Sun, Hong Zhang, **Ting Feng**, Yihong Qiu, Yisheng Zhu and Shanbao Tong. Early cortical connective network relating to audiovisual stimulation by partial directed coherence analysis. IEEE Transactions on Biomedical Engineering, vol. 56, pp. 2721-2724, 2009.

Ting Feng, Yihong Qiu, Yisheng Zhu and Shanbao Tong. Attention rivalry under irrelevant audiovisual stimulation. Neuroscience Letters, vol. 438, pp. 6-9, 2008.

Conference Presentations

Ting Feng, Delia Silva, David J. Foster. Mechanisms contributing to experience-dependent changes in the structure of hippocampal replay sequences. Society for Neuroscience Annual Meeting Abstracts, 630.01, 2015.

Ting Feng, Delia Silva, David J. Foster. Sequential activation of hippocampal place cells during replay slows down with experience. Society for Neuroscience Annual Meeting Abstracts, 397.12, 2012.

Ting Feng, Delia Silva, David J. Foster. Rapid development of hippocampal theta sequences with experience. Society for Neuroscience Annual Meeting Abstracts, 729.02, 2011.

Erin V. Vasudevan, **Ting Feng**, Amy J. Bastian. Structure learning in a locomotor adaptation task. Society for the Neural Control of Movement Abstracts, 2011.